AN EXPERIMENTAL STUDY INTO THE CO-COMBUSTION OF COAL AND DENSIFIED REFUSE DERIVED FUEL

A THESIS SUBMITTED TO THE UNIVERSITY OF MANCHESTER FOR THE DEGREE OF DOCTOR OF PHILOSOPHY IN THE FACULTY OF SCIENCE AND ENGINEERING

CLEVER KETLOGETSWE

MANCHESTER SCHOOL OF ENGINEERING

OCTOBER 2002

ProQuest Number: 10834372

All rights reserved

INFORMATION TO ALL USERS
The quality of this reproduction is dependent upon the quality of the copy submitted.

In the unlikely event that the author did not send a complete manuscript
and there are missing pages, these will be noted. Also, if material had to be removed,
a note will indicate the deletion.

ProQuest 10834372

Published by ProQuest LLC (2018). Copyright of the Dissertation is held by the Author.

All rights reserved.
This work is protected against unauthorized copying under Title 17, United States Code
Microform Edition © ProQuest LLC.

ProQuest LLC.
789 East Eisenhower Parkway
P.O. Box 1346
Ann Arbor, MI 48106 – 1346

Th 22931

JOHN RYLANDS
UNIVERSITY
LIBRARY OF
MANCHESTER

Table of Contents

Figures

Tables

Abstract

Thermal treatment of waste and the recovery of heat energy generated by the combustion process is now a recommended method for the disposal of the ever-increasing amounts of waste produced by modern society but there is a conflict because of the need to reduce emissions to the atmosphere. An experimental study has been performed to determine the emission levels and thermal characteristics for the combustion process of different mixtures of pelletised densified refuse waste derived fuel (dRDF) and coal.

A non-intrusive optical transmission method was employed to monitor the nitrogen dioxide ($N0_2$) emission levels continuously, while point measurement of carbon dioxide, carbon monoxide, oxygen and excess air concentrations were also recorded at various times during the combustion process using a gas sampling technique. The emission levels for the different fuel mixtures provide indicators which can be used to predict the performance of a full-scale plant.

The work was carried out in a small-scale laboratory furnace burning each mixture individually under stoichiometric combustion conditions. Mixtures of 50/50% coal/dRDF, 60/40% coal/dRDF and, 70/30% coal/dRDF were tested. In addition, the dRDF and coal were burnt separately and were tested for their thermal characteristics.

It was found that, under stoichiometric combustion conditions, the maximum mean temperatures for the combustion of the above fuels ranged between 900°C to 950°C. The 50/50% coal/dRDF mixture burns easily and quickly, and produces peak nitrogen emission levels at the maximum rates of combustion. However, reducing the proportion of dRDF to 30% delays the ignition process and shifts the peak for nitrogen dioxide emission towards the earlier stages of the ignition process.

In these conditions, where the combustion is slower, the peak nitrogen dioxide emission levels do not occur at the maximum rates of combustion, in contrast to the situation when the ignition rates are relatively high.

The experimental study has shown that the $N0_2$ emission levels for all the different fuel mixtures were below the specified limit of 200 mg/m^3. However, the results also showed that the oxygen rapidly consumed in the ignition stage when the proportion of dRDF is increased from 30% to 50%. In this case, oxygen values below the EU specified limit of 6% appeared which might give cause for concern about the required minimum destruction removal rate of 99.99%.

Declaration

No part of this thesis has been submitted in support of an application for any degree or qualification of the University of Manchester or any other University or Institute of Learning.

Copyright

Copyright in text of this thesis rests with the Author. Copies (by any process) either in full, or of extracts, may be made only in accordance with instructions given by the Author and lodged in the John Rylands University Library of Manchester. Details may be obtained from the Librarian. This page must form part of any such copies made. Further copies (by any process) of copies made in accordance with such instructions may not be made without the permission (in writing) of the Author.

The ownership of any intellectual property rights which may be described in this thesis is vested in the University of Manchester, subject to any prior agreement to the contrary, and may not be made available for use by third parties without the written permission of the University, which will prescribe the terms and conditions of any such agreement.

Further information on the conditions under which disclosures and exploitation may take place is available from the Head of the Department of School of Engineering.

Acknowledgement

The author graduated from Portsmouth University in 1995 with a master's degree in Environmental Engineering. Since that time he has been employed by the University of Botswana as a Lecturer.

In April 1999, the author was granted study leave to enrol in the School of Engineering of the University of Manchester in order to undertake a PhD in Environmental Engineering. It was agreed that he should study the co-combustion of waste derived fuel and coal. Since this was the first such combustion project to be undertaken within the Fluid Mechanic Research Group, it became necessary to design and commission a new combustion rig. The author wishes to express his sincere gratitude to Dr J.T. Turner who supervised the project.

The willing help of Dr David J. Smith and other members of the staff of the Goldstein Laboratory are also acknowledged. Without such assistance, a successful completion of the project could not have been achieved. Special thanks are extended to Dr Adrian Watson of the Manchester Metropolitan University for his willing help. Finally the author wishes to extend special thanks to Mr F. Cameron plant manager for Reprotech (Pebsham) Ltd and his secretary for the supply of densified refuse derived fuel (dRDF).

Nomenclature

G_{RT}	Gas residence time,	s
V	Volume of the reactor,	m^3
V_1	Volumetric flow rate of the gas,	m^3/s
h	Plank's constant,	Js
λ	Wavelength,	nm
ν	Frequency,	1/s
c	The velocity of light in a vacuum,	m/s
e_1	Energy level of the ground state,	kJ
e_2	Energy level of the final state,	kJ
I_0	Intensity of the light incident upon the gas element,	%
I	Intensity of the light at exit from the gas element,	%
Tr	Transmittance of the light through the flue gas,	%
α_λ	Molecular absorbance coefficient (dependent on the λ)	
Cp	Concentration of the pollutant,	ppm
L	Distance the light beam travels through the gas,	m
A_λ	The absorbance at each wavelength	
S_λ	Sample intensity at each wavelength	%
D_λ	Dark intensity at each wavelength	%
R_λ	Reference intensity at each wavelength	%
E_A	Uncertainty in the measured absorbance,	%
Q_m	Air mass flow rate,	kg/s
E	The velocity of approach factor,	m/s
d	The orifice diameter,	m

Δp	The pressure drop across the orifice plate,	pa
ρ	The air density,	kg/m^3
D	Pipe bore diameter,	m
β	The ratio of orifice bore to pipe bore	

Chapter 1 Introduction

1.1 General overview

The increased pressure from environmental legislators such as the European Union to minimise the volumes of biodegradable waste going to landfill sites is expected to stimulate the rapid development of waste-to-energy plants in many communities. It is noted that the new EU Landfill Directive (99/31/EC), which came into force in April 1999, requires Member States to reduce the amount of biodegradable solid waste going to landfill sites. The Directive also requires that the landfill gas produced in existing and new sites must be collected, treated, and used for power generation where appropriate. In a situation where the use of landfill gas for power generation is not economic the Directive requires that landfill gas must be contained burnt in a special designed burner (landfill gas flare). This pressure to minimise the volumes of waste going to landfill sites aims to reduce the emission levels of greenhouse gases (The Kyoto Protocol and Beyond (1999) and Porteous (2001)).

Considering these stringent requirements, coupled with the growing shortage of landfill sites close to areas of solid waste generation, it is obvious that waste disposal using the landfill method is becoming increasingly unattractive. This brings several questions including the use of other alternatives such as recycling and composting and their ability to divert significant volumes of biodegradable waste going to landfill sites. It must be noted that the success of recycling and composting schemes depend critically on economics which include costs of collection and reprocessing, as well as the often-higher costs of utilising the recycled end product(s).

Interestingly, a study by Border (1995)[1] showed that the largest potential market for reliable compost derived from waste would be the agricultural market. However, the penetration of waste-derived compost into the agricultural market has proved difficult presumably because there were no control measures to ensure that levels of contaminants especially potentially toxic elements such as mercury, lead, cadmium etc were relatively low. As a direct results of this, 1998 saw the introduction of the first UK standards for composts as given in table 2.1 (The UK Composting Association Report SCA03 (January 2002)).

Despite the introduction of the standards for composts in UK, composting facility excluding home compost still handles relatively small quantity of municipal solid waste as described in section 2.3. All these lead to the conclusion that these two alternatives are not capable of diverting worthwhile amounts of biodegradable waste from landfill.

In such a scenario, the concept of waste-to-energy looks increasingly attractive because it recycles the energy present in refuse to produce power and heat in a situation where combined heat and power system is employed. In so doing, this method of waste disposal provides three useful public services as an alternative to the disposal of waste to landfill. Despite all these advantages, the primary obstacles facing the rapid development of waste-to-energy facilities is public concern regarding the emissions generated during the combustion of waste in particular dioxins emission levels. Furthermore, it is also noted that the new Directive (2000/76/EC), which covers the burning of waste, requires strict control on nitrogen dioxides emission levels.

[1] Border, D. Taking a green product to market. The Waste Manager, March 12 – 15, 1995, in Williams 1998.

In fact, this is the first European Directive on the combustion of waste to prescribe limits for the $N0_2$ emission levels produced by the combustion of solid waste. This Directive requires Member States to reduce the emission of $N0_2$ to 200 mg/m^3. In the UK the current allowable $N0_2$ emission level is 300 mg/m^3 as shown in table 3.3 (HMIP Standards S2 1.05 (1996)).

Note, it needs to be explained that as a direct pressure from the European Union environmental law on minimising emission levels produced by the combustion of waste, the UK Government through the Environment Agency issued a number of Guidance Notes for process subject to integrated pollution control. The first series which covered the combustion of fuel manufactured or comprised of solid waste were the IPR series published in 1992 as given in table 3.3 (HMIP Standards IPR 5/3 (1992)). It is believed that the establishment of the first UK Guidance Notes (IPR series), was to response to the first two EU Directives 89/369/EEC and 89/429/EEC on the reduction of air pollution from the combustion of waste. In 1996 the IPR series UK Guidance Notes were superseded by the new S series as given in table 3.1.

The above observations are indicative of the growing legislative pressures on national governments and local authorities to reduce gaseous emission levels from combustion facilities. It is noted that The Kyoto Protocol to the United Nation Framework Convention on Climate Change (UN FCCC) also requires both the Organisation for Economic Cooperation and Development (OECD) and Non-OECD countries to reduce the emissions of greenhouse gas especially carbon dioxide.

With regard to climate change the UK Government responded by introducing climate change levy. This was introduced in April 2001 (Green (2000)). Consequently, energy generated from renewable sources is exempted from climate change levy.

Note, that in this context, renewable sources cover the burning of solid waste as presented in table 2.3. The techniques of converting waste-to-energy are summarised in figure 2.4.

The present investigation was designed to study the concentration of nitrogen dioxide emission generated during the co-combustion of various mixtures of pelletised densified refuse derived fuel (dRDF) and coal. Note that dRDF refer to a solid fuel manufactured from municipal solid waste as described in section 2.4.

In order to provide a comprehensive review on the thermal conversion of municipal solid waste and the application of optical techniques to measure gas concentrations, it was considered appropriate to review the entire subject prior to undertaking the combustion study.

This is done in chapters 2, 3, 4, 5, and 6. Chapter 2 therefore provide information on the classification of waste, waste management options, and how some of these options could adversely affect the energy recovery potential of large-scale waste-to-energy facilities if they were to be carried out at large scale. This chapter also covers subjects such as the minimum allowable combustion conditions for the combustion of waste, with or without energy recovery schemes.

The different components of UK and European Union environmental legislation which cover the combustion of municipal solid waste are described in chapter 3. Chapter 4 describes factors influencing the formation of $N0_2$ during the combustion process and methods which are employed to reduce $N0_2$ emission levels. This chapter also describes other methods which are used to measure $N0_2$ concentrations.

Chapter 5 concentrates on the use of spectrometers and absorption methods since this was the approach adopted in the present investigation. Chapter 6 describes the experimental apparatus, instrumentation and operational procedures used to calibrate the spectrometer and the pressure transducer employed in the present investigation. Chapter 7 describes the measurements of the emission levels and fuel bed temperatures achieved during the combustion of a number of fuel mixtures. Chapter 8 presents and discusses the results. Finally, chapter 9 draws conclusions from the experimental study.

1.2 Aims and objectives of the investigation

The aims of the investigation described in this thesis were as follows: –

i. To review the legislation relating to the combustion of waste derived fuels, and the environmental implications of these developments.

ii. To carry out a systematic investigation for various mixtures of coal and dRDF using a laboratory scale combustion system to determine their thermal and effluent generation characteristics.

iii. To consider the findings of the experimental study and draw conclusions relating to full-scale implementation of the technology.

Objectives were therefore specified as listed below: –

i. To design, construct and commission a flow and instrumentation system which enables the gaseous effluents generated by the co-combustion of coal and densified refuse derived fuel (dRDF) to be studied in the laboratory.

ii. To calibrate the optical instrumentation used to determine the NO_2 emission levels and assess the accuracy of this non-intrusive method as discussed in section 61.

iii. To compare the measured combustion and effluent generation characteristics of the different fuel mixtures and determine an optimum which might be appropriate for full-scale waste-to-energy operation, as discussed section 8.6.

Chapter 2 Waste as an alternative source of energy

2.1 Background information

In a situation where a method of converting waste to energy is part of the waste management system, it is important that the data on waste generated within the catchment area of the power generating plant is reliable. For example, if there is significant fluctuation in volume of waste throughout the year, there is a great chance that the system will fail to fulfil its objective of generating significant and reliable levels of power. For the method of converting waste-to-energy to be economically feasible and reliable the volume of waste per unit time must be consistent otherwise the system would become an incinerator.

Although from the above, its clear that the quantity of waste generated within the catchment area of the power generating plant is an important factor regarding the financial feasibility of the plant, it is noted that the waste-to-energy sector prefers to use municipal solid waste (MSW) because this category of waste generally contains more organic material and therefore, has a higher calorific value.

Despite the significant use of municipal solid waste for power generation in some countries as shown in figure 2.3 and the development of environmental legislation in many parts of Europe, the term "**municipal solid waste**" still has a relatively imprecise definition. As a result, use of municipal solid waste in the waste-to-energy sector frequently causes problems during applications for authorisation to operate a waste-to-energy system under section 6(3) of the Environmental Protection Act 1990. For this reason, it is considered appropriate that the classification of waste in the UK context should be considered in greater detail.

2.2 General classification of waste

When an authority is to set-up a facility for waste disposal and recycling and to convert the waste into energy, data on the composition of the waste is vital. For example, the quality of waste in terms of its heating value is a major factor influencing the economic feasibility of waste-to-energy plant. Also, data on waste is an important factor needed for the imposition of regulatory controls and waste disposal procedures by waste management authorities around the world.

Regarding the definition of municipal solid waste, there is still lack of consistency around the world. For example, in the UK, the term "municipal solid waste" is generally defined to include household waste, waste from civic amenity sites, street sweeping and park waste, and waste collected from trade premises by the local authorities (ENDS Report No 246 1995). In contrast to the above definition, the European Union (EU) Landfill Directive (99/31/EC) has a broader definition and describes municipal solid waste as including household, commercial, industrial, and other wastes which, because of their nature or composition, are similar to waste from the household stream.

The difficulty with this extended definition is that the composition of commercial, industrial and institutional wastes are poorly characterised. It is envisaged that this extended definition of municipal solid waste, as it appears in the new EU Landfill Directive may cause problems to Member States during the implementation phase, especially when considering the waste-to-energy sector because operators of such plants must comply with EU Directive on air pollution and even more stringent UK Environmental Agency Guidance Notes.

In the UK, Waste Management Authorities tend to define MSW as follows: (Guidance Note S2 5.01 (1996))

Household waste means waste from

i. domestic property, that is to say, a building or self-contained part of a building which is used wholly for the purposes of living accommodation

ii. caravan sites

iii. residential homes

iv. premises forming part of a university or school or other educational establishment

v. premises forming part of a hospital or nursing home.

Commercial waste means waste from premises used wholly or mainly for the purpose of a trade or business or for sport, recreation or entertainment with the exclusion of

i. household waste

ii. industrial waste

iii. waste from any mine or quarry and waste from premises used for agriculture.

Industrial waste means waste from any of the following premises

i. any factory within the meaning of the UK Factory Act (1961)

ii. any premises used for the purpose of, or in connection with, the provision to the public of transport service by land, water or air

iii. any premises used for the purpose of, or in connection with, the provision to the public of gas, water or electricity or the provision of sewage services

iv. any premises used for the purpose of, or in connection with, the provision to the public of postal or telecommunications service.

Combining the first two of these categories, household and commercial waste, disposed of by the local authority, constitutes a municipal solid waste (MSW).

In conclusion, the term municipal solid waste in the UK context is normally assumed to include all community wastes with the exception of waste from industrial processes and agricultural waste.

2.3 Waste management options

Several options are used in waste management systems to minimise the environmental impact due to the ever-increasing volumes of waste. Considering the UK situation, the disposal routes for the main elements of controlled waste are shown in figure 2.1. It can be seen that landfill is the preferred route for the disposal of solid waste. Estimates indicate that about 120 million tonnes/year of controlled waste is going to landfill sites each year. This includes 90% of household waste, 85% of commercial waste, 63% of the waste from construction and demolition, and 73% of industrial waste (Williams (1998)).

Figure 2.1 also shows that waste from construction and demolition is subjected to a relatively high proportion of recycling whilst, in the household and commercial sectors, the recycling rates are relatively low. This low recycling rate of household and commercial wastes reflects the facts that landfill is the most adaptable and

perhaps least expensive waste management option in most areas of the UK as shown in figure 2.3. In support of this observation, a study by Williams (1998) found that many landfill sites in the UK are located in areas where the geology and hydrogeology are suitable for landfill sites.

This author found that many landfill sites benefit from natural clay linings, which help to contain the potentially polluting liquids formed within the landfill, thus considerably reducing the engineering costs in most sites in the UK. In addition, many sites employ old quarries although there are still required to comply with the relevant environmental law: the government encourages the disposal of waste by backfilling these quarries as a measure to increase land reclamation process (Guidance Note S2 5.02 (1996)).

Although, from the above observations, the landfill method may look attractive, there are serious uncertainties regarding the future use of landfill, particularly with regard to the cost which appears certain to escalate. For example, it is noted that the new EU Landfill Directive, which came into force in April 1999, is expected to challenge the disposal of organic waste by landfill across the EU Member States. The Directive requires Member States to significantly reduce the amount of biodegradable solid waste going to landfill sites. Reductions of 75% of the total produced by 2002, 50% by 2005, and 35% by 2010 from the 1997 baseline levels are specified.

The Landfill Directive during application also requires that the landfill gas produced in existing and new sites must be contained and burnt in a special designed landfill gas burner. Note, that landfill gas flare produces mainly carbon dioxide which has a much weaker global warming effect compared to methane gas. The Directives also encourages the use of landfill gas for power generation where appropriate.

When these stringent landfill requirements are recognised, it is clear that landfill costs must soon increase. All these lead to the conclusion that a high percentages of the wastes originating from household, commercial and industrial sources must be diverted from landfill sites to waste-to-energy thermal plants. Those plants which in many situations combine both heat and power generation can also be expected to offer greater efficiency in the conversion process.

From the economic perspective, the implementation of the Landfill Tax, which came into operation in October 1996, adds another disincentive for the landfill option. The Landfill Tax is still fixed at £2/tonne for inert waste, however, for bio-reactive waste the tax was set at £7/tonne in 1996, £11/tonne in 2001, rising to £15/tonne by 2004 (DETR (2000)). When these costs are recognised, it is clear that the future of the landfill option is uncertain.

Regarding the utilisation of landfill gas for power generation, it is clear that the reduction of organic waste going to landfill sites as required by the new Landfill Directive, will reduce the opportunity for landfill to be considered as a "bio-reactor". This must have major impact on landfill operators. On the other hand, there will be a corresponding increase in the economic case for waste thermal reactors with energy recovery options which currently only account for about 3% of energy production in the UK (Jahnke (1991) and Bury (1994)). At the present time, it is estimated that waste disposal by thermal methods without energy recovery currently accounts for about 5% of household waste, 7.5% of commercial waste and less than 2% of industrial waste (Department of the Environment and Welsh Office (1995)).

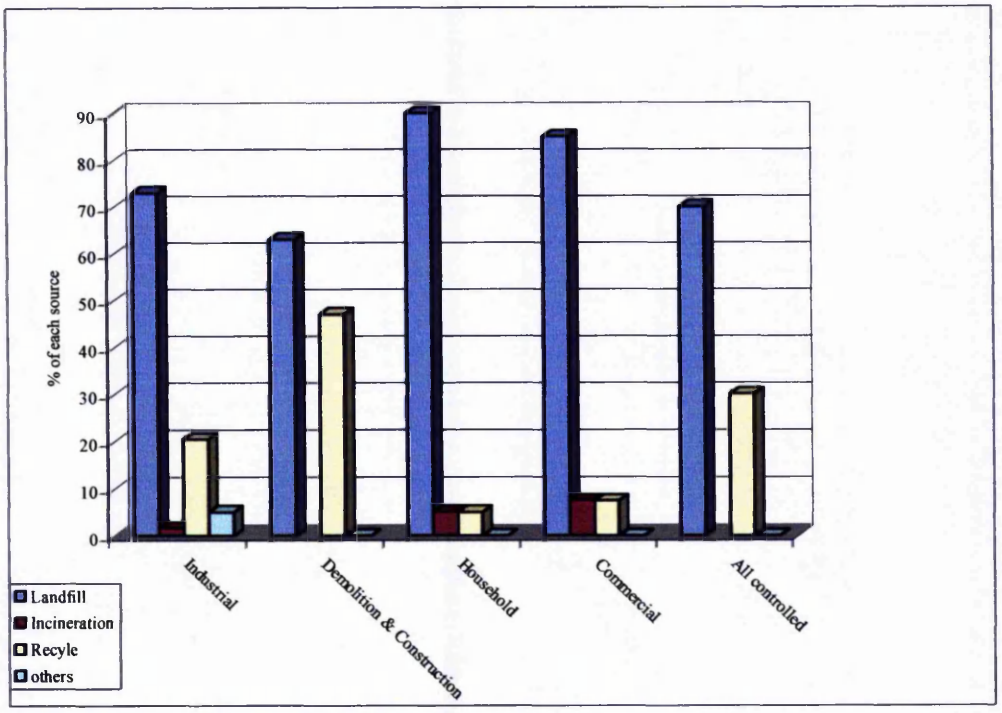

Figure 2. 1 Disposal route for the main elements of controlled waste in the UK.
Source. DoE. Making Waste Work (1995)

Regarding the recycling of household and commercial waste, it is noted that there is scope for action to increase the rate of recycling in the UK. This opportunity has been indicated by a number of legislative measures referred to in (IPC Guidance Note S2 5.02 (1996)).

Although scope for actions to increase the rate of recycling in the UK does exist, there are still uncertainties as to whether recycling could significantly reduce the volume of organic waste going to landfill sites as required by the new EU Landfill Directive. From a waste-to-energy perspective, there is a fear that if recycling programmes was to become more successfully, then these would adversely affect the energy potential (and hence the viability) of waste-to-energy systems because of the reduction in volume of biodegradable waste (major source of waste which holds a considerable

amount of exploitable energy). A detailed discussion on the effects of increasing the level of recycling on the heating value of municipal solid waste appears in section 2.7.

Another waste management option, which could have adverse effects on waste-to-energy systems, and especially landfill gas utilisation, would be the large-scale development of composting. Composting in the UK is seen as offering immense potential for significantly reducing the amount of organic waste going to landfill. As a result, the UK Government responded to the growing pressure to reduce biodegradable waste going to landfill sites and set a target of 40% home composting by the year 2000 (Department of the Environment and Welsh Office (1995)). The question then arising is how much biodegradable waste this policy, backed up by the Landfill Tax, would divert from landfill? It is noted that in 1997, just over one-third of local authorities had centralised composting schemes and, in 1998, composting facilities excluding home compost which is mainly vegetable and garden waste handled 0.9 million tonnes of green waste, about a fifth of the municipal waste that could be composted (DETR (2000)). All these factors lead to the conclusion that the government ambition to achieve 40% compost by the year 2000 was not met.

To address the uncertainty of whether the overall effects of this policy could affect landfill gas utilisation schemes, it is appropriate to consider factors which influence large-scale composting. These include the price, quality and consistency of the product. There must also be guarantees that the product will be free of contaminants such as heavy metals, glass and other inert materials, and plant and animal pathogens. Interestingly, a study by Border (1995) showed that the largest potential market for reliable compost derived from waste would be the agricultural sector. However, the penetration of waste-derived compost into the agricultural sector has proved difficult.

This was because there were no standards available. As a results, there was no guarantees that the product was free of contaminants. Consequently, in the UK, the development of large-scale composting has been mainly been restricted to the relatively simple and cheap use of '**green waste**' from civic amenity sites and local authority parks and gardens.

A number of Member States in the European Union including the UK through the Composting Association which was formed in 1995 have establish their own standards for composts and the European Committee for Standardisation is working to harmonise standards for soil improvers throughout the EU. Table 2.1 summarises major substances and their limit levels for the UK Composting Association. Table 2.2 summarises the obligatory information for composts.

Table 2. 1 The UK standards for composts

Parameter	Upper Limit
Human pathogens	
Salmonella spp	Absent in 25 g
E. Coli	1000 CFU g^{-1}
Potentially Toxic Elements	
Cadmium (Cd)	1.5 mg kg^{-1} dry matter
Chromium (Cr)	100 mg kg^{-1} dry matter
Copper (Cu)	200 mg kg^{-1} dry matter
Lead (Pb)	150 mg kg^{-1} dry matter
Mercury (Hg)	1 mg kg^{-1} dry matter
Nickel (Ni)	50 mg kg^{-1} dry matter
Zick (Zn)	400 mg kg_{-1} dry matter
Physical contaminants	
Total glass, metal and plastics > 2 mm	1% m/m of total air-dried sample (of which < 0.5% m/m of total air – dried sample is plastic
Stones and other consolidated mineral contaminants > 2 mm	5% m/m of total air – dried sample
Weed contaminants	
Weed propagules	5 viable propagules L^{-1}
Phytotoxins	
Plant tolerance	20% below control

Source: The UK Composting Association SCA03 2002

Table 2. 2 Obligatory information for composts

Designation of compost (compost-derived soil improver, growing medium constituents ets)
Contact details, name, address and telephone number of producer
Feedstocks from which the compost is derived
Organic matter content (% mass/mass dry matter
Moisture content if sold by mass (% mass/mass or g/l)
pH(plus a statement concerning its suitable for acid-loving plants)
Electrical conductivity (mS/m)
Total chloride concentration (mg/l)
Total nitrogen (N mass/mass dry matter)
Ammonium to nitrate ratio (NH_4-N : $N0_3$-N)
Carbon to nitrogen ratio (C : H)
Particle size grading (as X% less than y mm in diameter)
Batch identification code (s)
Storage instructions (e.g store in a cool, dry place)
Instruction for use
Appropriate safety advice
Health and safety warming with safety symbols as appropriate
The phrase "produced in accordance with The Composting Association Standards for Composts"
The Certification Number

Source: The UK Composting Association SCA03 2002

JOHN RYLANDS
UNIVERSITY
LIBRARY OF
MANCHESTER

It is interesting to note that a study by the UK Composting Association on the state of composting in the UK found that in 1999 there were a total of 90 operators running 197 sites, processing approximately 833,044 tonnes of material. The sites have been classified into three different types, compressing: 62 operators running 80 centralised sites processing 765,155 tonnes, 18 co-ordinators/operators running 65 on-farm sites processing 66,401 tonnes and 10 co-ordinators/operators running 52 community sites processing only 1,488 tonnes (The Composting Association Report SCA03 (2000)).

Considering the community sites processing only 1,488 tonnes/year, it is appropriate to conclude that compost option despite the introduction of standards composts is not capable of diverting waste from municipal solid stream from going to landfill. On this basis, the only attractive option with the potential to cause significant reductions in the volume of organic waste going to landfill would be to use the thermal method with energy recovery to improve the economics of the processes. These systems would reduce the greenhouse gas emissions especial methane which has a much stronger global warming effect. Note, that it is estimated that one tonne of biodegradable waste produces between 200 and 400 m^3 of landfill gas ((DETR (2000)).

It may be concluded that the use of the thermal method with energy recovery is the only option, if the volume of organic waste going to landfill is to be reduced significantly. However, it is also noted that the combustion of waste is a complex process due to the anticipated variations in the composition of the waste. The next section describes some of the most common problems associated with the combustion of solid waste.

2.4 Combustion of municipal solid waste

There are numerous problems associated with the combustion of solid waste. These are well-known and should be considered carefully when implementing any waste-to-energy scheme. The operational concept to be emphasised when dealing with the combustion of any waste stream is that the feedstock cannot be treated as a single combustible substance. Rather it must be seen as a heterogeneous mixture of combustible materials, each with its own combustion characteristics. This heterogeneity applies to chemical composition, including the major constituents (carbon, hydrogen, and oxygen), the pollutant forming minor constituents (nitrogen, sulphur, and chlorine), and the trace metal content (Tillman (1991)).

There are mixed opinions regarding the use of heterogeneous solid waste in power generating plants. For example, Rhyner et al (1995) pointed out that the use of a heterogeneous composition in which the components have different specific heat values would cause fluctuations in the heat output and steam pressure. The authors further reported that in a situation where refuse derived fuel is co-fired with another solid fuel such as coal, the ratio of refuse derived fuel to coal must be limited to 20% to avoid fluctuations in the heat output and steam pressure.

In its "as-collected" form, the wide range of size and composition of municipal solid waste makes it difficult to handle and feed as a fuel to most waste-to-energy facilities. When compared to coal, raw waste has a low heating value of approximately 9.7 MJ/kg and a high ash and moisture content (Goodger (1980)). Furthermore, the moisture content for a typical solid waste ranges from 15 to 40%, with a typical average value of 30% (Moss 1997 as reported in Williams (1998)).

Considering the operation of the waste-to-energy facilities, these characteristics would lead to high heat losses and low boiler efficiencies.

In order to improve boiler efficiency, a supplementary fuel is usually used. This supplementary fuel is also essential to provide the heat energy needed to remove the excess moisture by evaporation. The heat required to remove the moisture by vaporisation is approximately 2257 kJ/kg. This is another reason why a supplementary fuel is added in waste-to-energy plants where the raw waste represents the main source of the energy.

Since industrial companies have shown an increased interest in waste as an energy source in recent years, several processes have been employed to minimise the problems associated with the combustion of solid waste. These include removing the ferrous and other non-combustible materials, "top size reduction" by chopping, crushing, or grinding to produce a higher quality waste fuel referred to as "refuse-derived fuel" (RDF). RDF falls into two categories, coarse and densified. Densified which is abbreviated as dRDF refers to the combustible portion of MSW that has been extruded into pellets to reduce the cost of transportation and storage, while coarse RDF also refers to the combustible portion of MSW which is not compacted to form a solid fuel pellets. Figure 2.2 shows a typical flow diagram for the manufacturing of RDF/dRDF.

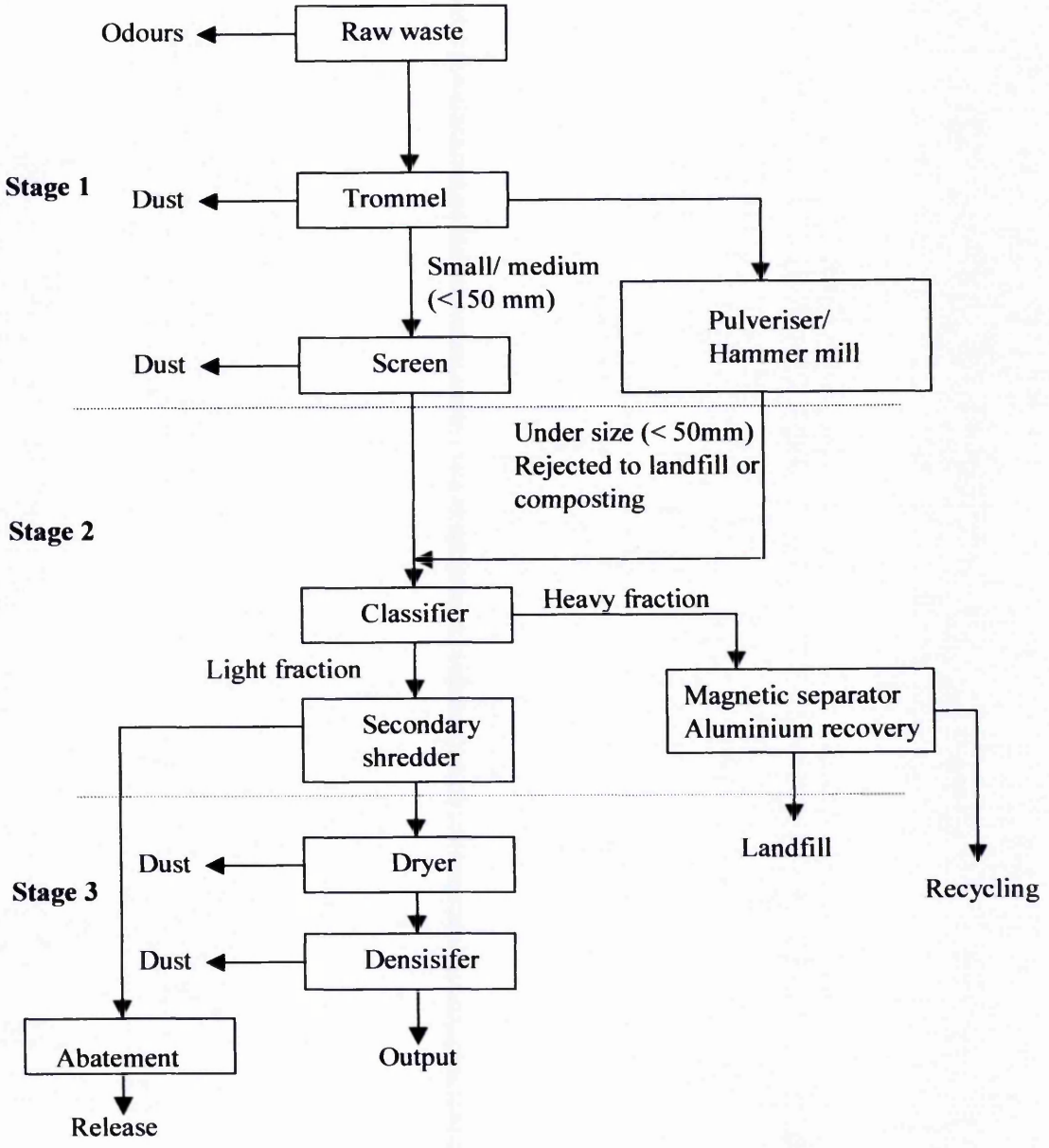

Figure 2. 2 A flow diagram for RDF/dRDF manufacturing

Source: The UK Guidance Note S2 5.01 (1996)

The manufacturing process compresses three stages as follows:

Stage 1 Sizing and screening

Here, the waste is transported from the storage hall, usually by conveyor, into a primary trommel mill (a revolving screen) to separate large and small objects, with a typical cut-off size of around 150mm.

The overzised fraction is pulverised in a hammer mill (shear, or knife mills may also be used) to create a more uniform object size. The undersized fraction, less than 50mm across may with further processing be recycled for composting or may be rejected to landfill.

Stage 2 Separation

The selected process material is fed into a classifier which may be mechanical or pneumatic which separates the wastes according to weight, with the lighter plastics and paper materials floating off and heaver objects such as metals and glass, passing out at the bottom. Where classification is pneumatic cyclones may be used to recover the product.

Stage 3 Densification

Prior to pelletisation the output from the classifier is dried at around 100°C by mixing the waste with hot gases in either a thermo-pneumatic dryer or a rotary dryer (after partial densification) to compressed into pellets to a density of around 560 kg/m^3 and a moisture content of about 10%. The waste gases from the drying line are generally treated in a wet scrubber before discharged to the atmosphere.

A typical composition of dRDF manufactured in the UK as a percentage of dry material is as follows (Guidance Note S2 5.01 (1996)).

- Paper/board 84%
- Plastics 11%
- Glass, wood, textiles, metals, etc 5%

2.5 Energy recovery from the combustion of solid waste

The potential for heat recovery from the combustion of municipal solid waste is influenced by its energy content and the design operating temperatures of the flue gases treatment systems in waste reactors. Modern flue gas treatment systems are designed for operating temperatures between 250°C and 300°C (ENDS Report No 246, July 1995)). Such systems include cyclones, scrubbers, bag filters and electroprecipitators. Consequently, in waste-to-energy plants, the operating temperature range of the flue gases treatment systems is achieved by incorporating a power boiler. In such a configuration, the plant becomes more environmental friendly because it displaces fossil fuel that would otherwise have to be burned to achieve the electricity generation.

The combustion of waste for power generation has long been seen as an attractive alternative source. For example, in 1977, the Member States of the European Community incinerated 20 million tonnes of their municipal waste. This figure represented about 20% of the total municipal waste generated at that time. More than 12 million of these 20 million tonnes of municipal solid waste were burnt with energy recovery to obtain heat, steam and / or electricity representing about 63% of the thermal treatment waste (Commission of the European Communities (1980 / 81)). The figures presented above can only be used as a guide and estimates do vary because very little of the municipal waste is weighted or analysed.

Although the combustion of waste for power generation has long been seen as an attractive alternative source, it is noted that this technique is not so common in the UK as it is elsewhere in Europe, Japan and Canada. Figure 2.3 compares the level of waste-to-energy in the UK with few selected countries.

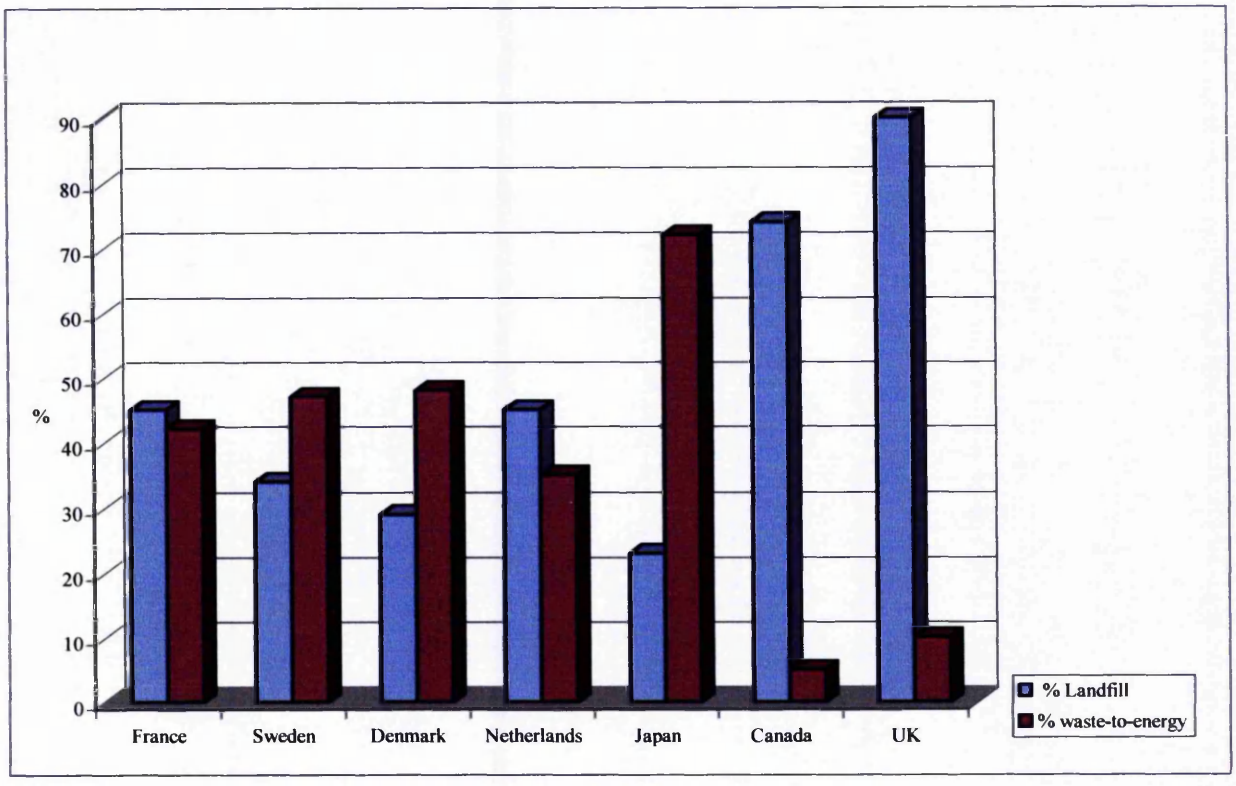

Figure 2. 3 Level of waste-to-energy in selected countries

Source. Integrated Waste Service Association (USA 1997/98)

The low rate of waste-to-energy systems in the UK is explained by the availability of least expensive landfill as discussed earlier in section 2.3. The current level of waste-to-energy conversion in the UK is estimated at 3% (Bury (1994)). It is assumed that this difference in waste-to-energy production as shown in figure 2.4 is due to differences in environmental legislation which is many situation is driven by the scarcity of landfill space. For example, in Germany, the legislation makes the recovery of energy from municipal solid waste a legal obligation in situations where there is an on-site use for heat or steam or where electricity generation would be more than 0.5MWe (Jonhke (1992)). As a result, the level of waste-to-energy conversion in Germany is estimated to be 35% (Integrated Waste Services Association (1997/98)). The recovery of energy from municipal solid waste covers a number of options.

The full range of options are summarised in figure 2.4. Figure 2.4 also shows that the thermal conversion of municipal solid waste for power generation or to produce combustible gas is divided into three streams.

Combustion is a flame initiated reaction which requires an excess air to ensure sufficient oxygen for the oxidation reaction necessary to convert the carbon and hydrogen in the waste into mainly $C0_2$. Figure 2.4 shows that the process releases the energy content of the hydrocarbons in the waste into the flue gases in the form of heat.

Note, that this process provides the following environmental benefits, (SELCHP Technical Report (1997))

- Achieve approximately 75% weight reduction and 90% volume reduction of input wastes.
- Minimise the volumes of residues to landfill and hence the environmental impact of landfill.
- Reduce UK greenhouse gas emissions.

It needed to be explained here, that in many counties the bottom ash from waste-to-energy plants is used in building roads and in several types of construction materials. In Germany 60% of waste-to-energy bottom ash is used as material for road base or in highway sound barriers. The Netherlands uses more than 90% of the bottom ash as road base and to make concrete products (Integrated Waste Service Association (1997/98)). Note, that such beneficial use of the ash further saves on landfill space.

Gasification is a thermal upgrading process in which the majority of the carbon in waste is converted into the gaseous form, leaving an inert residue, by partial combustion of a portion of the fuel in the reactor with air, or with pure oxygen.

Relatively high temperatures are employed, 900 – 1100°C with air and 1000 – 1400°C with oxygen (Whiting (1999)). Air gasification as show in figure 4.2 is most widely used technology forming a low heating value. Figure 4.2 shows that gasification process transfer the energy content of the waste into the gas phase as chemical energy which can be re-employed as chemical feedstock or as power via additional processing.

Pyrolysis is the thermal degradation of hydrocarbons materials at temperatures between 400 and 800°C (Rampling 1993)) in the absence of oxygen such that gasification does not occur as indicated in figure 4.2. Such processes devolatilise and decompose solid organic material by heat without combustion occurring. The products of this process include gas, liquid and solid char with the relative proportions of each depending on the method of pyrolysis and the reaction parameters, such temperature and pressure.

All these lead to a conclusion that thermal conversion waste-to-energy offer a means of energy production from renewable sources and potentially attractive method of waste disposal with limited environmental impact. It needs to be explained here that the present investigation is focussing on combustion process.

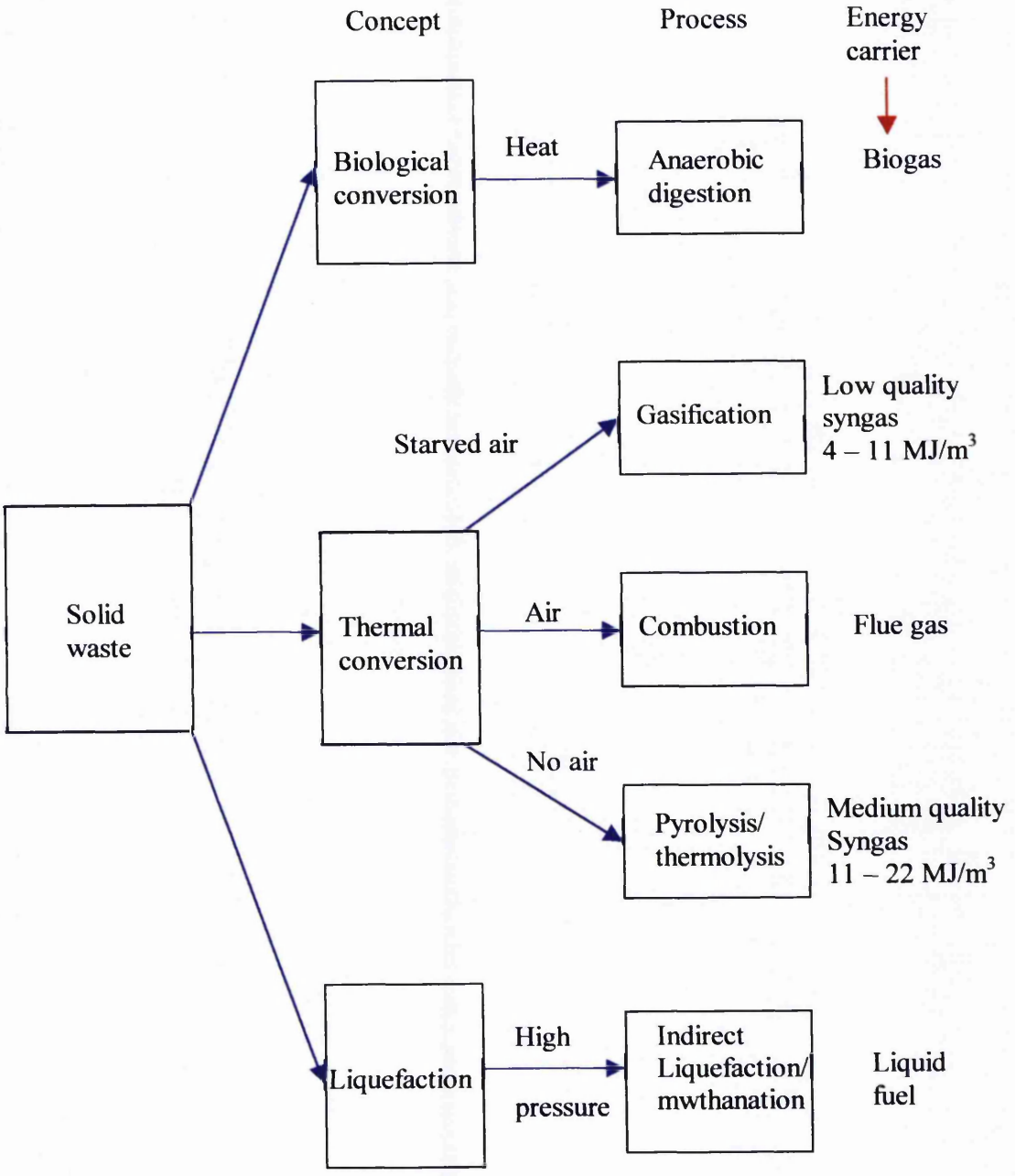

Figure 2. 4 Energy conversion options for solid waste
Based on Whiting (1999)

While there are several barriers that have contributed to a low rate of waste-to-energy in the UK, it is encouraging to note that the implementation of Non-Fossil Fuel Obligation (NFFO) schemes in 1990 has led to a net increase in waste-to-energy

JOHN RYLANDS
UNIVERSITY
LIBRARY OF
MANCHESTER

facilities in the UK. The next section describes some of the most important measures which were taken by the UK Government under the NFFO schemes to encourage waste-to-energy conversion.

2.6 The effect of non-fossil fuel obligation schemes on energy recovery

As a basis for subsequent discussions, it is noted that the UK Electricity Act (1989) makes provision for the Secretary of State for Trade and Industry to place an NFFO on any or all of the Regional Electricity Companies (RECs). This obliges the RECs to take a certain proportion of electricity generated from non-fossil fuel sources such as those listed in table 2.3. This obligation, in the context of waste, applies to the recovery of energy from waste via, for example, waste thermal reactors, gasification, pyrolysis or the combustion of landfill gas for electricity generation or combined heat and power (CHP) schemes.

Under this NFFO, the RECs are required to purchase electricity from waste-to-energy facilities at a price equal to the "utility's avoided cost". In this context, the utility's avoided cost refers to the overall disposal costs which local authority would pay if it were to use another alternative method such as landfill. The overall cost will include, for example, the costs of collection, transportation and other service charges. Consequently, electricity prices paid by the ERCs under the NFFO are higher than those from coal, oil and gas generated electricity. This economic incentive, supported by freedom from the fuel levy for NFFO facilities, has resulted in a significant increase in the number of waste-to-energy facilities in the UK since the 1990's. A breakdown of the first two renewables order under the NFFO is shown in table 2.3

Table 2. 3 Energy from waste projects accepted under the 1990 and 1991 renewables tranches

Project Type	No of projects	Total declared capacity (MW)
NFFO 1 (1990)		
MSW Combustion	4	41
Poultry Litter	2	25
Scrap Types	1	20
Landfill gas	25	36
NFF0 2 (1991)		
MSW Combustion	10	261
Poultry Litter	1	9
Scrap Types	1	8
Other waste combustion	2	13
Landfill gas	28	48
Totals		
MSW Combustion	14	302
Poultry Litter	3	34
Scrap Types	2	28
Other waste combustion	2	13
Landfill gas	53	84
Cumulative Total		
Energy from waste schemes (excluding sewage and slurry digestion)	74	**461 MW**

Source. ENDS Report No 265, February 1997.

In order to encourage the development of waste-to-energy technology, the UK NFFO scheme has been designed to provide an initial guaranteed market up to 2016 (ENDS Report No 265 (February 1997)). This is in the expectation that once waste-to-energy techniques are fully established, and become more competitive with fossil fuel

JOHN RYLANDS
UNIVERSITY
LIBRARY OF
MANCHESTER

generated forms of electricity, the techniques will become economically viable without further financial support.

Moreover, while the concept of waste-to-energy appears to be gaining support from the environmental legislators (Guidance Note S2 5.01 (1996)), it is also noted that the implementation of the 1999 EU Landfill Directive has created some uncertainty about the future of landfill gas utilisation for electricity generation. Thus, the Landfill Directive may also make the use of thermal (incineration with energy recovery) methods for the disposal of organic waste more attractive.

Figure 2.5 illustrates the energy potential of various waste streams in the UK. From this, it can be seen that industrial, commercial and municipal solid waste represents a potentially significant renewable energy resource. In fact figure 2.5 show that the 15 million tonnes of commercial and industrial waste disposed of annually in the UK could provide an energy value equivalent of 15 million tonnes of coal, while the 20 million tonnes of municipal solid waste could provide an energy value of equivalent of 6.5 million tonnes of coal. However, there is still some uncertainty about the possible effects of recycling schemes on the heating value of industrial, commercial and municipal solid wastes.

Section 2.7 therefore discusses the possible effects of recycling schemes with particular reference to their potential impact on the heating value of municipal solid waste.

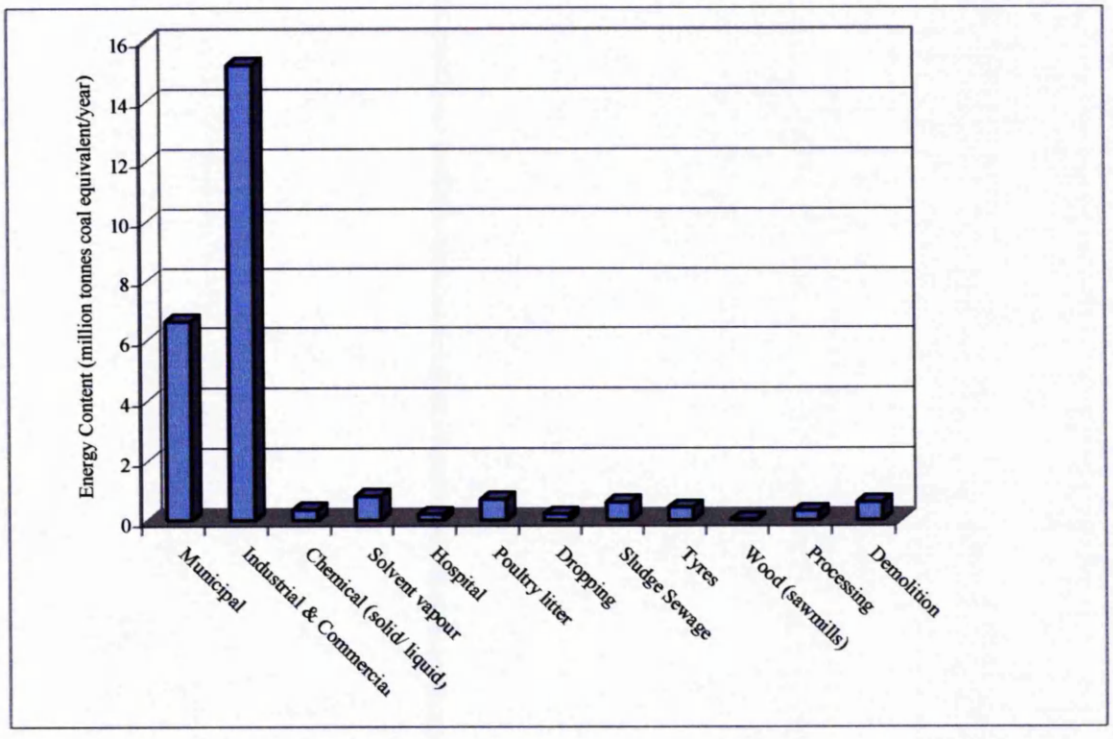

Figure 2. 5 The potential of various waste substances for energy recovery

Source. DoE Waste Management Paper 1 (1992)

2.7 Effects of recycling schemes on the heating value of MSW

There has been concern that recycling schemes may reduce the calorific value of municipal solid waste and adversely affect the potential for energy recovery of large-scale waste-to-energy facilities (Recycling Waste Management Paper 28, 1992). Contrary to the above concern, a study by Brereton (1996) found that recycling programmes have resulted in an increase in the net heating value of MSW by approximately 9% since the implementation of "section 49" of the UK Environmental Protection Act (1990).

This author pointed out that the increase in the net heating value results from the removal of a substantial fraction non-combustible waste with a low heating value from the MSW mix.

Barton (1988) also observed that, if separation systems capable of removing non-combustible materials such as glass and metals as discussed in section 2.4 could be adopted, then the net calorific value of the MSW would increase as heat losses to the ash during combustion of the remaining refuse are reduced.

To reinforce the above observations, Stessel (1996) pointed out that plastics in waste include low-density polyethylene, high-density polyethylene, polystyrene, polyvinyl, polyester, alkyds, epoxies, melamine, and urethane foam. Considering this complex mixture of plastics in the waste stream and as shown in figure 2.6, it is assumed that a complete removal of plastics in the waste stream would not be economic. Based on observations in figure 2.6, it is appropriate to conclude that the percentage of plastic material in municipal solid waste stream will increase. It is estimated that each household in the UK is producing 2.4 kg per annum (Environmental Statistics No 20 (1998)). Wolpert (1994) also observed that the gross calorific value of MSW, which is typically 9.7 MJ/kg, is already boosted by 4% of plastic film at 27 MJ/kg and 4% dense plastic at 30 MJ/kg.

Regarding the level of plastic material in municipal sold waste stream, it is interesting to note that the present study has confirmed that the level of plastic material in dRDF is relatively high. Figure 2.6 presents a photograph of the plastic materials which were removed during the preparation of the dRDF fuel pellets by the author.

Figure 2. 6 Plastic materials removed from dRDF pellets.

On the basis of the above observations, there seems to be no evidence that the viability of energy recovery from the combustion of municipal sold waste, and especially dRDF, would be adversely affected by an increase in recycling activities. Furthermore, considering that there appears to be no secure and stable market for most recycled products, it is unlikely that recycling activities would adversely affect the energy recovery potential of large-scale waste-to-energy facilities.

2.8 Combustion conditions for waste reactors

According to the EU Directives, 89/429/EEC and 2000/76/EC on the combustion of waste, the following combustion conditions must be satisfied:

i. the minimum oxygen level in the gases within the combustion chamber should be 6%;

ii. the maximum carbon monoxide level in the fluid gases should be 100 mg/Nm^3;

iii. the maximum organic compounds expressed as carbon in the combustion gases should be 20 mg/Nm^3;

iv. the combustion gases in the combustion chamber must be kept at temperature of at least 850°C for two seconds or more in the presence of at least 6% oxygen.

The above conditions are the minimum requirements to ensure satisfactory thermal destruction of the products of incomplete combustion. In accordance with these combustion requirements, as set by EU Directives 89/429/EEC and 2000/76/EC, modern MSW reactors therefore usually incorporate at least one specially designed afterburner. This burner is switched on automatically when the temperature of the combustion gases after the last injection of combustion air falls below 850°C or 1100°C if hazards waste with a content of more that 1% of halogenated organic substances, expressed as chlorine are incinerated (EU Directive 2000/76/EU). This burner is also used during plant start-up and shut-down operations in order to ensure that the temperature of 850°C or 1100°C as the case may be is maintained at all times during these operations and as long as unburned waste is in the combustion chamber.

Note, that three important factors must be fulfilled to ensure the effective destruction of products of incomplete combustion. These are high temperatures, turbulent airflow conditions, and a sufficiently long gas-residence time.

Here, however, it is noted that a comprehensive definition of the gas-residence time is still lacking in the environmental legislation.

In particular, it is not made clear whether the two seconds minimum gas-residence time applies to the average residence time in the high temperature zone under the worst furnace condition, or the minimum time spent by the gas in the high temperature zone.

The increased environmental concern over the emissions from the combustion of solid waste has, over the past few years, stimulated the development of more accurate techniques for measuring gas-residence times in waste reactors. Since this controlling factor is so relevant to the present investigation, section 2.9 discusses modern techniques which are used to assess the gas-residence time in practical waste reactors.

2.9 Gas-residence time as applied in waste reactors

The new Directive 2000/76/EU on the combustion of waste makes the same provisions for the operating conditions as the previous Directive 89/429/EEC. Before emergence of the new Directive, existing waste reactors which were commissioned before the 1st December 1996 were often granted an exception with regard to the two seconds requirement in their authorisation under the integrated pollution control scheme. In contrast, the new Directive imposed the gas-residence time requirement on existing, as well as new plants.

At the present time, the gas-residence time is calculated according to BS 3316, Part 2, 1987. According to this standard, the residence time is given by the equation

$$G_{RT} = \frac{V}{V_1} \qquad 2.1$$

where G_{RT} = gas residence time

V = volume of the reactor

V_1 = volumetric flow rate of the gas

It should be realised that this equation represents the ideal case of a plug flow reactor, where it can be assumed that every elemental volume of the gas will spend the same time in the reactor. However, in practice, real flows never satisfy these conditions because of the superimposition of boundary layers and separation which produce much more complicated flow patterns. Such real flow effects lead to channelling, internal re-circulation, and the presence of stagnant flow regions.

Previous studies have shown that calculating the gas-residence time according to BS 3316 Part 2, 1987 often over estimates the real residence time (Nassezabeh et al (1995)). Consequently, the Environment Agency now recommends the application of computational fluid dynamics (CFD) to assess gas-residence times in waste reactors (IPC Guidance Note S2 5.01 (1996)).

With particular reference to the application of CFD in municipal waste reactors, Nassezabeh et al (1995) explained that the gas-residence time is normally measured by injecting a tracer such as helium gas, mercury vapour, sulphur compounds or radioactive material at a secondary air entry. The time required for the tracer to pass through the system is determined by analysing the concentration of the tracer at the exit as a function of time. At the very least, such an approach can be expected to take into account the real flow effects such as channelling, internal re-circulation and the presence of stagnant regions.

2.10 Concluding remarks

This chapter has discussed some aspects of waste treatment which underlie the present project. In particular, the following features have identified:

- The proportion of its energy produced by the UK from waste is very low in comparison with other European states as shown in figure 2.3.
- The UK commits a high proportion of its waste to landfill as shown in figure 2.3.
- The UK Government is taking active steps to encourage waste-to-energy conversion through its recent legislation as discussed in chapter 1.
- The varied composition of municipal waste creates major problems for any attempt at recycling, particularly with regard to plastic as shown in figure 2.6.

Chapter 3 Legislation controlling the combustion of waste

3.1 Principal regulations

To ensure that the waste industry in the UK complies with the relevant European Union (EU) Directives, the UK Government has published Guidance Notes (S2 series) for processes subject to Integrated Pollution Control (IPC). The S2 Series Guidance Notes supersede Her Majesty's Inspectorate of Pollution Chief Inspector's Guidance Notes IPR types, published in May 1992.

The new series of guidance notes are listed in table 3.1. Note S2 1.05 is of particular interest in the present investigation. The S2 series covers the burning of solid fuel manufactured from waste, or comprising waste in an appliance with a net thermal input of 3 MW or more. Particular reference will be made to the extraction of energy from waste schemes using refuse derived fuel (RDF), wood, treated wood, straw, poultry litter and tyres as given in table 2.3.

In the context of IPC Guidance Note (S2 series), the term "thermal input" describes the rate at which fuel can be burned at a maximum continuous rating (MCR) multiplied by the net calorific value of the fuel. This is expressed as megawatts thermal (MW (th)).

As a basis for subsequent discussion, of the approximately 35 million tonnes per year of waste from household and commercial sources produced in the UK, some 65 000 tonnes per year is converted to RDF and used for power generation (Guidance Note S2 1.05 (1996)).

Although this represents only 0.2% of the total production, in terms of quantity, this represents a very large volume and could contribute a significant percentage of the pollutants derived from the processing plants. Therefore, to avoid increasing the net

environmental burden from energy processing plants, Her Majesty's Inspectorate of Pollution has published achievable targets for various types of fuel from waste. Table 3.2 summaries the major substances and their achievable values.

Table 3. 1 Guidance notes issued for combustion processes

S2 Series	Process and Plant Capacity
S2 1.05	Combustion of fuel manufactured from or comprised of solid waste in appliances 3 MW (th) and over
S2 1.04	Waste and recovered oil burners 3 MW (th) and over
S2 1.12	Reheat and heat treatment furnaces 50 MW (th) and over
S2 1.03	Compression ignition engines 50 MW (th) and over

Source. Guidance Notes (S2 series 1996)

Table 3. 2 Achievable substance releases to air

Substance	mg/Nm^3					
	RDF	Tyres	Poultry litter	Clear wood	Treated wood	Straw
Total particulate matter	25	25	25	25	25	25
Hydrogen chloride	30	10	30	-	30	30
Hydrogen fluoride	2.0	-	-	-	-	-
Oxide of sulphur (as sulphur dioxide)	300	300	300	300	300	300
Oxide of nitrogen (as nitrogen dioxide)	300	150	300	300	300	300
Carbon monoxide	100	50	200	100	100	250
Dioxins and furans (ng/m^3)	0.1- 0.5	0.1- 0.5	0.1- 0.5	0.1- 0.5	0.1- 0.5	0.1- 0.5
Mercury	0.1	0.1	0.1	-	0.1	-
Cadmium	0.1	0.1	0.1	-	0.1	-
Arsenic, chromium, copper, lead, manganese and nickel	1.0 Total	1.0 Total	1.0 Total	-	1.0 Total	-
Formaldehyde	-	-	-	-	5	-
Hydrogen cyanide	-	-	-	-	5	-

Source. Guidance Notes (S2 series 1996)

The combustion of solid fuel such as RDF will also release significant effluents to water and produces solid residues which must be disposed to landfill. In practice, the discharge of effluents to water will be limited to boiler blow-down, boiler water

treatment and occasionally, to maintenance discharges during maintenance operations. According to the Guidance Note S2 1.05, when effluents from the combustion processes plant are released to controlled water and sewers, continuous measurements should be made of the following parameters:

i. volumetric flow rate
ii. pH
iii. temperature
iv. oxygen demand
v. toxic metals
vi. grease and oils
vii. suspended solids.

In addition to the regular monitoring carried out by the operator to demonstrate compliance with the set limits, the operator is expected to ensure that a full analysis is carried out covering a broad spectrum of substances. This must be performed at regular intervals.

The procedures for enforcing the overall regulations covering the combustion of waste involve several government organisations. For example, public authorities exercise control measures over the operation of incinerators in three ways.

i. The Waste Regulation Authorities are responsible for enforcing the waste management regulations. For example, where controlled waste is finally disposed of to landfill, the applicant must advice HMIP which, in turn, is required to notify the Waste Regulation Authorities for the area in which the process is located. Applicants should be aware that Waste Regulation Authorities will wish to be satisfied that the analyses are sufficient to ensure

that wastes are acceptable under the terms of the waste management licence of the disposal facility and fulfil the description requirement of the Duty of Care.

ii. The Health and Safety Executive (HSE) must ensure that the incineration processes are operated in such a way as to protect personnel at work as well as the environment. This organisation also ensures that conditions in the authorisation of a process do not impose any requirements which would put at risk the health, safety or welfare of personnel at work

iii. The National River Authority (NRA) is responsible for processes which involves the discharge of any effluents to controlled waters. The inspector must ensure that their minimum requirements are met by the authorisation conditions.

At European Union level, all the processes involving the combustion of solid fuel manufactured from, or comprising, municipal solid waste are subject to the requirement of EU Directives 89/369/EEC, 89/429/EEC and 2000/76/EU. UK Directive EPA 1990 implements the provisions of Directive 89/369/EEC in England and Wales.

Since the UK is a Member State of the European Union, it is considered appropriate to discuss the influence of the EU Directives on the incineration of municipal solid waste. This topic is therefore considered in section 3.2.

3.2 EU legislation on municipal solid waste reactors

The emissions from waste incinerators, and especially the emission of grey or black smoke, led to strong public opposition to the use of incineration in the late 1970s and

early 1980s. As a direct result of this, 1989 saw the introduction of the EC (subsequently EU) Directives 89/369/EEC and 89/429/EEC and the closure of a number of old incineration plants in the UK. Council Directive 89/429/EEC on the reduction of air pollution from existing municipal waste incineration plants entered into force in all Member States by 1st December 1990.

The first of these Directives (89/369/EEC) sets out air emission limits for acid gases, dust and heavy metals which must be achieved by all new plants. The second Directive (89/429/EEC), which was applied to all existing waste incinerators, set lower limits for these substances and required that all such plants be upgraded to achieve the limits shown in table 3.3 for new plants by 1st December 1996. Surprisingly, no specific limits were set for the emission of dioxins. Instead combustion conditions of at least 850°C for a minimum of two seconds in the presence of at least 6% oxygen were specified to minimise the products of combustion especially the level of dioxins and furans. Alternatively, other appropriate control techniques could be employed to reduce the level of dioxins and furans, subject to the necessary approval from the competent authorities.

Despite the implementation of these EU Directives, the public still tends to reject the use of the waste-to-energy option as a basis for reducing the net environmental burden from both the energy and waste management sectors. This rejection appears to stem from the fact that the combustion of waste is known to be a major potential source of the dioxins which are so widely feared by the general public.

It is known that dioxins and furans are most likely to be formed after incineration during the flue gas cooling, and treatment processes, because of the large drop in the flue gas temperatures which occur there. The critical operating window for cooling

and treatment of the flue gases is between 450°C and 200°C (Paul and Ellen Connett (1994)), Chagger et al (1998), Guidance Note (IPR 5/3 1992)). According to this Guidance Note, the formation of dioxins and furans can be avoided by cooling the gases rapidly through this critical temperature range. Such cooling may be accomplished by the use of a heat exchanger, regenerative boiler, or by water spray cooling.

In modern waste incinerators, it is required that the waste should not be fed to the plant at start-up until the auxiliary burners or after burners have heated the combustion zone to 850°C as discussed in section 2.8. This temperature is clearly well above the temperature range at which the formation of dioxins is likely to occur. Also, the fact that the new Council Directive 2000/76/EU article 11 requires continuous monitoring of temperature near the inner wall of the combustion chamber indicates a strong determination to minimise the formation of dioxins and furans during the waste incineration.

All of these factors lead to the conclusion that the emission levels of dioxins from waste incineration plants can be below the achievable levels presented in table 3.2 if the best available control techniques are employed.

The public concerns regarding the emission of dioxins from waste plants have been noted by a number of authors including Elliot et al (1998), Rappe et al (1985), Chagger et al (1999) and Williams (1992). It is therefore appropriate to review the effects of dioxins on public health.

3.3 Dioxins and risks to human health

The main obstacle to the development of waste-to-energy systems in most communities appears to be the public perspective about the environmental and health consequences to the community living close to such plants. For example, between 1982 and 1990, a total of 248 waste-to-energy projects were cancelled in the USA, most of these cancellations were because of public opposition (Curlee et al (1994)).

Public concerns regarding the emission of dioxins appear to stem from the fact that MSW contains a high percentage of plastics as illustrated in section 2.7. However, a majority of the scientific reports on the subject reject both the notion that plastics make a significant contribution to the production of dioxins and the assertion that the conversion of waste-to-energy contributes a significant percentage of dioxins (Curlee et al (1994)).

In a recent development, a report of the Committee on Carcinogenicity (COC/2000/S1) set up by the UK Department of Health, investigated the incidence of cancer in over 14 million people living near to 72 solid waste incinerators in Great Britain. The analysis showed that there was no evidence of adverse health effects being caused by emissions from such plants.

Elliott et al (1996) conducted a similar investigation. The population living in areas within 7.5km from MSW incinerators were examined and all the incinerators starting before 1976 were included. Significantly, these authors could find no evidence for the decline in risk with distance from the incinerators. Nor did this study find any link between cancer and the emissions from the waste incinerators.

In a similar study, Elliott et al (1998) investigated public concern in two Canadian population samples living in areas close to municipal solid waste incinerators. The results of this investigation showed a relatively low level of impacts reported in both incinerator communities, contrary to what might be anticipated on the basis of reading the very common line of argument to be found in the popular press, sometimes referred to as "Not In My Back Yard" (NIMBY) literature. The fact that the investigation by Elliott et al (1996) centred on older incineration plants, and the finding that the combustion of waste could not be linked to health problems, should surely increase the environmental desirability of modern waste-to-energy plants since these incorporate even more design features to minimise the level of emissions.

As a basis for subsequent discussion, a dioxin emission limit of 1 nanogram per cubic meter (ng/m^3) is imposed on all waste reactors by HMIP as shown in table 3.3. Interestingly, the Committee on Carcinogenicity report found that, in practice, most existing waste reactor plants are already achieving dioxin emission levels close to $0.1 ng/m^3$. Thus, they are operating at a level 90% below the specified threshold.

The Committee on Carcinogenicity also noted that, because of these tighter emission limits, the conversion of waste-to-energy would contribute less than 1% to a person's normal dioxin intake from typical "background" levels if operated to the new standards. Considering the evidence that there is no link between the emissions from waste reactors and public health, the obvious conclusion to be drawn is that a large fraction of municipal waste should soon be diverted from landfill and used as fuel in waste-to-energy plants.

The growing shortage of landfill sites close to areas of solid waste generation which is a problem especially in big cities, is expected to stimulate the rapid development of

waste-to-energy plants in many communities. This is in line with current pronouncements by UK Government authorities, such as the Environmental Agency, that the amount of waste incinerated in the UK should be doubled by 2003 and should reach 10 million tonnes per year by 2010 DETR (1999). Also, considering the fact that the new EU Landfill Directive requires a higher proportion of biodegradable waste to be diverted from landfill over the next 20 years, there is no doubt that the conversion of waste-to-energy will soon play a major role in waste management.

3.4 New EU Directive on combustion of waste

The waste incineration industry in the UK operates in a rapidly changing environment due to recent control measures initiated by the EU.

However, perhaps the EU Directive's biggest impact on municipal incineration, in the UK is to place tighter controls on N0x emissions. The new Directive (2000/76/EC), dealing with the reduction of air pollution from municipal waste incineration, is the first EU Directive to set emission limits for nitrogen dioxide.

Article 21 of this Directive requires all Member States to bring into force the laws, regulations and administrative provisions necessary to comply with this Directive not later than 28th December 2002. The Directive defines air emission limits for nitrogen dioxide of 200 mg/m^3. This compares with the UK national limit of 300 mg/m^3 currently in force as shown in table 3.3.

Interestingly, the 1989 EU Directives dealing with the reduction of air pollution from municipal waste incineration did not set limits for the emission of dioxin. However, the new Directive sets a limit of 0.1ng/m^3 dioxin for all incineration and co-incineration plants. This again compares with a limit of 1 ng/m^3 set in the UK for all

types of incineration plant. According to the ENDS Report No 285 (1998), modern waste reactors in the UK now incorporate more design features to minimise the level of emissions. As a result, it is unlikely that the newly specified limits will force the closure of incineration plants in the UK.

The new Directive is designed to replace EC (subsequently EU) Directive 89/369/EEC and 89/429/EEC on the prevention of air pollution from new and existing municipal waste incineration plants.

Considering the need for tighter control on the emission of nitrogen dioxide from waste reactors, it is obvious that the measurement and monitoring of $N0_2$ produced during the co-combustion of dRDF and coal must be of considerable a practical interest. Since this is the principal area of study in the present investigation, considerable attention has been paid to this aspect of the problem. Chapter 6 therefore describes the major experimental tools and supporting systems used to measure $N0_2$ concentration in the project described in this thesis.

Prior to the investigation of $N0_2$ concentration, it is appropriate to review factors influencing the formation of this gas during the combustion of solid fuel such as dRDF. Then, the methods employed to reduce this formation will be discussed. This is done in chapter 4.

Table 3. 3 Comparison between the emission limits set by EC Directives and the HMIP Standards

Plant size (tonnes/hour)	EC Directive 89/429/EEC (applied to existing plants) (1989) mg/Nm^3		EC Directive 89/369/EEC (applied to new plants) (1989) mg/Nm^3		HMIP Standards IPR 5/3 applied to new and existing plants (1992) mg/Nm^3	EU Directive 200/76/EU (applied to new and existing plants) daily average) (2000) mg/Nm^3	HMIP Standards S2 1.05 Applied to new & existing plants (1996) mg/Nm^3
	e < 1	**1 < e < 6**	**e < 1**	**1 < e < 3**	**3 tonnes/hour**	-	-
Total particulate matter	600	100	200	100	30	10	25
Carbon monoxide	100	100	100	100	100	50	100
Volatile organic compound (excluding particulates, expressed as total carbon)			20	20	20		
Oxide of sulphur (as sulphur dioxide)				300	300	50	300
Hydrogen chloride			250	100	30	10	30
Hydrogen fluoride				4	2	1	100
Oxide of nitrogen (as nitrogen dioxide)					350	200	300
Cadmium & Mercury				0.2	0.1 each	0.05	0.1 each
Arsenic & nickel				1	1		
Other metals[b]				5	1	0.5	1
Dioxins and furans (ng/m^3)					1[c]	0.1	0.1 – 0.5

Sources. Royal Commission on Environmental Protection, 17th Report 1993, Institute of Waste.
Official Journal of the European Communities, December 2000.

Key

[b] = Total of chromium, copper, lead and manganese plus (in the HMIP standard but not in the EC directive) tin.

[c] = HMIP's guidance note says that the emission of dioxins should be reduced as far as possible by techniques with the aim to achieving a guide value of 0.1 nm/Nm^3.

e = Plant size (tonnes/hour)

Chapter 4 The significance of nitrogen dioxide

4.1 Permissible level of nitrogen dioxide

In the UK, the permissible $N0_2$ emission levels produced by waste thermal reactors are being gradually reduced from 400 mg/m^3 to 200 mg/m^3 (ENDS Report No 285 (1998), Gerstrom et al (1999)). This reduction of $N0_2$ emission levels is necessary to comply with the new EU Directive 2000/76/EC. This is the first Directive on the combustion of waste to prescribe emission limits for the $N0_2$ produced by the combustion of solid waste. Because of the legislative pressures to reduce the $N0_2$ emission levels produced by waste reactors and, particularly, waste-to-energy plants, it is apparent that measurements of the gaseous emissions due to the combustion of waste are important. This is the origin of the present investigation. Prior to the measurement of these $N0_2$ emission levels, however, the factors which influence the formation of $N0_2$ during the combustion process will be discussed.

4.2 Sources of $N0_2$ during the combustion process of MSW

There are three mechanisms for the production of $N0_2$ emissions during the combustion process of municipal solid waste (MSW). These are referred to as thermal, prompt and fuel N0x and occur at different temperature levels during the combustion process.

Thermal N0x dominates at high temperatures and is strongly influenced by the oxygen concentration levels. In a situation where the combustion temperatures are above 1100°C, thermal N0x is dominating (Baukal and Romano (1992)). These same authors noted that prompt N0x is produced by the relatively fast reaction between nitrogen, oxygen and hydrocarbon radicals.

The hydrocarbon radicals are intermediate species, produced during the combustion of most solid fuels, and especially when the fuel contains highly volatile matter such as is the case for dRDF.

Prompt N0x dominates at lower combustion temperatures. However, in a conventional combustion system, prompt N0x accounts for approximately 10% (Swithenbank et al (1999)). In their investigation, these authors concluded that prompt N0x could be neglected as a significant contributor in waste reactors presumably because, in a full-size system, the combustion chamber will first be heated to a temperature in excess of 850°C before the waste is introduced into the combustion chamber. Note, here, that the exhaust gas should be subjected to a temperature above 850°C for at least 2 seconds in the presence of at least 6% oxygen concentrations to satisfy the requirements of the EU Directives (1989, 2000).

Fuel $N0_2$ is produced by the direct oxidation of organo-nitrogen compounds, contained in the fuel. In practice, $N0_2$ is not a concern for high-quality gaseous fuels such as natural gas or propane which normally have no organically bound nitrogen. However, fuel $N0_2$ is a problem for fuels such as fuel oil, coal and dRDF. Several authors, including Baukal and Romano (1992), Swithenbank et al (1999), have noted that the major source of this gas during the combustion of municipal waste is the nitrogen in the fuel which is estimated to represent between 0.4 to 0.8% by volume.

Considering these three mechanisms for the formation of $N0_2$, and the fact that the UK EPA requires waste reactors to achieve a minimum destruction removal rate of 99.99% (Oppelt (1989) and Liem and Wilson (1991)) – it is apparent that some correlation between the characteristics of the combustion processes and the formation of nitrogen dioxide will be unavoidable.

This is because, to achieve the levels of destruction and removal conditions specified in the UK EPA, waste reactors are often operated at elevated temperatures, high excess air and long residence times. Consequently, these combustion conditions favour the formation of nitrogen dioxide and especially, thermal $N0_2$ which is dominating at high temperatures. Despite this, several techniques to reduce the $N0_2$ emission levels in the exhaust gas stream have emerged. It is considered appropriate to discuss some of the most commonly used techniques.

4.3 Methods of reducing N0x from combustion of solid fuel

Several techniques are available to reduce the $N0_2$ emission levels produced by the combustion of solid waste. Firstly, the air can be replaced by oxygen in the combustion facility to reduce the $N0_2$ emission levels. This method also has the direct benefit that the destruction removal efficiency is increased. For example, a study by Baukal and Romano (1992) showed that the temperature of a conventional oxygen-enriched burner flame is 150°C to 200°C greater than the flame temperature for an air burner. Since replacing air with oxygen offers such clear environmental benefits, this method is becoming increasingly attractive to waste reactors used to process toxic substances or the incineration of contaminated waste containing dioxins. However, it is assumed that this method would not be cost effective for companies which handle municipal solid waste in large scale operations.

Waste management companies, which have incorporated a method of converting waste-to-energy in their systems, are now employing techniques to reduce N0x emission levels after the combustion stage. These options include selective non-catalytic reduction (SNCR), selective catalytic reduction (SCR), and wet technology.

Collectively, these are referred to as dry and wet techniques. Dry N0x reduction techniques, i.e. SCR and SNCR, largely depend upon the injection of ammonia (NH_3) to reduce the $N0_2$ emission levels. NH_3 reacts with the N0 and $N0_2$ present in the flue gas to form an intermediate stage compound which subsequently decomposes to nitrogen gas and water vapour. The overall reaction is given by the two equations:

$$4NH_3 + 4N0 + 0_2 = 4N_2 + 6H_20 \qquad 4.1$$

$$4NH_3 + 2N0_2 + 0_2 = 3N_2 + 6H_20. \qquad 4.2$$

The literature reveals that there is an operating window for SCR which is between 250°C and 500°C. This window will depend upon the specific catalyst employed (Gerstrom et al (1999) and Takacs and Moilanen (1991)). Regarding SNCR, the operating window is relatively narrow for the injection of NH_3, and is approximately between 870°C and 950°C (Gerstrom et al (1999) and Takacs and Moilanen (1991)). These authors also noted that, if injected at a temperature above 950°C, the NH_3 would oxidise to N0. Interestingly, dry N0x reduction techniques can reduce the N0x emission levels significantly typically by 35 to 45%.

Furthermore, the injection of NH_3 has been shown to inhibit the formation of dioxins in the cooler parts of the waste reactor (IPC Guidance Note S2 5.0.1 (1996)). It is noted that when hazardous waste with a content of more than 1% of halogenated organic substances is to be incinerated then the new EU Directive requires that the combustion temperature must be raised to 1100°C. This high combustion is generally achieved by employing special auxiliary burner(s). In a situation where afterburners are used, it is apparent that dry techniques would not be appropriate and there will be less opportunity to reduce the formation of dioxins in the cooler parts of the reactor.

Although there are significant environmental benefits to be derived from the use of ammonia injection, Takacs and Moilanen (1991) and Swithenbank et al (1999) have also observed that there are some associated operational problems. The major problem appears to be the need to achieve a uniform mixture of the NH_3 and the N0x over the entire cross section of the exhaust duct so that the chemical reactions can take place effectively. Any non-uniformity in the distribution of N0x across the exhaust duct ahead of the catalyst will create local regions of high or low NH_3/N0x ratio. These non-uniformities are assumed to continue into the active catalyst layers and can cause variations in the N0x emission levels and may lead to the presence of ammonia in the exhaust gases.

Such conditions would be highly undesirable because NH_3 adsorbs onto the fly ash, which is usually used in construction industry in many countries for example, in Germany, and the Netherlands (Rashid and Frantz (1992) and The Integrated Waste Service Association (1997 - 1998)).

Takacs and Moilanen (1991) further noted that a concentration of NH_3 greater than 5 parts per million could result in an ash with an objectionable odour. It is assumed that such characteristics would limit its use in the construction industry.

Another strategy which is receiving widespread attention is to modify the combustion process, for example, by the application of flue gas re-circulation (FGR), staged combustion, or water injection. According to IPC Guidance Note S2 5.0.1 (1996), the FGR has the potential to replace approximately 10% to 20% of the secondary air. The overall effect of applying this technique is to reduce the peak combustion temperatures. In turn, this helps to reduce the production of thermal N0x.

4.4 Techniques used to monitor $N0_2$ levels

The decision to make measurements of the $N0_2$ emission levels using an optical spectrometer stimulated the need to review other monitoring techniques. Several methods have emerged in recent years which enable nitrogen dioxide emission levels to be measured. For example, Gera and Gautam (1993) used the chemiluminescence technique to monitor the concentration of $N0_2$ produced during the combustion of different mixtures of RDF and coal. Beine et al (1999) employed the passive diffusion tube technique for measuring $N0_2$ emissions.

Although the use of these psuedo-chemical methods, and particularly that of the passive diffusion tube and chemiluminescence techniques, to measure $N0_2$ has grown in recent years, there are number of serious limitations of the techniques.

Beine et al (1999) showed that the passive diffusion tube technique overestimates the $N0_2$ concentration when compared with the value measured by chemiluminescence analysis by an average of about 30%. It is not known which of the two methods is more accurate.

The introduction of laser technology into the combustion and environmental engineering industries has enhanced the quality of data available to describe the generation of pollution. This is due to the high degree of sensitivity of laser based instrumentation when compared with the intrusive chemical sensor techniques.

Peng et al (1995) transmitted a laser beam through an ionised chamber containing a sample of air at atmospheric pressure to detect the presence of $N0_2$. Their measurements covered both the ultraviolet and visible regions from 224 to 230 nm and 448 to 460 nm respectively. In this investigation, a coumarin 47-laser dye laser

was used to cover the wavelength range from 448 to 460 nm, while measurements in the range 224 to 230 nm were obtained by frequency doubling the output of the dry laser. Frequency doubling is an optical techniques which enables a high power beam in the visible region to be shifted into the ultraviolet region.

In an entirely different approach, Brown et al (1991) employed pulsed photothermal laser deflection to measure the concentration of smoke and $N0_2$ in an exhaust duct. In their investigation, they used a broadband XeCl excimer laser producing light at 308 nm to pump a tunable dye laser operating at 451 nm. After the beam emerged from the sample cell, it was dumped into a calorimeter to measure the transmitted power. These authors showed that the pulsed photothermal laser deflection system demonstrated excellent sensitivity and good linearity down to $N0_2$ emission levels of 3 ppm. They also showed that the system performed well at levels as high as 200 ppm.

Although it appears that the used of optics in the measurement of pollutants has generally enhanced the quality of the available data, Peng et al (1995) showed that there is a serious practical limitation of these methods. When $N0_2$ gas is exposed to wavelengths shorter than 400 nm, it may dissociate to form N0 and atomic oxygen. This behaviour is expressed by the equation

$$N0_2 + h\lambda \rightarrow N0 + 0 \qquad 4.3$$

where Planck's constant $h = 6.626*10^{-34}$ J/s.

λ = wavelength of light (nm)

The potential for $N0_2$ to dissociate due to its exposure to ultraviolet light is very significant in the present investigation because of the particular optical method used. In another similar development, Davidson et al (1988) measured $N0_2$ emission levels

over the wavelengths 264 to 649 nm range using a 300W xenon arc lamp. In their findings, they noted that difficulties arose because of the dissociation of NO_2.

Considering the above observations, it is obvious that there may be major disadvantages if UV methods are used to monitor NO_2 emission levels because of the tendency of the NO_2 to dissociate below the wavelength of 400 nm. Further, examination of the literature has revealed that the actually threshold on wavelength for the dissociation of NO_2 gas is 397 nm (Zacharias et al (1990)).

As a result, the wavelength of 439.34 nm was used in the present investigation. It can be assumed that using the above wavelength to monitor the NO_2 emission levels produced during the co-combustion of coal and dRDF should not cause any errors due to dissociation.

There is one further influence which needs to be considered. This relates to the residence time for the exhaust gas at the sampling point. Since this is very short in the combustion apparatus which will be described, it is assumed that the dissociation process will be weak even below the threshold wavelength. However, during the calibration experiments which are described in chapter 6, dissociation of NO_2 was assumed to occur below the threshold wavelength since the residence times of the NO_2 samples in the calibration cell were then typically between 20 and 25 minutes.

The optical absorption method chosen to determine the concentration of NO_2 in the combustion chamber exhaust duct utilised a Xenon light source covering the UV and visible ranges. A detailed description of the mode of operation of this system, and its calibration, will be given in chapter 6.

Chapter 5 Optical techniques

5.1 The transmission of light through an absorbing medium

In the present investigation, an optical technique was used to monitor the $N0_2$ concentration levels during the co-combustion of coal and dRDF. This approach was selected because optical techniques, unlike other more intrusive techniques such as gas sampling tubes, are capable of withstanding hostile combustion conditions within the flue stack and achieve the sensitivity necessary for sampling low concentration of pollutant gases. Further, optical techniques do not disturb the characteristics of the fluid flow whereas the disturbance associated with gas sampling methods can often lead to uncertainties in the derived results.

Apart from the use of an optical method in the present investigation, it was important to emphasise that optical techniques can be used for a wide range of property measurements and in the control of combustion emissions. It was therefore considered appropriate to discuss optical measurement techniques in general, prior to the description of the particular system used in the present investigation.

All the optical techniques used in continuous emission monitoring (CEM) are based on principles associated with the interaction of the incident light with the gas molecules. In these CEM applications, the wavelength of the light used ranges from the ultraviolet to the infrared (Pavia et al (1996) and Jahnke (2000)). Figure 5.1 shows the regions of the electromagnetic spectrum, and the wavelengths where gas molecules are known to interact with the incident light energy.

These are the regions where optical instrumentation can be designed to measure the effects of these molecular interactions. The basic concepts of light as a form of energy and some of its principle characteristics will be discussed in the next section.

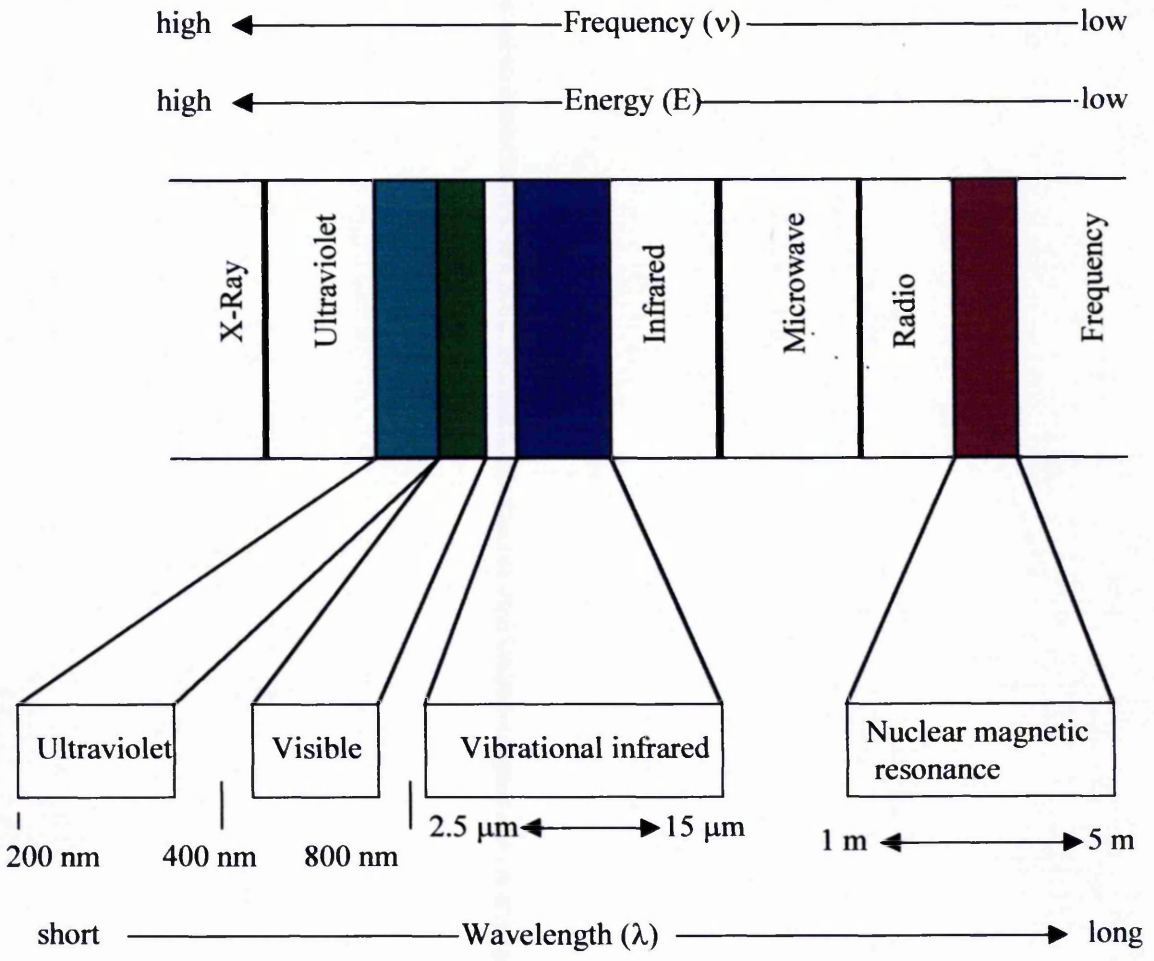

Figure 5. 1 Sections of the electromagnetic spectrum used for continuous emission monitoring systems.

Source. Based on Pavia et al (1996)

5.2 Light energy

Light is a form of energy which, in the most simple representation, can be shown as a travelling wave motion as shown in figure 5.2. This sine wave shows how the amplitude of the optical wave changes with time at any position along the path of the ray.

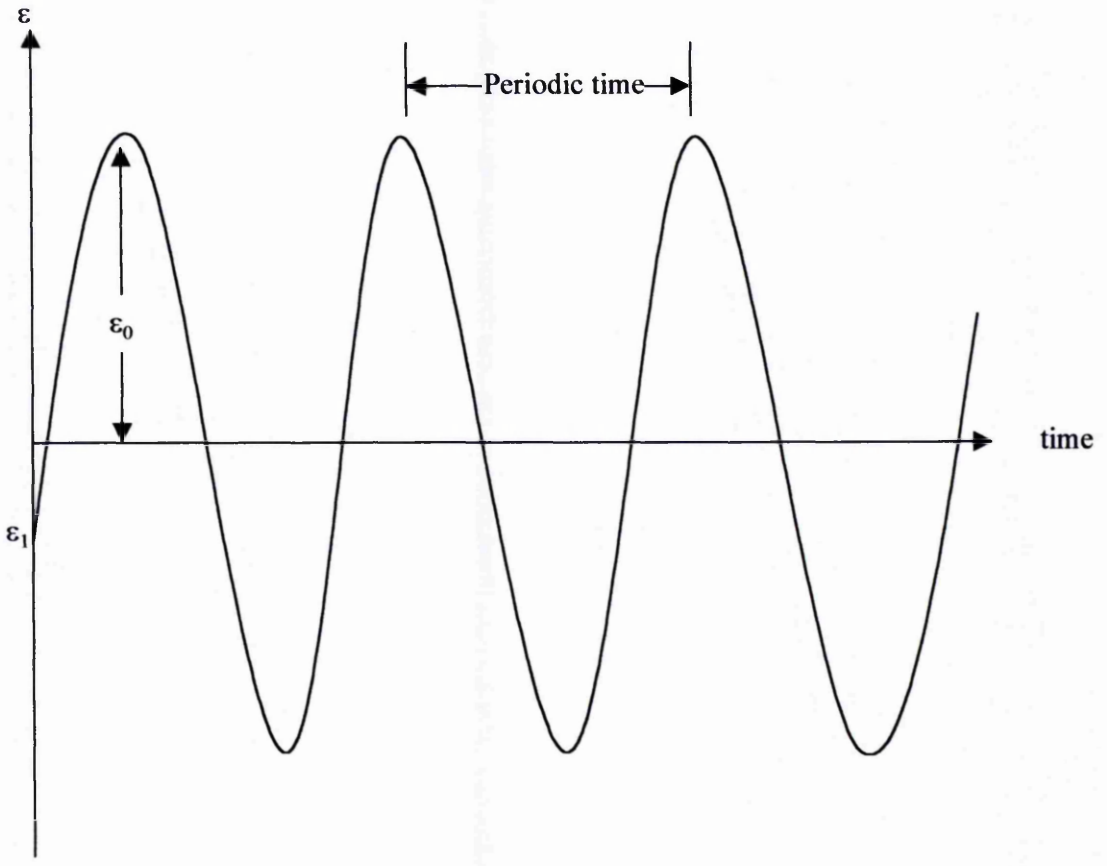

where ε_0 = the amplitude of the electromagnetic field

ε_1 = the field at the source

ν = frequency of the wave

$\frac{1}{\nu}$ = *periodic time*

Figure 5. 2 Representation of a light wave

Source. Based on Laufer (1996)

The frequency ν and wavelength λ of the optical wave are related to the velocity of propagation of light c in free space. The relationship is

$$c = \nu\lambda \qquad 5.1$$

where c the velocity of light in a vacuum.

The travelling wave shown in figure 5.2 is just a simple representation of the way in which electromagnetic radiation, and optical waves in particular, propagate. In certain situations, however, light behaves as if it were composed of discrete packets of energy called photons. Then, in a beam of light having frequency ν, each photon carries an amount of energy defined by the Einstein Planck relation (Laufer (1996)). This states that

$$e = h\nu = \frac{hc}{\lambda} \qquad 5.2$$

where h, known as Planck's constant, equals $6.626 * 10^{-34} \quad J/s$.

In a situation where a beam of photons is transmitted through a cell containing molecules or atoms that can exist at several well-defined energy levels, a fraction of the energy of each photon can be absorbed. It has been shown that the amount absorbed is proportional to both the density of the pollutant gas and the energy level of the photons. During the absorption process, the energy gained by the molecules causes these to be excited into a higher energy level (or state), as illustrated in figure 5.3. Here e_1 and e_2 represent the energy levels of the ground and final states respectively. The molecules raised to this excited state will be in an unstable condition and, subject to external influence, may revert back to the original ground state.

During this decay process, they must dispose of their energy to matches the energy difference ($e_2 - e_1$). These processes are represented schematically in figure 5.3 and are called absorption and spontaneous emission (Laufer (1996)).

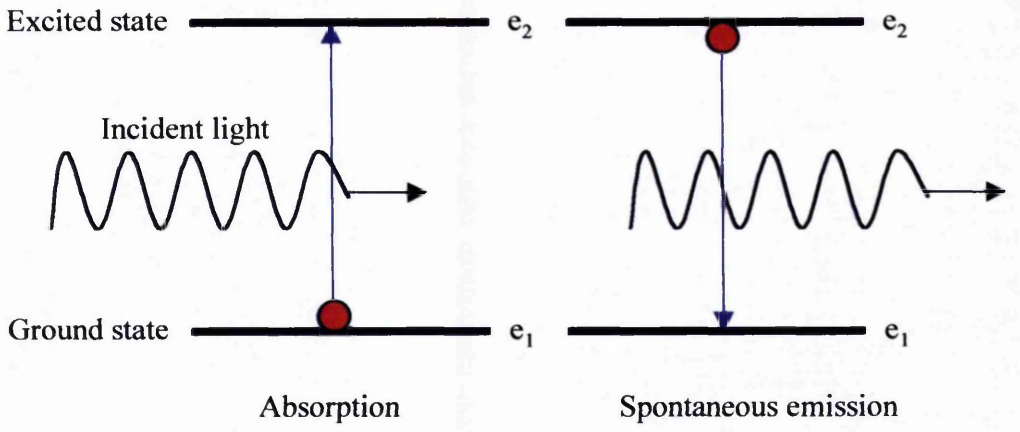

Figure 5. 3 Typical two level electron energy system
Source Based on Laufer (1996)

When the absorption takes place, the intensity of the incident light will be reduced from 100% to some value which depends both on the density of the photons and the gas molecules. Typical responses showing the reduction in the intensity of the transmitted light which occurs due to the interaction with the gas molecules, are shown in figure 5.4.

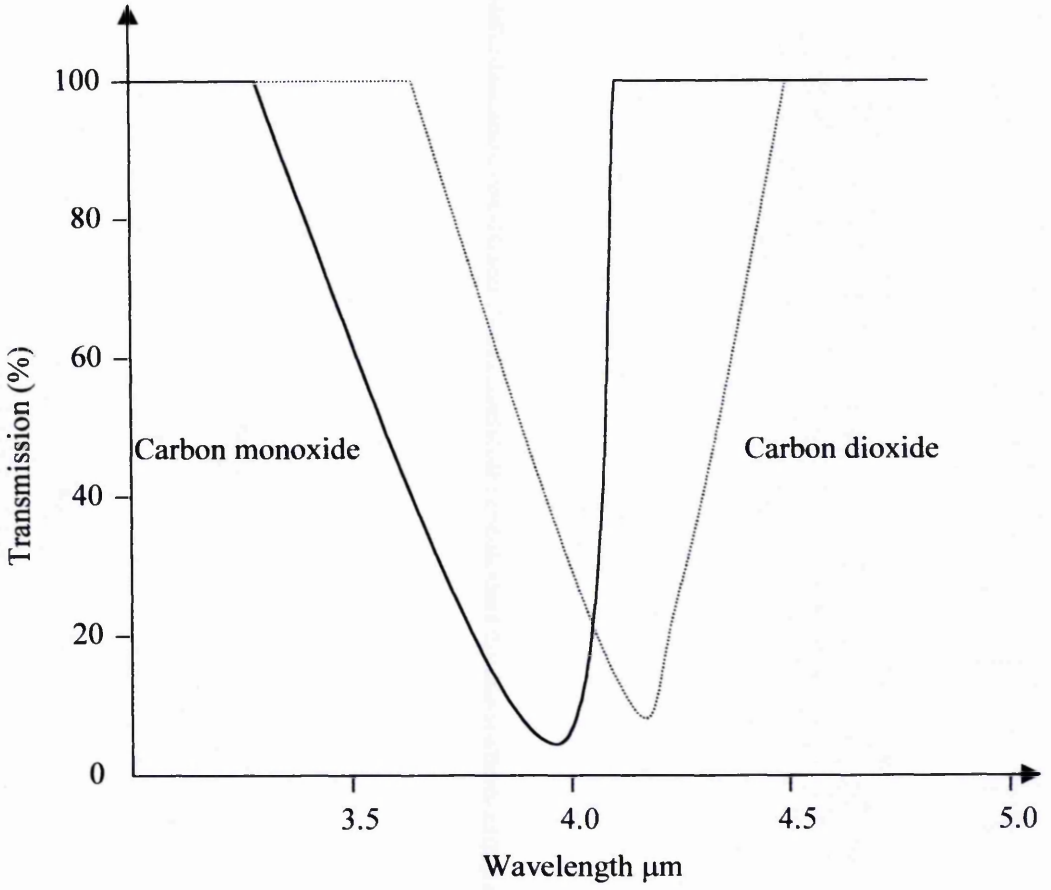

Figure 5. 4 A typical transmission spectrum

Source. Based on Parr (1995)

This figure shows a sharp fall in the intensity of the transmitted beam between 3.2 to 4.2 μm for carbon monoxide and between 3.75 and 4.45 μm for carbon monoxide. These reductions in the transmitted energy are associated with the absorption characteristics of the gas molecules and the parts of the transmission spectrum where light energy is absorbed most strongly are called the absorption bands for the particular gas considered.

The absorption characteristics can also be plotted in the form of an absorption spectrum as shown in figure 5.5. It is convenient to make use of the relationship between the fractional amount of light energy absorbed and the concentration levels of the absorbing gas. This relationship will be discussed in the following section.

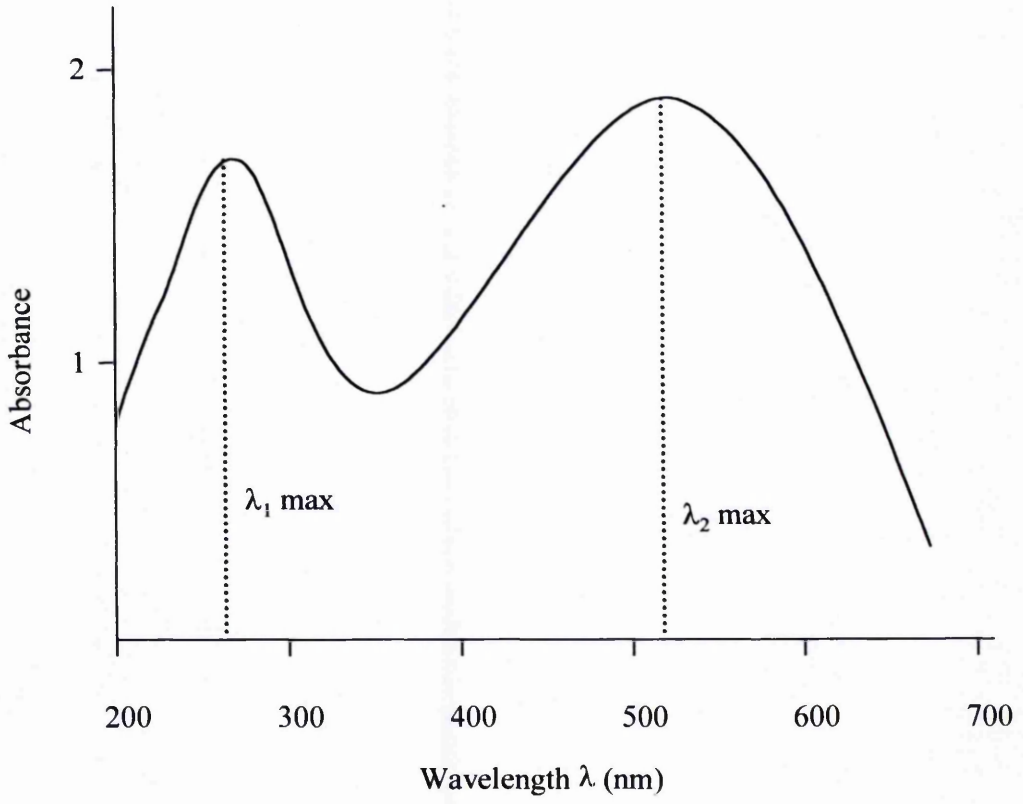

Figure 5. 5 A typical absorption spectrum

Source. Based on Harwood and Claridge (1997)

Note that absorbance (A) is the logarithm of the ratio $\frac{I_0}{I}$.

where I_0 = intensity of the light incident upon the gas element

I = intensity of the light at exit from the gas element

I0 and I are usually expressed as percentage. Note, that the intensity of the light incident upon the gas element is then 100%.

When half of the incident light is absorbed, then the intensity of the light at exit from the gas element is 50% and the expression for A is used

$$A = \log (100/50) = 0.301 \qquad 5.3$$

When 90% of the incident light is absorbed, I = 10% and

$$A = \log (100/10) = 1.0 \qquad 5.4$$

When 99% of the incident light is absorbed, I = 1% and

$$A = \log (100/1) = 2.0 \qquad 5.5$$

Note, as the intensity of the light at exit from the gas element decreases to zero than absorbance increases to infinity. The useful practical range, however is $0 < A > 1.0$ corresponding to $100\% > I > 10\%$ (Metcalfe (1994)) and (Andrews (1990)).

It can then be seen that figure 5.5 represent absorbance responses which are above the useful practical range. This theoretical data can be compared with the data in Appendix A, figures A.29 and 30 which show the absorbance signal plotted against the nitrogen dioxide concentrations for selected test run. The measurements in figures A.29 and 30 show the linear relationship between the absorbance and $N0_2$ concentration.

5.3 Relationship between absorption and the gas concentration

The Beer-Lambert Law is used to relate the amount of light energy absorbed to the concentration of the pollutant gas. To explain this relationship more clearly, consider figure 5.6 which shows the incident radiation, a cell contained the sample of gas, and the beam of transmitted light.

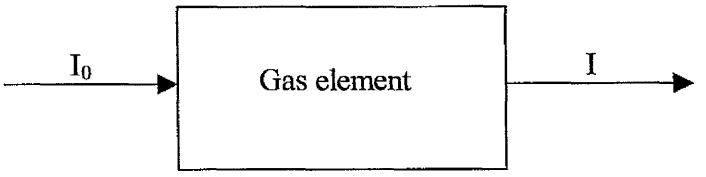

where I_0 = intensity of the light incident upon the gas element

I = intensity of the light at exit from the gas element

Figure 5. 6 A typical optical system for measuring the concentration of pollutant gases

Source. Based on The Royal Society of Chemistry (1995)

The Beer-Lambert Law states that the intensity of the light passing through any transparent medium decreases exponentially with distance and is dependent on the wavelength of the light and the gas concentration.

Thus, the factor $\alpha_\lambda Cp L$ is introduced and the expression for T_r is used

$$T_r = \frac{I}{I_0} = e^{-\alpha_\lambda Cp L} \qquad 5.6$$

is used where T_r = transmittance of the light through the gas element

I_0 = intensity of the light incident upon the gas element

I = intensity of the light at exit from the gas element

α_λ = molecular absorption coefficient (dependent on the wavelength λ)

Cp = concentration of the pollutant

L = distance the light beam travels through the gas.

The absorption coefficient α_λ is dependent on the wavelength of the light and on the molecular properties of the pollutant gas.

It is a quantitative expression of the degree to which a molecule will absorb light energy at a given wavelength. Thus, if no absorption occurs, α_λ will be zero, and the transmittance will be equal to 100% (as is shown in figure 6.152). Alternatively, if the electrons in a molecule make a transition from one state to another due to the influence of light of a certain wavelength then the absorption coefficient will have a non-zero value and the reduction of light energy through the gas element will depend on the pollutant concentration Cp and the path length L. Such a system is shown in figure 5.4

Many modern optical instruments employ this principle and are designed to measure pollutant gas concentrations. The principal requirement is for a light source which emits at a wavelength which will cause some transition in the gas molecule of interest. A suitable optical path must then be identified across the flue gases so that the light source and the detector can be suitably located.

To make use of equation 5.6, the intensity of the light entering the gas I_0 is determined by taking a reading from the detector when the duct or cell is empty of the pollutant gas. Subsequently, the gas concentration is obtained by the application of Beer-Lambert expression where the quantities α_λ and L must be known (Metcalfe (1994), and Jahnke (2000)). Typically, a calibration response will be generated experimentally for known gas concentrations, rather then attempting to use theoretical values for α_λ. This approach was adopted in the present study and will be described in detail in chapter 6.

Instruments designed to measure the absorption of light energy due to molecular interactions are commonly classified as spectrometers or spectrophotometers (Jahnke

(2000)). Spectrometers are designed to separate the beam of light received at the detector into different wavelengths so that the intensity of each component can be determined. Such techniques make spectrometers capable of scanning a relatively wide range of wavelengths. Spectrophotometers, on the other hand, use filters or some other mechanism to measure the absorption of the light over a relatively small range of wavelengths and they do not separate the wavelength components of the light received at the detector. A special type of spectrophotometer, used in the infrared region, is called the nondispersive infrared (NDIR) analyser. Section 5.4 describes a typical NDIR system.

JOHN RYLANDS
UNIVERSITY
LIBRARY OF
MANCHESTER

5.4 Nondispersive infrared analysers

The basic layout of a nondispersive infrared analyser (NDIR) is shown in figure 5.7.

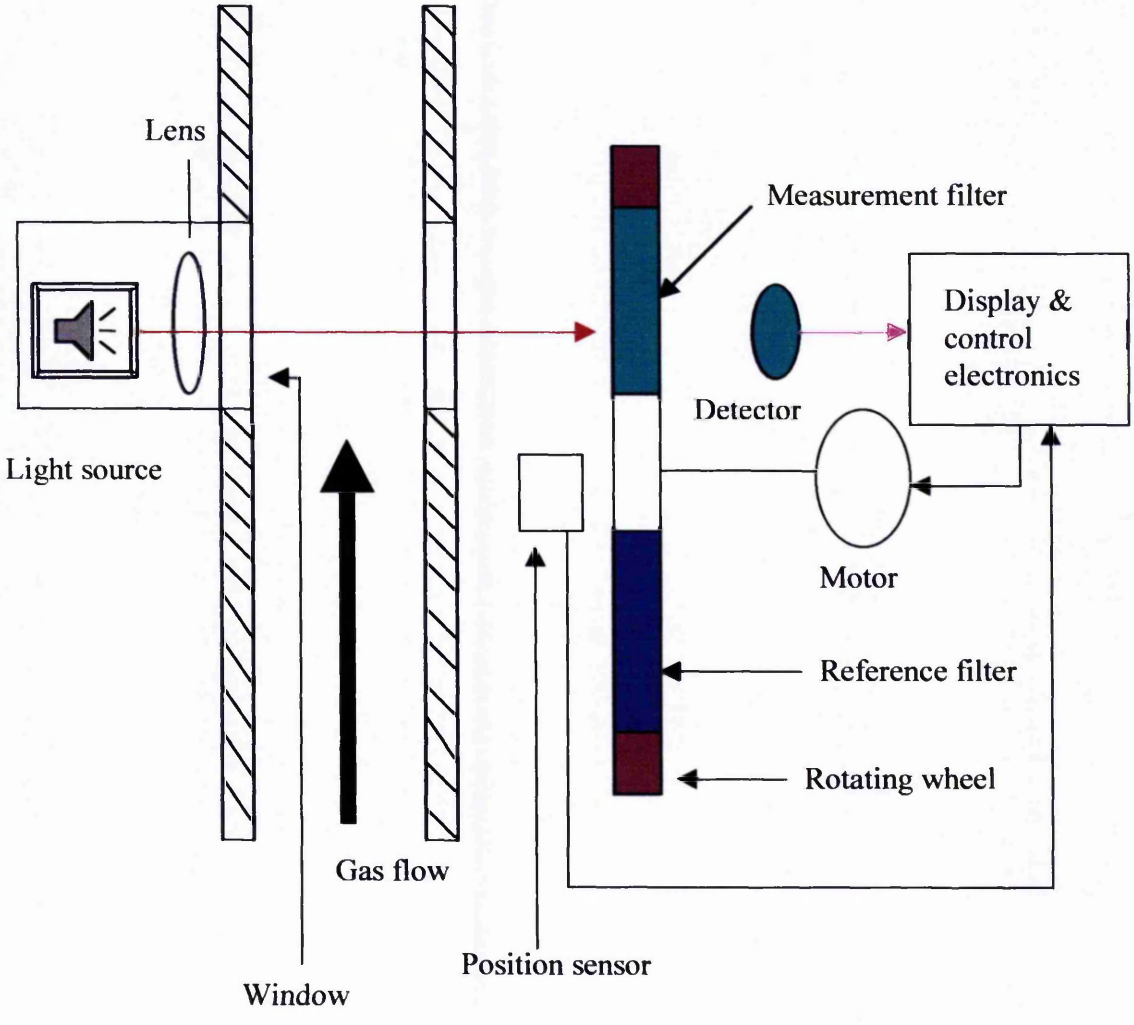

Figure 5. 7 A typical layout for a nondispersive infrared system using reference and measurement filters

Source. Based on Parr (1995)

A single infrared beam is transmitted through the flue gases in the duct or cell to a photo-detector. The rotating wheel carries two optical filters - known as the reference and the measurement filters.

These are interposed between the emerging beam and the photo-detector as the wheel rotates. The reference filter allows only the reference wavelength to reach the detector. This wavelength must be selected from a part of the spectrum where there is no absorption, either by the gas being monitored or by any other component which may be present. The second measurement filter allows the measurement wavelength (in the infrared part of the spectrum) to be transmitted without any loss of intensity. A position-measuring device (usually a simple optical detector) informs the display electronics which filter is in place at any given time.

The ratio of the detector signals transmitted through the two filter yields a value for the transmittance of the light $T_r = I/I_0$ at the selected measurement wavelength. This ratio can be related to the concentration of the pollutant gas as shown in equation 5.3. With regard to the reference signal, assuming $Cp_{ref} = 0$, a value for I_0 can easily be obtained since

$$I_{ref} = I_0 e^{-\alpha(\lambda)CpL} \qquad 5.7$$

Since, by definition, $\alpha_\lambda = 0$ at the reference wavelength, this reduces to

$$I_{ref} = I_0 e^0 = I_0 \qquad 5.8$$

Since there will be no absorption of the light intensity which is transmitted through the reference filter, the value of I_0 remains unchanged. Making the assumption that the spectral characteristics of the light source are such that the intensity I_0 is the same at the two wavelengths, the value of T_r enables an estimate of the concentration of the pollutant gas to be made.

In another arrangement, two cells are used to replace both the measurement and the reference filters. These cells are known as the sample and reference cells. Figure 5.8 illustrates this arrangement. The reference cell contains a gas, such as nitrogen gas, which does not absorb light energy at the wavelength used in the instrument. The optical system enables a single infrared beam to be transmitted through both cells. When the beam of photons is transmitted through the sample cell which contains the pollutant molecules, a fraction of the energy of each photon is absorbed. The ratio of the detector signals from the two cells gives the transmittance directly as illustrated in equation 5.6.

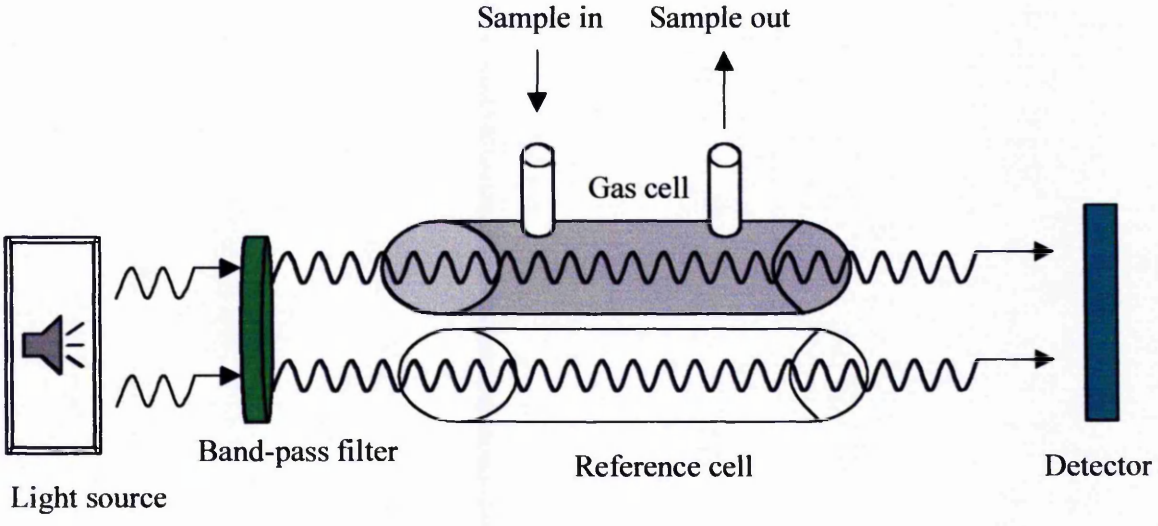

Figure 5. 8 A typical layout for a nondispersive infrared system using two cells
Source. Based on Jahnke (2000)

Differential optical absorption spectroscopy (DOAS), which is shown schematically in figure 5.9 is another technique which is applied widely because of the advantage that it can be employed to monitor more than one pollutant at a time.

In this approach, a reference wavelength is selected from a part of the spectrum where it is known that there is no absorption by the gas being monitored.

The measurement wavelengths are then selected from parts of the spectrum where the absorption peak for the gas to be monitored is at maximum.

When measurements are made for $S0_2$ for example, as shown in figure 5.9 the reference wavelength would be 578 nm while the wavelength 285 nm would be the most appropriate to monitor the concentration of $S0_2$.

In the present investigation, a similar approach, where the output of the instrument is related to reciprocal of the transmittance was used. The details of the system are described in chapter 6.

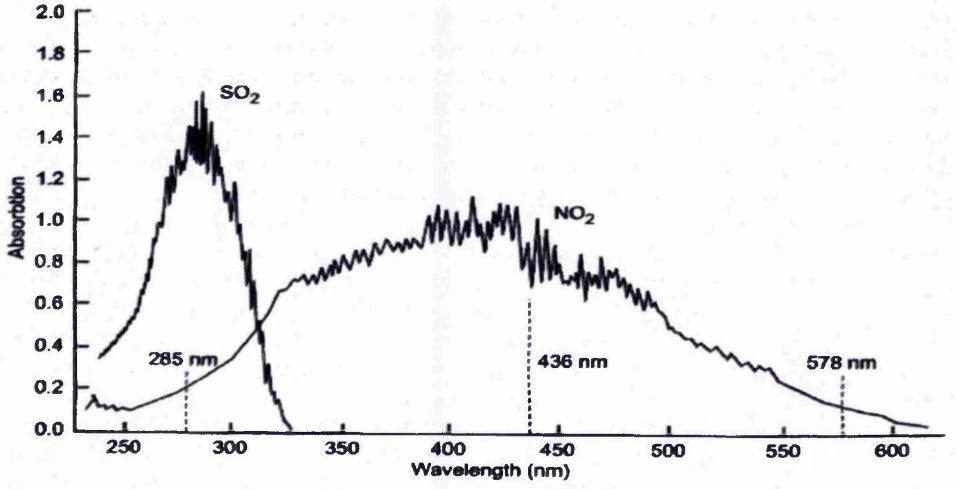

Figure 5. 9 The UV-visible spectrum of $S0_2$ and $N0_2$

Source. Janhke (2000)

Chapter 6 Experimental apparatus and instrumentation

6.1 Optical spectrometer (physical basis and principal features)

The system[2] consists of an ultraviolet light source, a fibre optic delivery system, a collimating lens, a detector lens, and a miniature diffraction grating and linear detector (all mounted on a PC card) which acts as the spectrometer. In the present investigation, this system was first used to measure the known gas concentration in the calibration cell, prior to its use to determine the $N0_2$ emission levels from the flue duct.

A schematic arrangement of the experimental apparatus is shown in figure 6.1. The PX-2 xenon (9.9W) ultraviolet light source was connected to the spectrometer (PC 2000) through a 15–pole sub-D PC connection box. This box controlled the electrical power into the 12 V light source and made it possible to synchronise the flashes of the lamp with the capture of data from the spectrometer.

The spectrometer was mounted on a 1MHz ISA-bus analogue to digital conversion card (ADC) and was installed in one of the parallel interface slots of the 600 MHz used in the experiments. The spectrometer (PC 2000) consists of a diffraction grating and a 2048 element linear CCD array detector enabling operation over an optical range from 200 to 1100 nm. However, in particular, since the slightly more restricted type 3 spectrometer grating was actually purchased, the useful wavelength for which data could be collected was restricted to the spectral range from 240 to 908 nm. All the operating parameters of the optical system, including the data sampling rate, were controlled through a desktop computer.

[2] Spectrometer system with absorbance/transmission optics, spectra win basic data acquisition software, type PC 2000 – purchased from Ocean Optics Europe.

The computer software package supplied with the optical spectrometer system was used to process the data (Spectrometer PC 2000 manufacturer's catalogue). This software package offered important data acquisition features, including the use of time and boxcar integrators, and the capability to calculate the time averages of the measured optical and derived properties.

The "boxcar integrator" averages a group of adjacent detector elements. For example, selecting a value of 5 means that each data point will be averaged with 5 points to its left and 5 points to its right. The greater this value, the smoother the data and the higher the signal-to-noise ratio (SNR). However, it is also noted that, if the value is set too high, then a loss in spectral (or frequency) resolution will occur. In the present investigation, a value of 4 was chosen after running a series of tests and evaluating the changes in the absorption spectrum between individual frequency components.

The "average integrator" sets the number of discrete spectral acquisitions which are accumulated before a spectrum is displayed. The larger this value, the better will be the signal-to-noise ratio. However, after a series of tests, it was concluded that a value of 6 would be quite sufficient. These functions made it possible for the spectrometer to set the background absorbance level to zero across the UV-visible spectrum, as shown in figure 6.7.

Following the manufacture's recommendations for the use of the instrument, the "absorbance signal" A_λ for any optical wavelength λ is given by the expression

$$A_\lambda = -\log_{10}\left(\frac{S_\lambda - D_\lambda}{R_\lambda - D_\lambda}\right) \qquad 6.1$$

Where S_λ = sample intensity at each wavelength

D_λ = dark intensity at each wavelength

R_λ = reference intensity at each wavelength

λ = wavelength considered.

Finally, the absorbance of the particular gas which is to be studied (in this case $N0_2$) is related to the concentration of the species by the equation 6.2.

$$A_\lambda = \alpha_\lambda CpL \qquad 6.2$$

where A_λ = the absorbance at wavelength λ

α_λ = molecular absorption coefficient (dependent on wavelength λ)

Cp = concentration at the pollutant

L = distance the light beam travels through the flue gas.

Equation 6.2 indicates that there should be a linear relationship between the absorbance at a given wavelength and the concentration.

Rearranging equation 6.2, the gas concentration is given by equation 6.3 so that

$$Cp = \frac{A_\lambda}{\alpha_\lambda L} \qquad 6.3$$

In most electronic instruments designed to measure the interaction of the incident light with the gas molecules, there is often random error (or uncertainty) in the true measured value because of electronic noise. With the inclusion of this error term, equation 6.2 therefore becomes

$$A_\lambda = \alpha_\lambda LCp(\pm E_A) \qquad 6.4$$

where E_A represents the uncertainty in the measured absorbance.

Modern instruments, including the one used in the present investigation, are now designed with features such as a boxcar integrator to enable the operator to reduce the effects of the random electronic noise. Here, the error term "E_A" is placed in brackets to indicate that its effects were minimised by the data processing methods during the course of the investigation. For example, figure 6.7 show that the background absorbance recorded after the operator adjusted the boxcar integrator, average integrator and time integrator was fluctuating between 0 and 0.005. This can be compared with the useful practical upper limit absorbance value of 1 corresponding to transmittance value of 100% as described in section 5.2.

In the present investigation, the software package supplied with the optical spectrometer was used to evaluate the absorbance values for selected wavelengths using equation 6.1. For the reasons explained in section 4.3 the data for $N0_2$ levels was collected for a wavelength of 439.34 nm. This enabled the $N0_2$ emission levels generated during the co-combustion of coal and dRDF to be determined by application of equation 6.3.

To enable this procedure to be applied, it was necessary to obtain the molecular absorbance coefficient factors α_λ for the selected wavelengths in a series of calibration experiments using a specially designed cell developed and used by Mott (1989). Initially, some modifications were made to the existing calibration cell constructed by Mott (1989). This work is described in section 6.2.

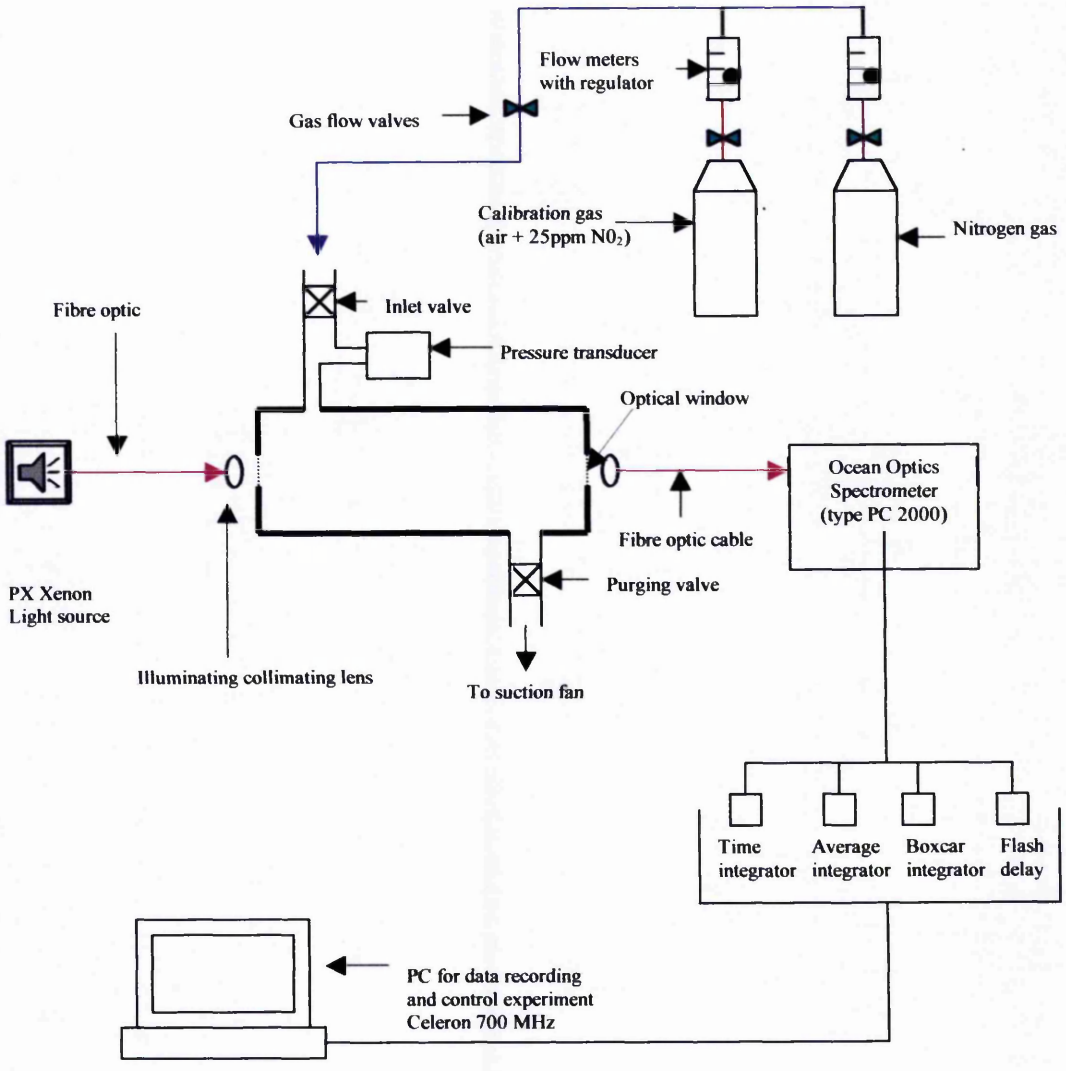

Figure 6. 1 Schematic arrangement of the optical calibration apparatus

6.2 Modification of calibration cell

A calibration cell constructed from a thick walled stainless steel tube with an inside diameter of 12 mm was used. As mentioned earlier, this cell was derived from an earlier study by Mott (1989) and, in its original form, had an effective optical length (between the windows) of 2000 mm. For the present study, it was decided to reduce this length to 500 mm so that it corresponded more closely to the optical path length for the combustion rig. Additionally, windows made from quartz were substituted for the original glass, since quartz does not absorb radiation in the UV to visible region.

Both ends of the stainless steel tube were fitted with round flanges of approximately 70 mm diameter. These flanges incorporated a circular recess to accommodate the new quartz windows which were in the form of circular discs of 60 mm in diameter and 5 mm thick. In addition, one end of the calibration cell provided a housing for the location of a K-type thermocouple as shown in figure 6.2. This thermocouple enabled the cell temperature to be monitored continuously during the data-recording process. When coupled with a measurement of the internal pressure of the cell, it became possible to calculate the gas concentrations for each condition.

Nitrogen dioxide is known to be highly toxic. An exposure of 5 ppm for 10 minutes will cause throat irritation and breathing difficulties (British Oxygen Company Information Sheet). Also, it has been suggested that this gas can have both acute, short-term and chronic, longer-term effects, on health, particularly in people with asthma (DETR (1998)).

On the basis of these considerations, it was decided to follow the system derived by Mott (1998) and incorporates some safety features to protect the operator and others

in the vicinity. For this purpose, the calibration cell was surrounded by two box-type enclosures.

The inner-most, which housed the calibration cell, was constructed of an acrylic plastic (Perspex) and incorporated an extraction port as identified in figure 6.2. An extraction port was connected to an extraction fan using a flexible tube so that any gas leaking from the calibration cell could be expelled to the atmosphere outside the building.

The outer box was constructed of wooden material "blockboard" and a second extraction fan was also provided to extract air from the space between the two boxes. Figure 6.2 shows a photograph of the assembled calibration cell enclosed only in the inner-box.

To facilitate the charging and purging of the calibration cell, two valves were incorporated: these will be referred to as the gas inlet and the purging valves. For safely reasons, the purging valve was linked to the extraction port using a small flexible tube. Another important feature of the calibration cell was the pressure transducer (North Lodge, Mediamate strain gauge type). This pressure transducer is manufactured from 300 series stainless steel to offer good resistance to corrosive substances such as refrigerants, ammonia, water and hydraulic fluids. Its operating pressure range is 0 to 3 bar gauge and its temperature range is $-40^{\circ}C$ to $100^{\circ}C$.

Nitrogen dioxide gas is known to be highly corrosive gas (Stohr et al (1997)). Thus, to avoid the risk of damaging the standard reference pressure gauge which had been used in the earlier study by Mott (1989), a pressure transducer was substituted.

The main function of this transducer was to monitor the internal pressure of the calibration cell during the charging processes as described in section 6.4. The pressure transducer was first calibrated prior to measurements of the $N0_2$ emission levels.

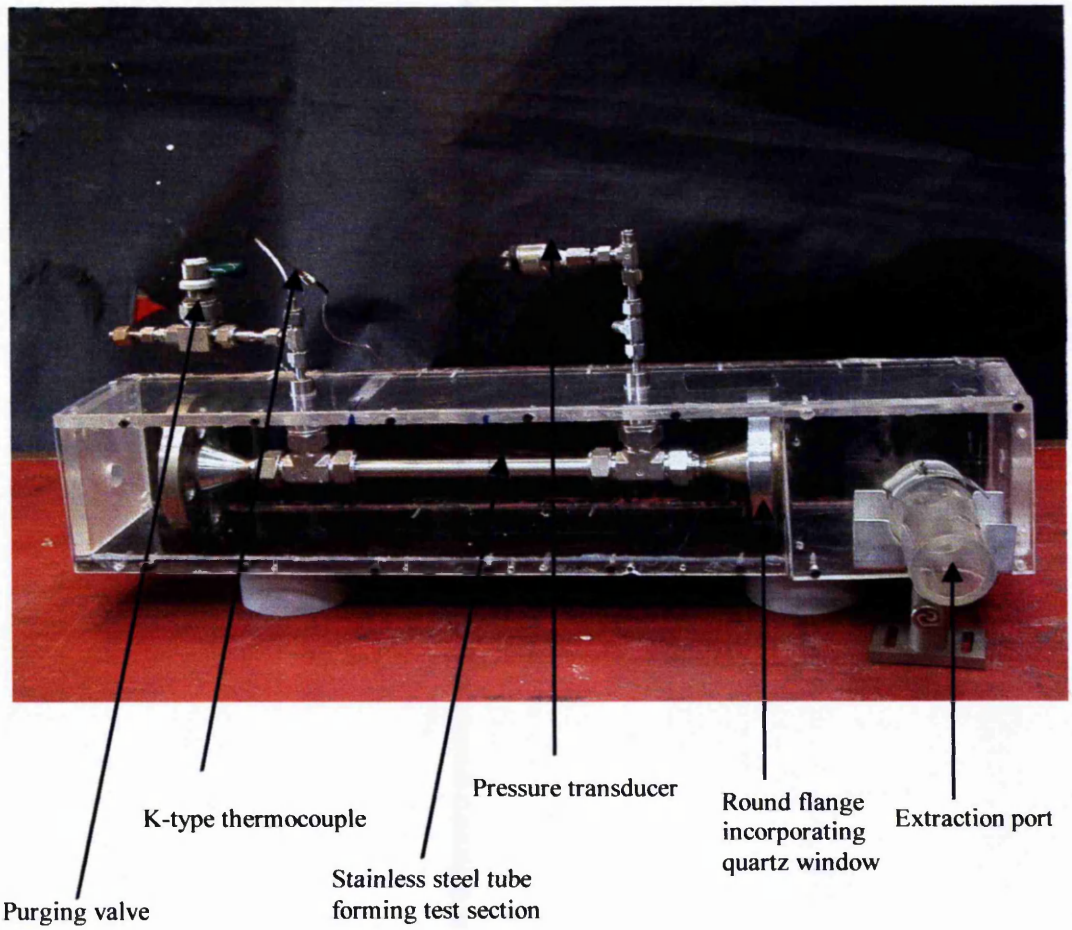

Figure 6. 2 Assembled calibration cell in the inner safety enclosure

6.3 Calibration of the pressure transducer

Prior to determination of the response of the optical instrumentation, the relationship between the digital readout on the transducer display and the gas pressure in the calibration cell was investigated.

This pressure transducer made it possible to relate the electrical transducer signal shown on the digital voltmeter, to the pressure of the gas mixture in the calibration cell. Figure 6.3 shows the arrangement of the apparatus used to calibrate the pressure transducer in schematic form.

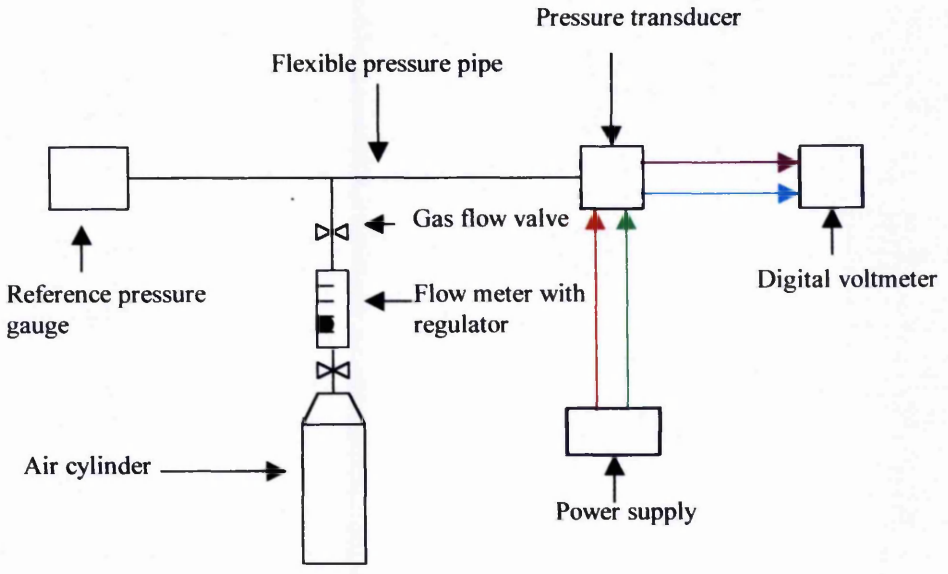

Figure 6. 3 Schematic arrangement of the pressure transducer calibration apparatus

Following the manufacture's recommendations for the use of this pressure transducer, the transducer was supplied from a 5V power supply. To carry out the transducer calibration process in the most efficient and accurate manner, the outlet valve on the gas cylinder and the flow control valve were slowly opened to increase the pressure in the pressure pipes in small increments.

Then, the pressure readings from the standard reference pressure gauge, and the voltage output from the digital voltmeter were recorded. Table 6.1 presents the data recorded during this calibration process and also gives a summary of the calibration statistics. The sample mean of a numerical sample for both the applied or reference

pressure (x) and the transducer signal (y), denoted by $\bar{x}$ and $\bar{y}$ respectively, could then be evaluated. Using the method of least squares, the best straight line relating the pressure transducer output signal to the applied pressure was found to be y = 1.46x - 0.176.

Table 6. 1 Data recorded during the pressure transducer calibration process

Observation	Applied pressure (kPa) (x_i)	Transducer readout (mV) (y_i)	Estimated y value (y_0)
1	1	0.53	1.64
2	5	6.65	7.48
3	10	14.2	14.78
4	15	21.71	22.08
5	20	29.02	29.38
6	25	36.65	36.68
7	30	43.88	43.98
8	35	51.45	51.28
9	40	58.61	58.58
10	45	65.45	65.88
11	50	72.86	73.18
12	55	80.28	80.48
13	60	87.55	87.78
14	65	94.76	95.08
15	70	101.80	102.38
16	75	109.26	109.68
SUM	$\sum x$ 601	$\sum y$ 874.64	$\sum y_0$ 8983.9

The variables x and y in table 6.1 were used to generate a calibration equation as shown in figure 6.4. Although the calibration data confirms that the output of the pressure transducer varied linearly with the applied pressure, figure 6.4 also shows that there is a slight zero error.

The method of least squares was used to determine the best-fitted straight line through the x y data points. The best-fit line occurs where the sum of squares for residuals (SSres) is the least possible value when compared to any and all other possible lines

which can be fitted to the data. It is obvious that the smaller the distances from the data points in a plot of x, y data to a line drawn through these data the better the line describe the data.

According to Mark and Workman (1991) the least squares solution to the best-fit line through a set of x y data points is given by

$$\sum_{i=1}^{N}(y_i - y_0)^2 = \sum(y_i - c - m_i x_i)^2 \qquad 6.5$$

where c = is the intercept for the best-fit line

m = is the slope for the best-fit line

y_1 = is any y observation used to determine the best-fit line

y_0 = is the estimated value of y_i using the best-fit line with slop (m) and intercept (c)

x_i = is any x observation used to determine the best-fit line

Note that the summation is taken over the entire sample and this solution given

$$\sum_{i-1}^{N}(y_i - y_0)^2 \qquad 6.6$$

The best least square fit-line is more precisely termed the minimum sum of squares. It is also referred to as the sum of squares for residuals or the sum of squares value to error.

In order to determine the minimum sum of squares the intercept (c) and the slop (m) which meet the criteria of minimum variations are calculated first.

The expression for the best-fit line intercept is used

$$c = \bar{y} - m\bar{x} \qquad 6.7$$

Intercept (c) = - 0.176

where $\bar{x}$ and $\bar{y}$ are the mean of all x_i and y_i value from the data points given in table 6.1.

The slop (m) for the best-fit line is given by

$$\frac{\sum_{i-1}^{N}\left(x_i - \bar{x}\right)\left(y_i - \bar{y}\right)}{\sum_{i-1}^{N}\left(x_i - \bar{x}\right)^2} \qquad 6.8$$

Slop (m) = 1.46

The overall line equation is then given by

$$y_0 = c + mx_i \qquad 6.9$$

Note that equation 6.6 can then be used to evaluate whether the calibration line is a good predictor of y_i given any value of x_i in the data range. If the value is equal to zero the calibration line is a perfect fit to the data. However, it was noted that the SSres approach is not appropriate when the standard deviation within the data is large. As a result, a method of r^2 was used to calculate the correlation coefficient through x_i and y_i data points. The approach was also used to calculate the correlation coefficient through the x_i and the estimated y_0 data points using the best-fit line with slop (m) and the intercept (c). The results are as follows

Correlation coefficient through the x_i and y_i data points = 1

Correlation coefficient through the x_i and y_0 data points = 0.99

Here, it needs to be explained that correlation coefficient through data points were calculated using Microsoft excel. Overall the results suggest that the variances in y_i and y_0 are not significantly different and that the calibration line is a perfect fit to the data.

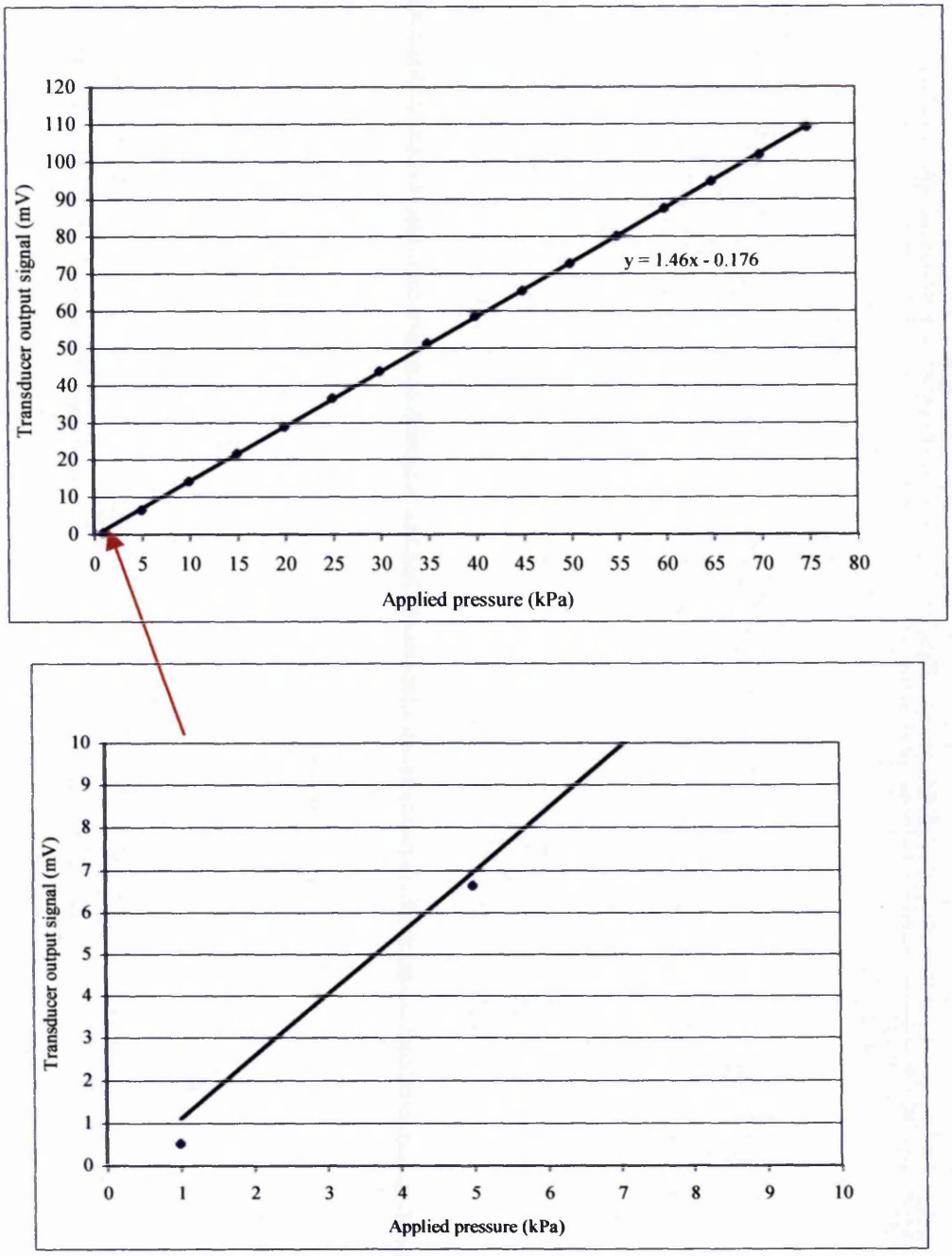

Figure 6. 4 The relationship between applied pressure and the digital readout of the pressure transducer signal

After the calibration process, the pressure transducer was inserted into its location on the branch pipe connected to the calibration cell as shown in figure 6.2.

The procedures to determine the molecular absorption coefficients for selected wavelengths were then carried out in a systematic series of experiments. The methods used will be discussed in the next section.

6.4 Data recording

The calibration gases used in the experiments were 25 ppm of nitrogen dioxide (balanced in air) and nitrogen. The $N0_2$ gas was prepared and supplied by the British Oxygen Company (BOC). To obtain concentrations as low as 5 ppm, the $N0_2$ gas was diluted with nitrogen gas. Firstly, the partial pressures corresponding to each specific concentration were calculated and their corresponding electrical transducer signals were noted as shown in table 6.2. The absorbance signals were observed and recorded at atmospheric pressure.

To perform the data recording for each concentration at atmospheric pressure, the calibration cell was first evacuated to around 0.25 bar absolute which corresponded to an electrical transducer signal of – 12mV. Then, with the electrical transducer signal display indicating a signal of – 12mV, both the intake and purging valves were shut as shown in figure 6.1. The data acquisition system was then prepared. First the system was switched to the "scope mode" as shown in figure 6.5. Then, with the xenon light source switched on, but without any concentration of $N0_2$ in the calibration cell, the data acquisition parameters were adjusted to give an indicated intensity of the transmitted light of approximately 3500 counts/second.

Following the manufacturer's recommendations for the use of this instrument, the light source was switched off so that the "dark spectrum" could be stored.

It must be noted that, in a situation where the optical path between the transmission and receiving lenses can be easily blocked, it is not necessary to switch off the light source. However, during the calibration experiments now described, it was not easily possible to block the optical path between the transmission and receiving lenses because of the location of the calibration cell within the innermost safety enclosure. Thus it became necessary to switch off the light source so that the "dark spectrum" could be recorded and stored for each successive measurement.

Following this, the light source was switched on again and the system was left on for approximately 4 to 5 minutes to enable the light source to become stable before the reference spectrum was recorded and stored. Note that the dark and reference spectra were both stored before any $N0_2$ gas was introduced into the calibration cell.

Next, the system was switched to the transmission mode as shown in figure 6.6. This was done to test the stability of the radiation arriving at the detector for 100% transmission. Finally, the data processing system was switched to the absorbance mode and the absorbance versus wavelength distribution for the cell in the absence of $N0_2$ was recorded and illustrated in figure 6.7. The data acquisition system was now ready to record the absorbance signal for given concentrations of $N0_2$ gas in the cell.

For example, to record the absorbance signal for a concentration of 25 ppm, a calibration gas ($N0_2$ balanced in air) was slowly introduced into the calibration cell until the electrical transducer signal display recorded 0mV.

The data recording system was started and data were recorded every second for a duration of one minute. This resulted in a sample size of 60 values.

This relatively long data collection time was chosen because it provided sufficient experimental data and allowed a sensible average value for the absorbance to be determined for each set of experimental conditions. Use of equation 6.1 then enabled the absorbance signal at any given wavelength to be calculated.

When the data recording had been completed, for the first measurement of the concentration, the calibration cell was evacuated and purged before the next test run – see section 6.4. When the purging process had been completed, the calibration cell was again evacuated until the same pressure as mentioned earlier was reached (corresponding to an absolute pressure of – 0.25 bar). Now it must be noted that to record the absorbance data for a diluted mixture is slightly different from recording the absorbance data for an undiluted concentration. For example, to record the absorbance signal for 10 ppm, the calibration gas (25 ppm balanced in air) was slowly introduced into the calibration cell and the electrical transducer signal was seen to increase from – 12mV to – 8.1mV. The outlet valve on the gas cylinder was then shut and nitrogen gas was then slowly introduced into the calibration cell to increase the electrical transducer signal display to 0mV (corresponding to 1bar absolute). The mixture was allowed between 20 and 25 minutes to reach equilibrium before the optical data was recorded. The same procedures were repeated for the remaining mixtures.

The absorbance signals representing the different concentration levels are presented in figures 6.8 to 6.12. Section 6.5 describes the operational procedures which were performed to evacuate and purge the calibration cell.

Table 6. 2 Pressure transducer electrical signal corresponding to specific concentration levels

$N0_2$ concentration levels (ppm)	Pressure transducer electrical signal (mV)	
	Nitrogen gas	25ppm $N0_2$ + Air
5	10.1	1.9
10	8.1	3.9
15	7.8	4.2
20	5.9	6.1
25	0	12

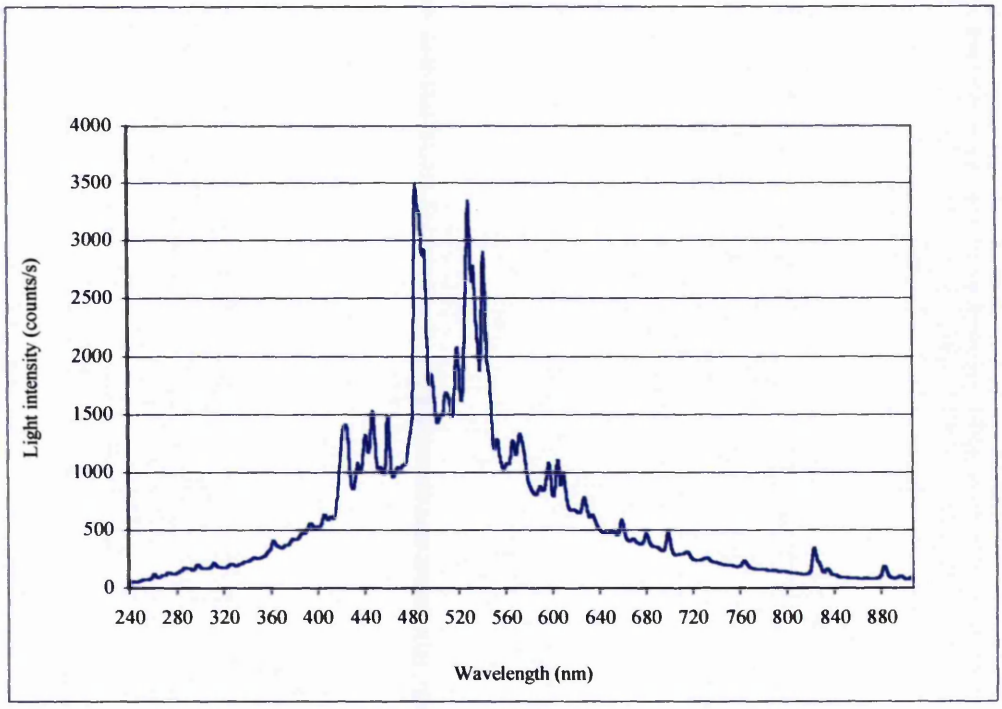

Figure 6. 5 Output of PS-2 Xenon light source.

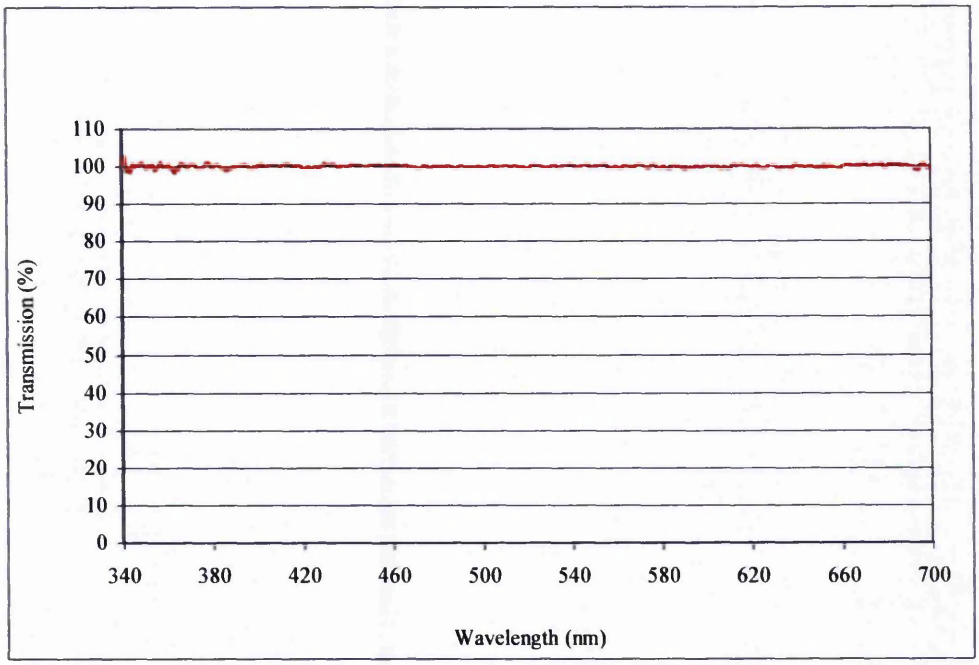

Figure 6. 6 A typical transmission spectrum for empty calibration cell.

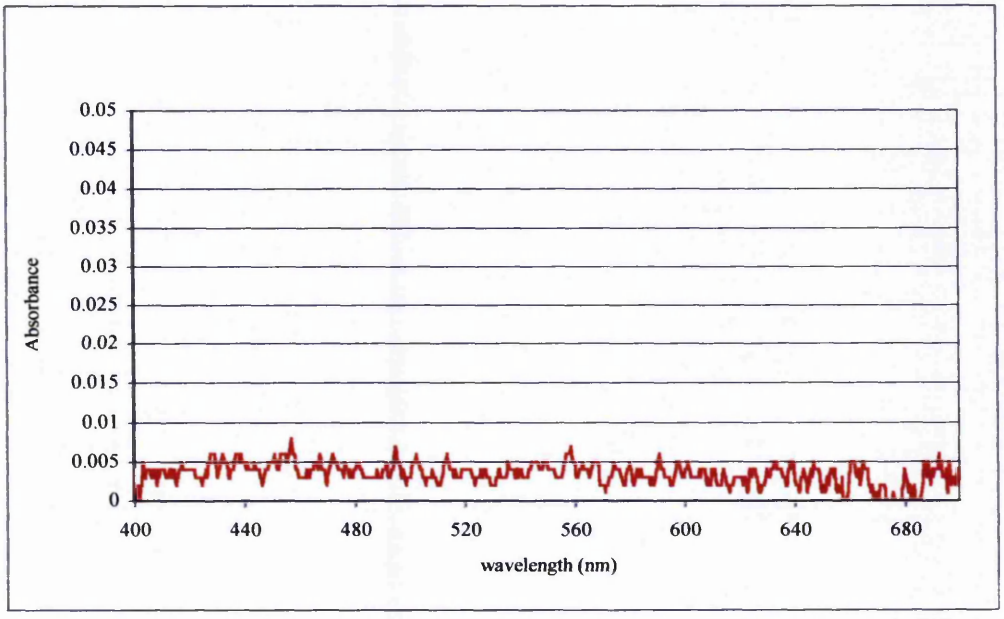

Figure 6. 7 A typical absorbance spectrum for the empty calibration cell.

6.5 Evacuation of the calibration cell

This process was carried out at the end of each calibration step to ensure that no trace of residual $N0_2$ gas remained in the calibration cell after the previous experiment. Clearly, any trace of residual gas being retained from one test to another would contaminate the results. To eliminate this contamination, a vacuum pump and a high-pressure cylinder of nitrogen gas were used to purge the cell between each calibration test.

To perform the evacuation and purging processes, a purging link from the calibration cell was connected to the intake valve of a vacuum pump. With the motor switched off, and the vacuum pump intake valve shut, nitrogen gas was slowly introduced into the cell until a gauge pressure of approximately 1bar was recorded. The electric motor which drove the vacuum pump was then switched on and the intake valve on the vacuum pump was slowly opened to give a negative pressure of – 0.25 bar equivalent to – 12 mV on the pressure transducer display. These operational procedures were repeated after every experiment.

6.6 Presentation of calibration results

Typical data to show the absorbance of $N0_2$ measured for five different concentration levels are presented in figure 6.8 to 6.13. Figure 6.14 is based on these distributions but shows the results for four selected wavelengths. Finally, the molecular absorption coefficients for these same selected wavelengths were determined from the slopes of the best least squares straight lines drawn through the data presented in figure 6.14. These values are presented in table 6.3.

In the bulk of the combustion molecular absorption coefficient for the wavelength 439.34 nm was used to calculate $N0_2$ emission levels for the unknowns during the combustion stage. The wavelengths quoted in this investigation correspond to those indicated by the instrument.

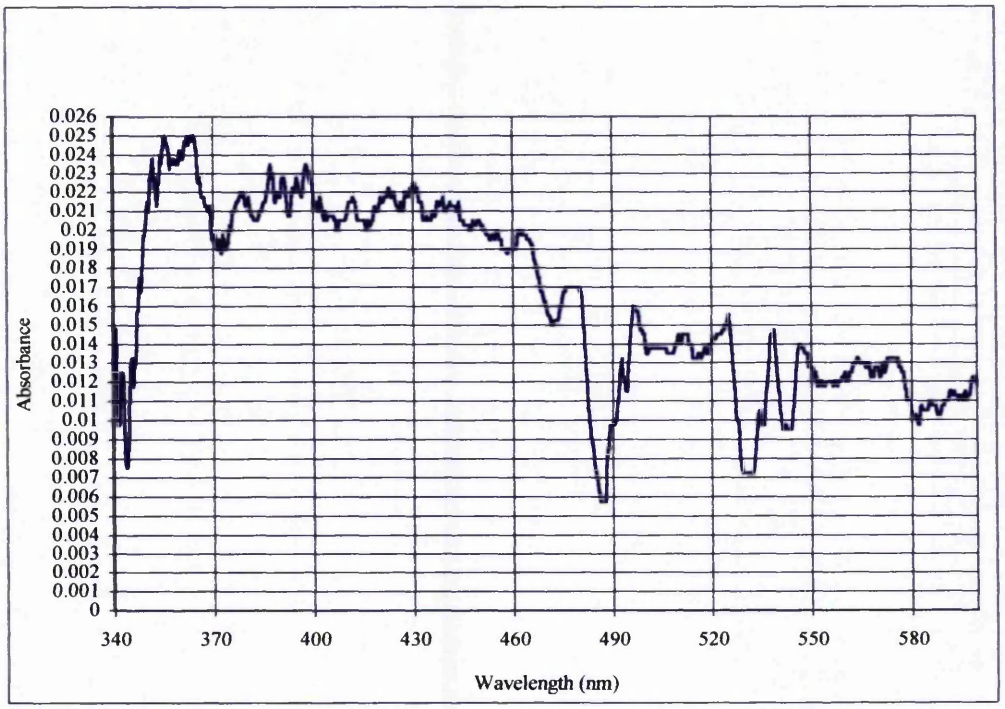

Figure 6. 8 Absorbance signal corresponding to 5 ppm of $N0_2$

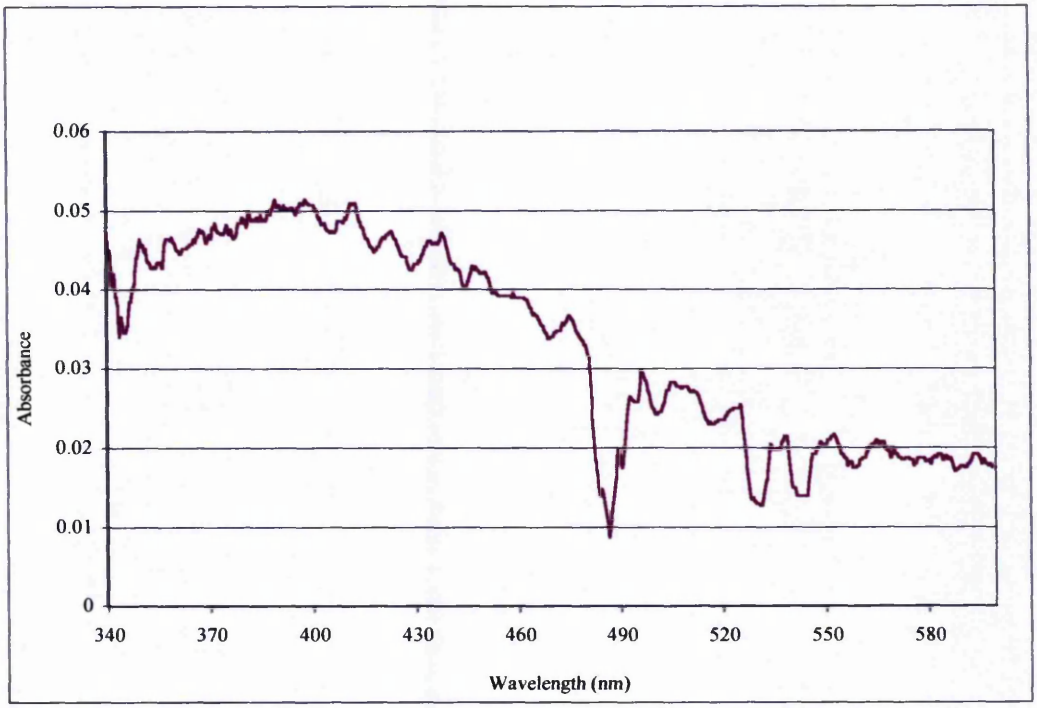

Figure 6. 9 Absorbance signal corresponding to 10 ppm $N0_2$

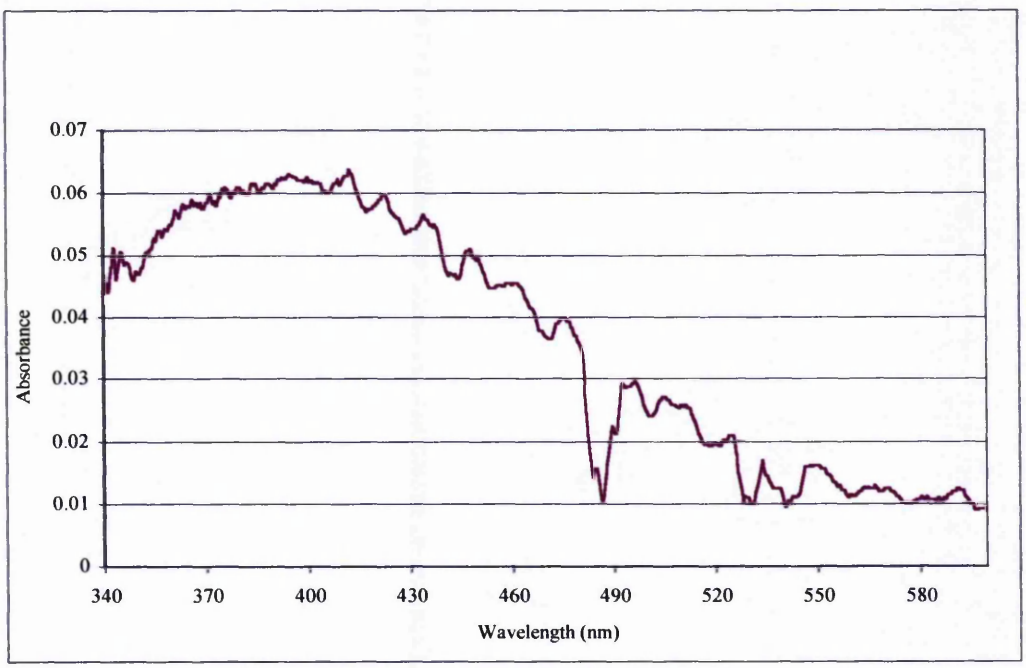

Figure 6. 10 Absorbance signal corresponding to 15 ppm $N0_2$

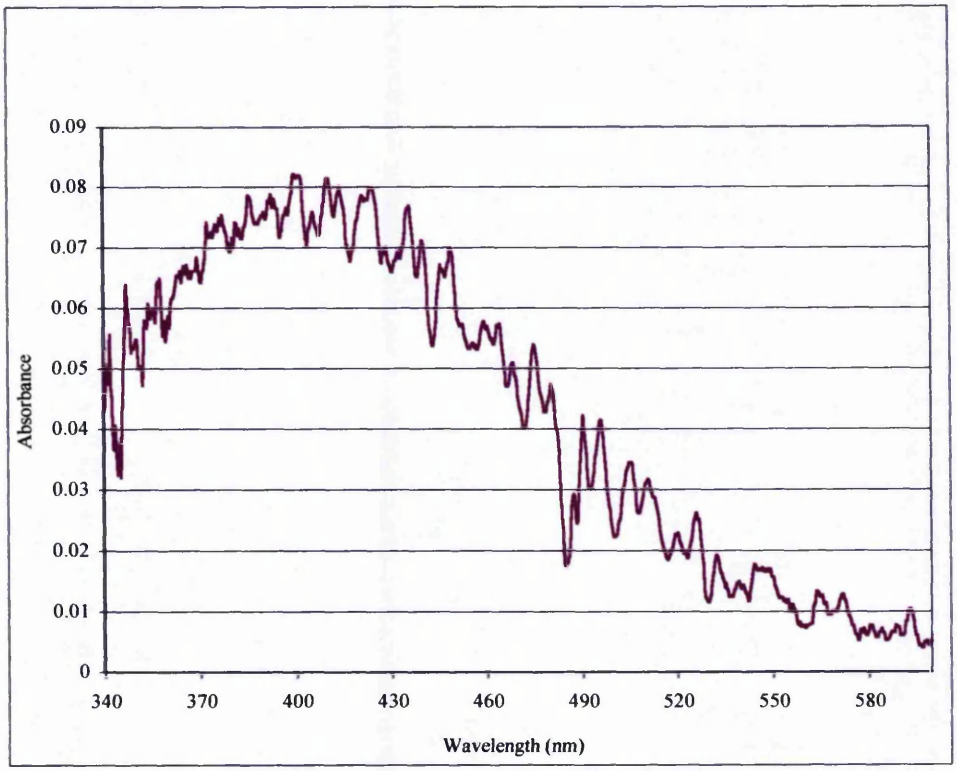

Figure 6. 11 Absorbance signal corresponding to 20 ppm $N0_2$

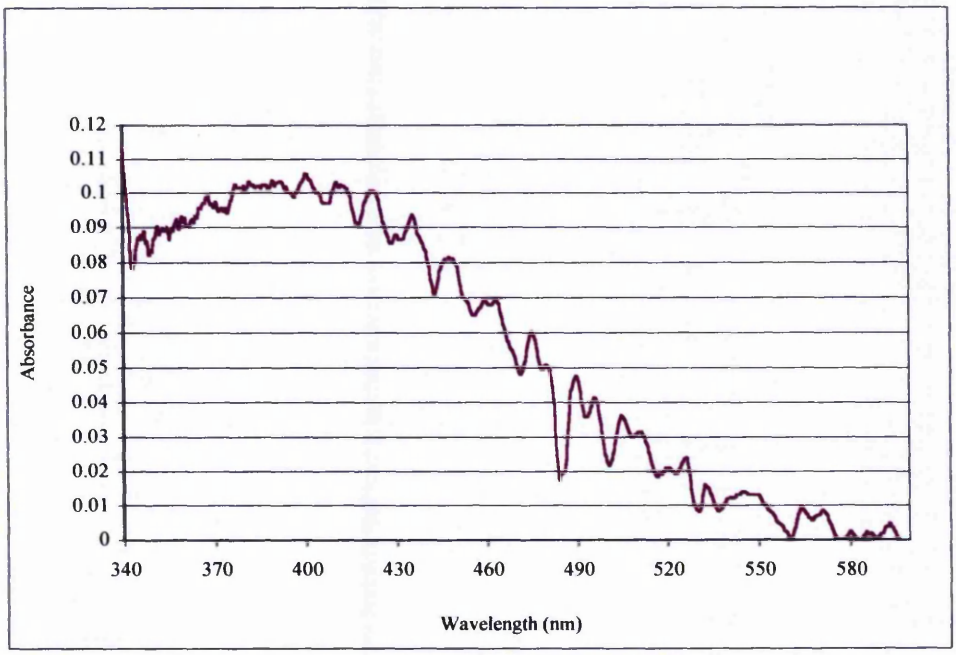

Figure 6. 12 Absorbance signal corresponding to 25 ppm $N0_2$

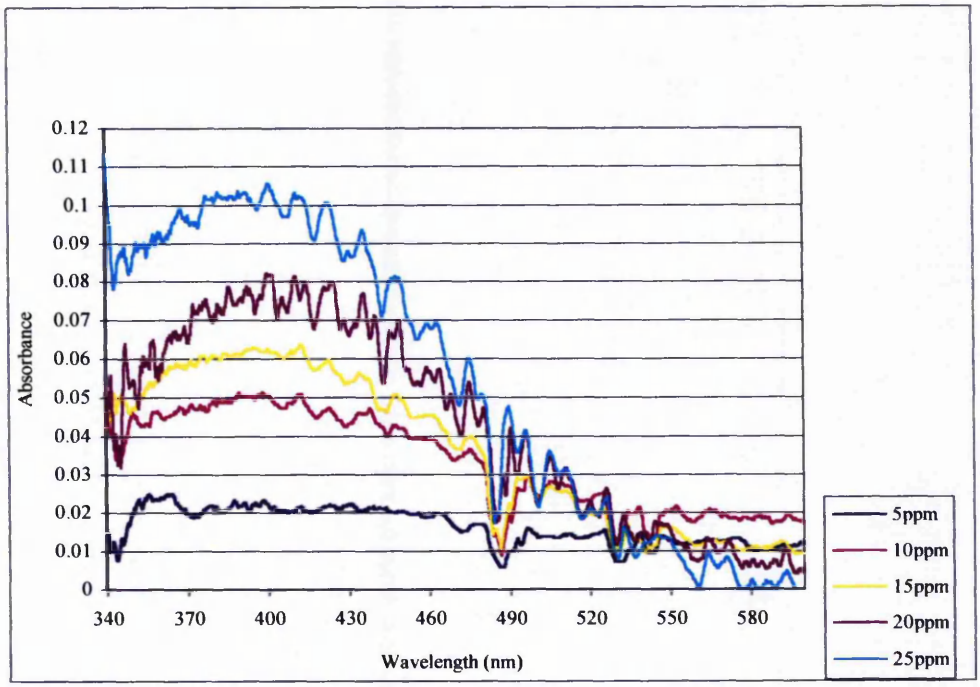

Figure 6. 13 Absorbance signal for all five concentrations

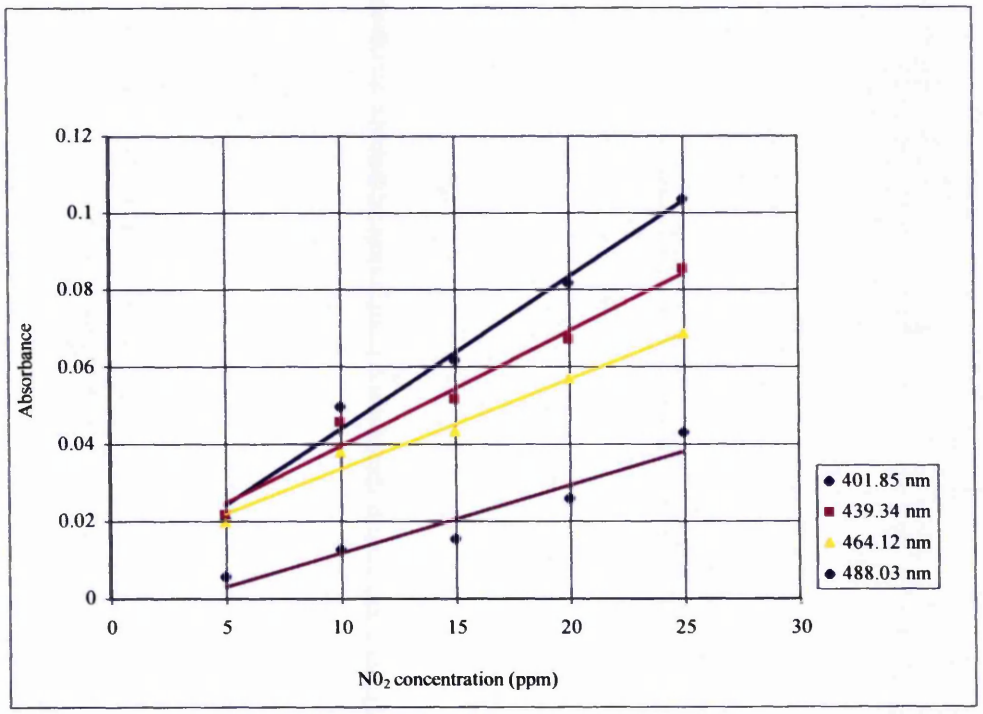

Figure 6. 14 Absorbance as a function of $N0_2$ concentration for four selected wavelengths

Table 6. 3 Molecular absorbance coefficients for selected wavelengths

Selected wavelengths	Molecular absorbance coefficient
401.85 nm	4.2
439.34 nm	3.6
464.12 nm	3.2
488.03 nm	1.7

6.7 Discussion of results

The results presented in figure 6.13 show the positions of the most significant absorbance peaks lying between 350 and 450 nm. These findings are consistent with the results attained by Davidson et al (1988) who measured the ultraviolet absorption spectrum of $N0_2$ from 250 to 650 nm as discussion in section 4.4. The data obtained by these authors showed a similar pattern to that presented in figure 6.13, with virtually identical wavelengths for the absorbance. Figure 6.14 presents the data in the form of the absorbance signal versus the $N0_2$ concentration. This data suggests that the absorbance is a linear function of the concentration.

The data is consistent with the data presented by Peng et al (1995), Brown and Pitz (1991) and Lindau (1991) for measurement of the $N0_2$ emission levels. However, it is noted that, although the $N0_2$ spectrum within the UV-visible region has been investigated several times before, there is only very limited data in the literature on the molecular absorption coefficients for most of the wavelengths.

In fact, most of the previous authors, including Brown and Pitz (1991), Davidson et al (1988), Lindau (1991), and Peng et al (1995) appear to have been more interested in the relationship between the absorbance signal and concentration levels, rather than in

any determination of the molecular absorption coefficients. As a result, this agreement with the previous work, and the linearity of the relationship as mentioned in the previous page, indicated that the output of the calibration experiment was satisfactory.

For comparison the four wavelengths of 401.85, 439.34, 464.12 and 488.03 nm were selected for detailed study. The molecular absorbance coefficients were then determined at these particular wavelengths in a systematic series of experiments.

The results show that light of wavelength 401.85 nm is more sensitive to molecules of $N0_2$ compared with the other three wavelengths. This is indicated by its relatively high molecular absorbance coefficient as shown in table 6.3. In contrast, a wavelength of 488.03 nm is relatively insensitive to $N0_2$ so that to make this the choice would obscure the detection of small concentration levels.

Although wavelength 401.85 nm has the highest molecular absorbance coefficient it was decided to use wavelengths 439.34 nm in the combustion experiments. A wavelength 401.85 nm would be too close to the dissociation threshold limit of $N0_2$ as previously illustrated. In fact, the dissociation threshold limit of $N0_2$ is approximately 397 nm as suggested by Zacharias et al (1990).

6.8 Description of apparatus (combustion rig)

Figures 6.15 to 6.17 shows the major components of the combustion test rig. A laboratory scale furnace was constructed in the form of a cylinder with a circular cross section, having an inside diameter of 300 mm and a length of 1000 mm. This furnace was manufactured in mild steel and was then lined internally with a 30 mm thick refractory material.

The grate was made of a 5 mm thick mild steel plate which was clamped between the lower flange of the combustion chamber and the air receiving section. The furnace was supported so that the axis of the cylinder lay in the vertical direction with the grate at the bottom and the exhaust ducting above. The cross sectional area of the furnace was approximately $0.071 m^2$.

The primary air was fed underneath the grate as a forced draught from a centrifugal fan, the airflow rates being controlled by a butterfly valve and measured by an orifice plate. The air mass flow rates across the fuel bed were determined according to the relationship (International Standard Organisation ISO 5167-1 (1999))

$$Q_m = CE\frac{\pi}{4}d^2\sqrt{2\rho\Delta p} \qquad 6.10$$

where C = the discharge coefficient

E = the velocity of approach factor

d = the orifice diameter

Δp = the pressure drop across the orifice plate

ρ = the air density

The velocity of approach factor E is given by the expression

$$E = \sqrt{(1-\beta)} \qquad 6.11$$

where β = the ratio of orifice bore to pipe bore (d/D)

The mass flow rates for selected tests are presented in Appendix B.

A band of ten K-type thermocouples (of 3 mm diameter) was located in a horizontal plane at a height of 300 mm above the top surface of the grate. These thermocouples were inserted radially through the wall of the combustion chamber around the circumference so as to protrude from the inner surface with different immersions at 10 mm spacing up to a maximum of 90 mm from the wall. An analogue to digital conversion card (PC1-DAS 1000) was used to record the thermocouple signals from which the flue gas temperatures could be determined for these ten positions during the course of each experiment.

A sight window was also located in a horizontal plane at a height of 30 mm above the grate. This sight window was used at the start of each experiment, during the fuel charging stage and while igniting the fuel bed. Before the exhaust gases were vented to the atmosphere, they were passed through a wet scrubber. This consisted of three water atomising nozzles, located at approximately 120 degrees from each other around the circumference of the scrubbing drum, which were used to provide a continuous spray of scrubbing water during the combustion process.

This wet scrubbing system was incorporated in an attempt to reduce the level of pollutants vented into the atmosphere during the combustion process. The scrubbing water was supplied from the mains water supply system, and the operating pressures were controlled using a standard water control valve and pressure gauge.

The major components of the test rig are shown in figure 6.15 to 6.17. The combustion chamber is shown in figure 6.15. The lower section (air receiving) of the ductwork, and the upper fixed section are also shown in figures 6.16, and 6.17.

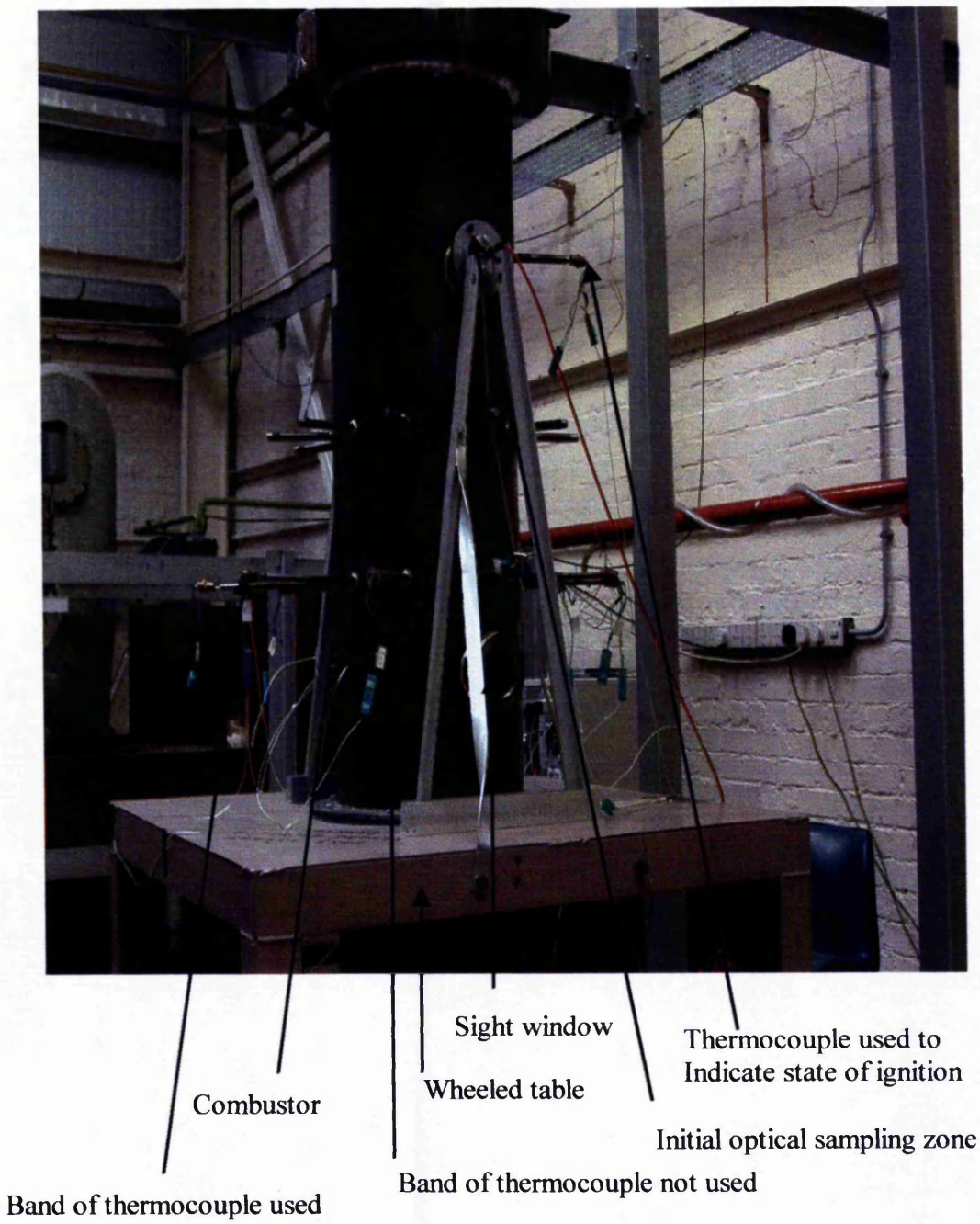

Figure 6. 15 Combustion chamber

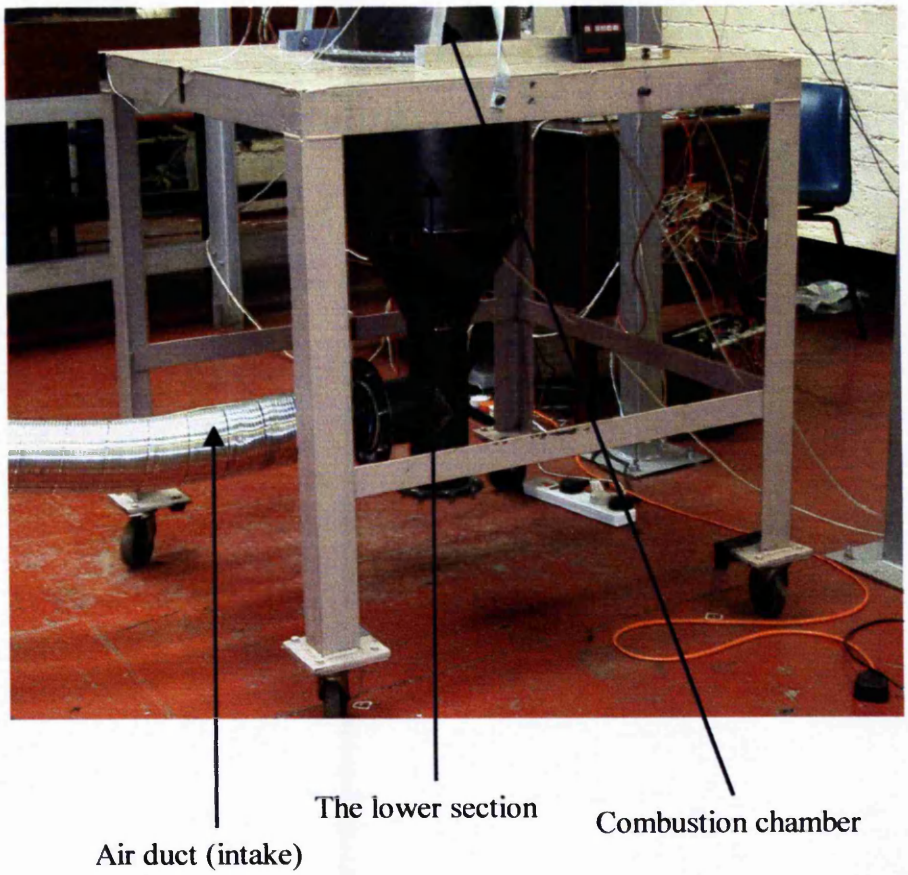

Figure 6. 16 Lower section (air receiving) of the combustion apparatus

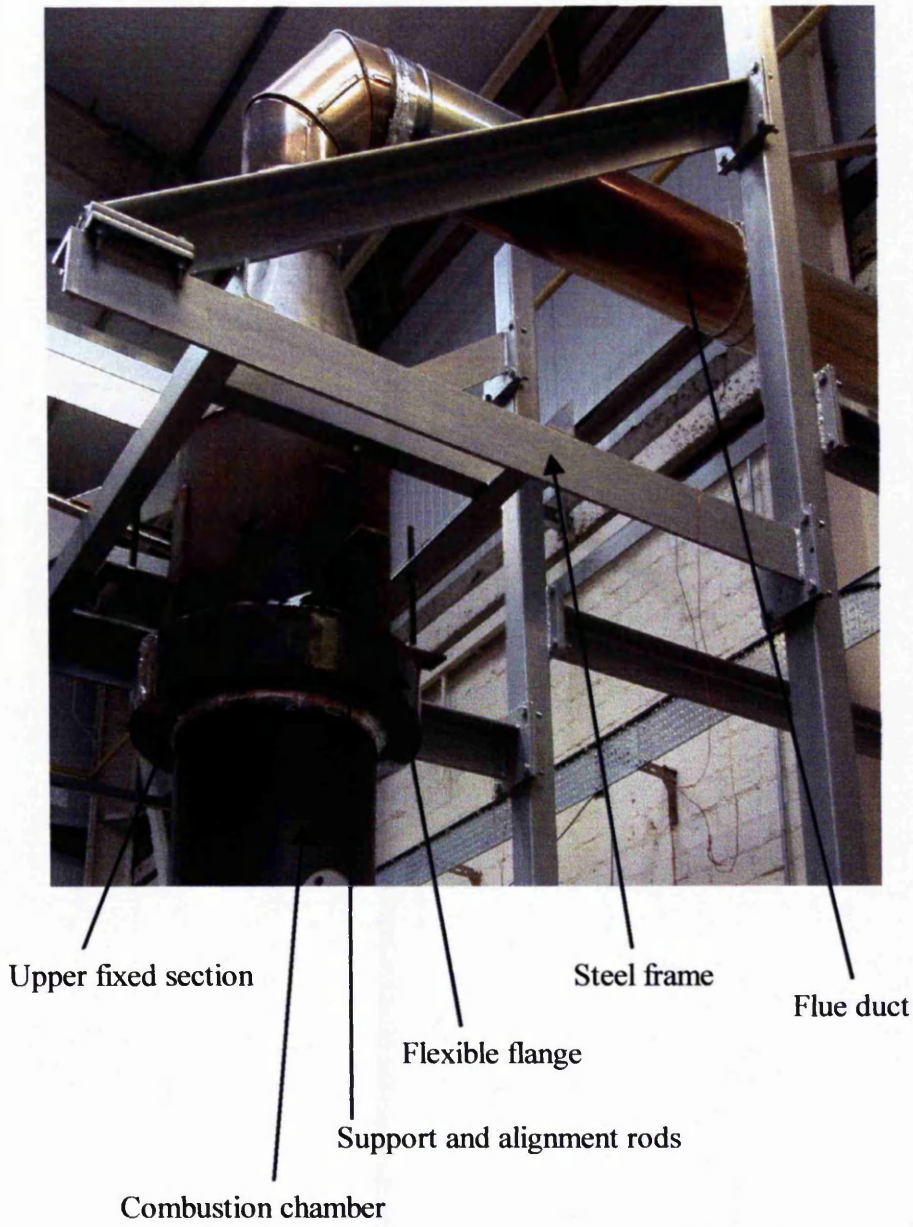

Figure 6. 17 Upper section (fixed) of the combustion apparatus

6.9 Location of the optical sampling point

In the initial design, the optical sampling zone was located at approximately 700 mm above the grate, as shown in figure 6.15. Windows made from glass with a high thermal resistance were used to provide optical access for the light beam and the detector. However, preliminary test results revealed that strong attenuation of the incident light could occur due to contamination of the windows. This problem was assumed to stem from the presence of soot in the flue gas forming a thin layer on the inner surface of the glass windows. The attenuation of the incident light due to the contaminated glass windows made it impossible to separate this effect from the attenuation due to the presence of $N0_2$ in the flue gases. It was assumed that the high percentage of volatile matter in the dRDF would make the optical conditions even worse.

In an attempt to avoid attenuation of the incident light due to contamination of the windows, it was decided that the two circular glass windows should be replaced by aluminium plates each having a central hole of 3 mm in diameter to provide optical access. However, it was realised that the exhaust gases could escape through these viewing holes and contaminate the optical lenses. A low-pressure zone was therefore created between each lens and the aluminium plate in an attempt to minimise the contamination of the optical lenses. This was achieved by attaching a small pipe of 5 mm in diameter on each plate as shown in figure 6.18.

The open end of each 5 mm pipe was located approximately 1.5 mm below the axis of the optical path while the other end was connected to a suction pump using a flexible tube. This arrangement created a localised low-pressure zone below each central hole and the optical lens.

Replacement of the glass windows with the aluminium plates showed some improvement on the overall results. However, the presence of other obstacles such as the hot small particles which frequently travelled across the optical path and were capable of scattering some fraction of the incident light were assumed to have an adverse effect on the overall results. Figure 6.19 illustrates this particle or spark phenomenon as it was observed during one combustion experiment.

It was noted that these combustion conditions were unavoidable because of the channelling effect associated with the combustion of a solid fuel which included a relatively high proportion of volatile matter such as dRDF. As a result, it was considered advisable to move the optical sampling zone to a new location further along the exhaust duct as shown in figure 6.20.

JOHN RYLANDS
UNIVERSITY
LIBRARY OF
MANCHESTER

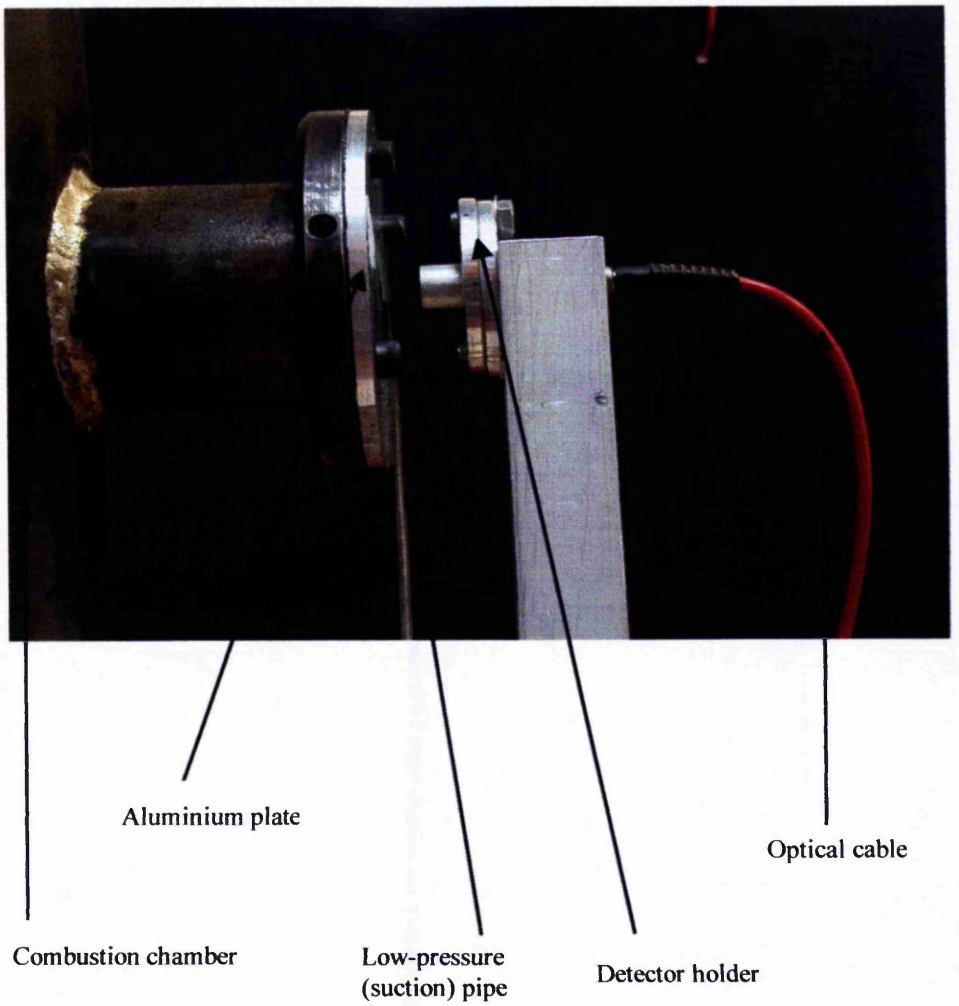

Figure 6. 18 Initial arrangement and position of the optical sampling zone

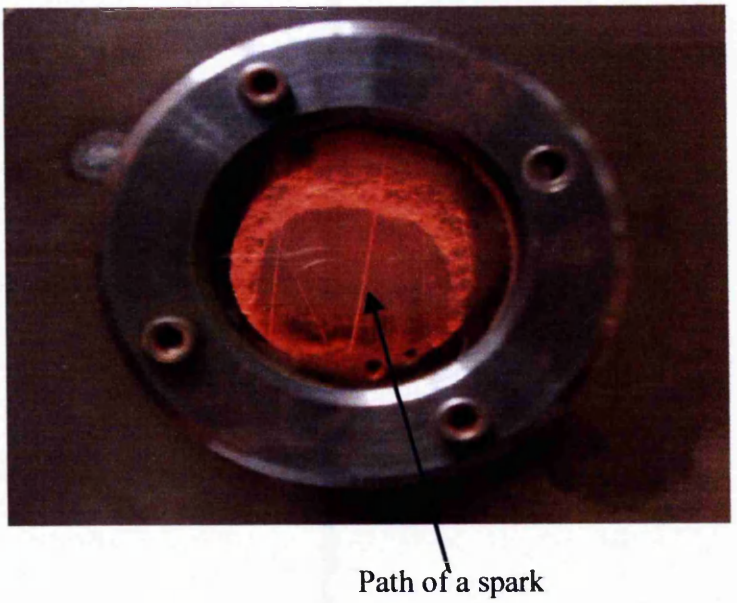

Figure 6. 19 Random movement of sparks – seen through the viewing window

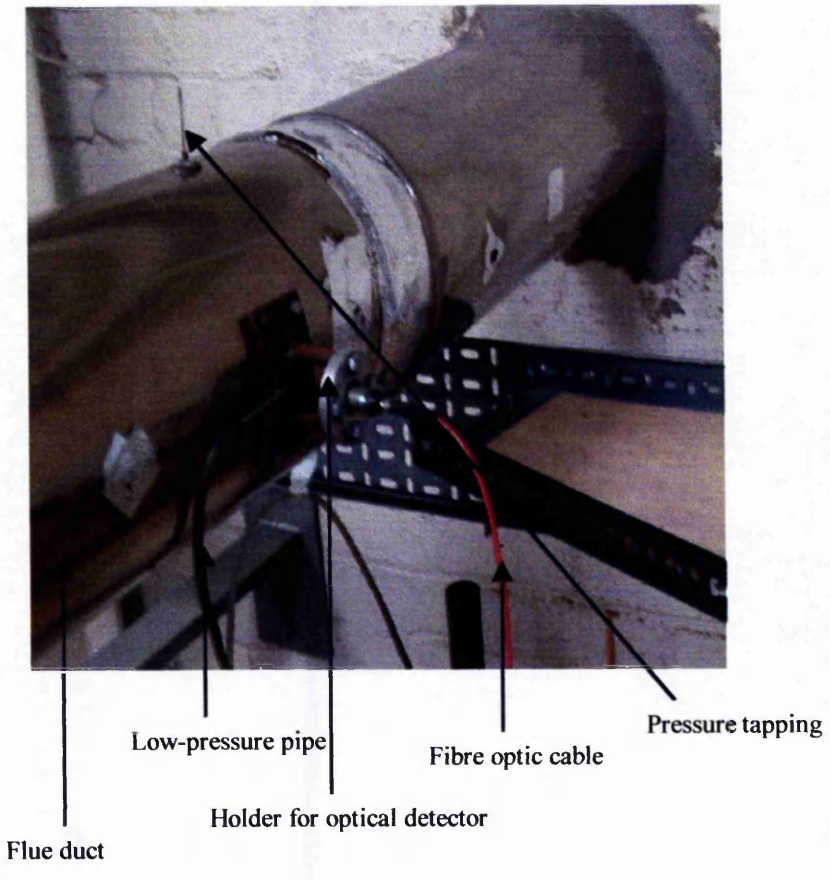

Figure 6. 20 Revised position of the optical sampling zone

Preliminary tests results obtained with the optical sampling zone located at the far end of the exhaust duct showed some improvement. However, to make it even less likely that the light beam would suffer from attenuation due to the presence of solid particles (or droplets) in the exhaust gas, a particle separator was incorporated into the exhaust duct before the optical sampling zone. This system included fine wire mesh filters and was designed to impose sudden changes in the direction of the exhaust gases to separate out any particulate material. Figure 6.21 shows the particle separator located between the upper fixed section and the optical sampling zone.

Figure 6.22 shows the separator in a schematic form to indicate how the sudden changes in the direction of the exhaust gases were achieved. A vertical metal shield was incorporated to divide the volume of the particle separator into two equal volumes so that the flow was forced to travel around several sudden changes in direction.

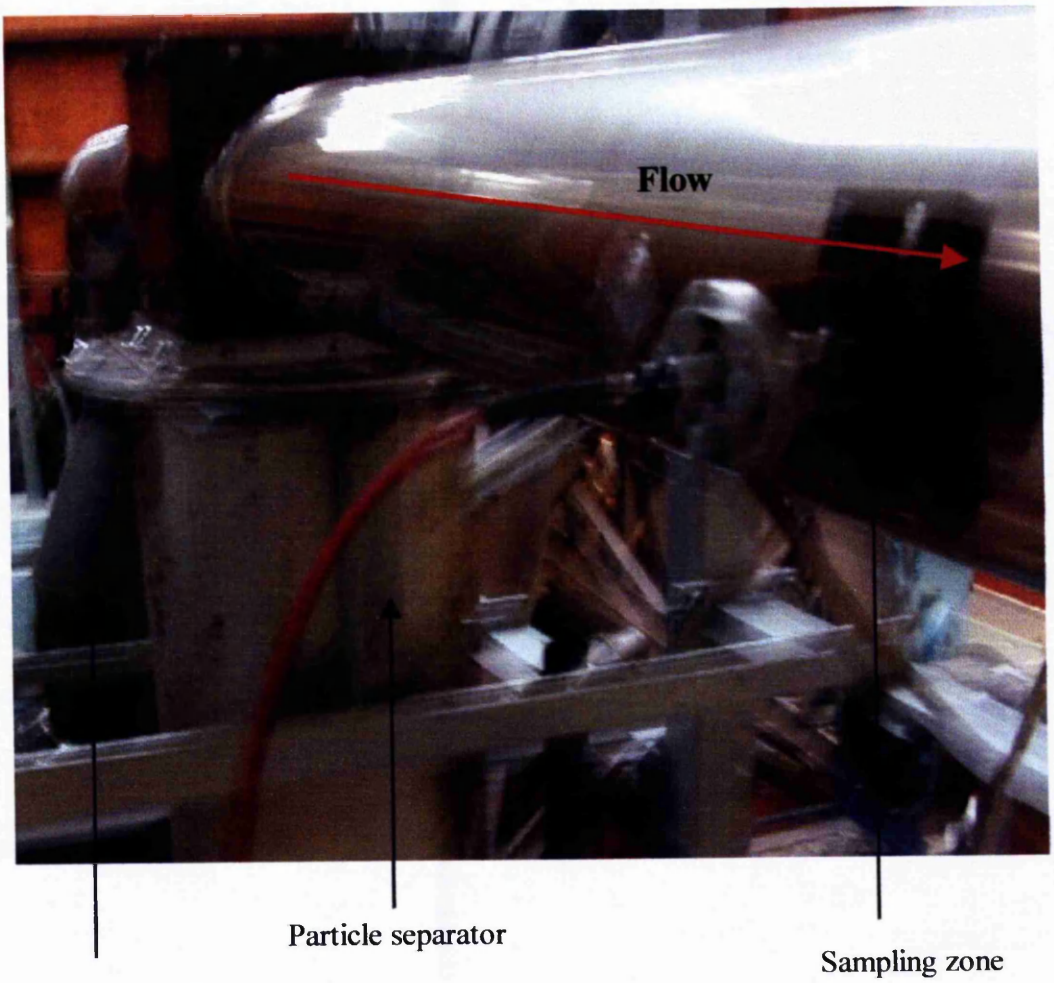

Figure 6. 21 Location of the particle separator in the horizontal exhaust duct

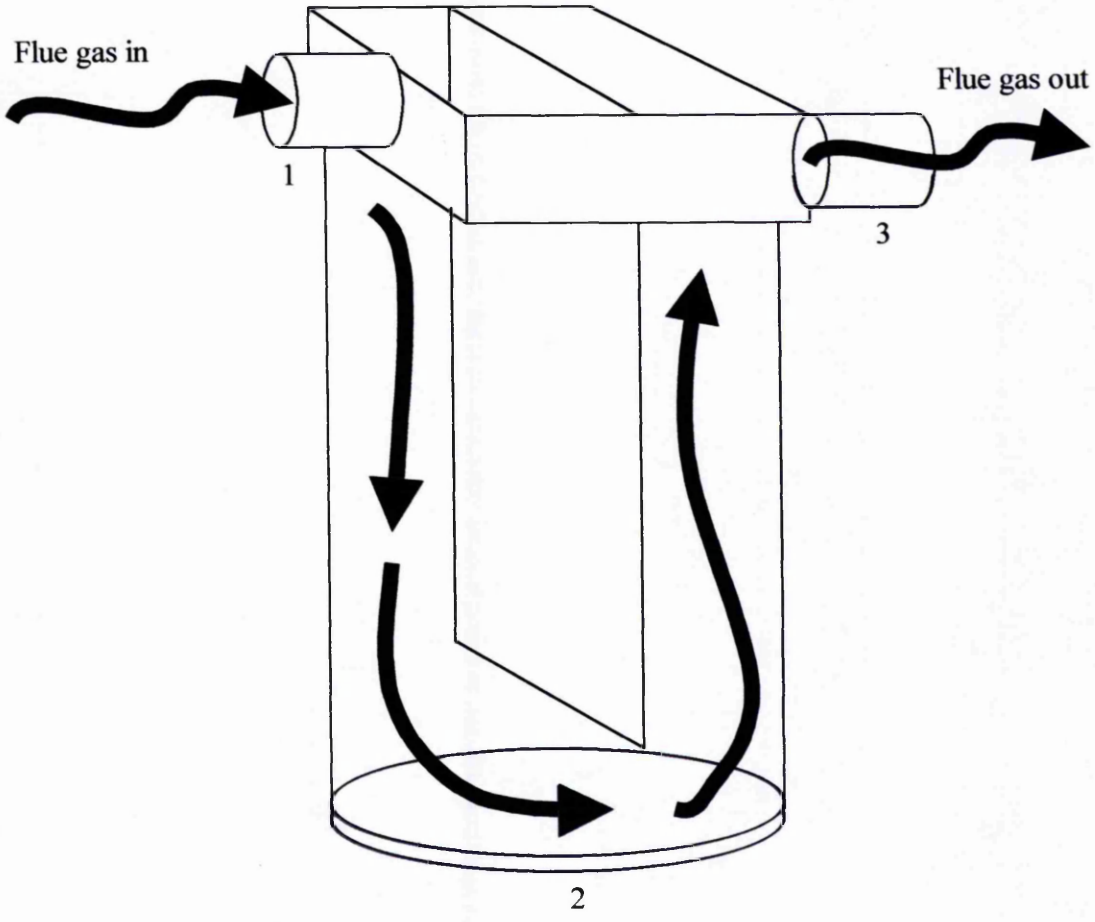

Figure 6. 22 Gas flow patterns within the particle separator unit.

Although this investigation has placed most emphasis on measurement of the $N0_2$ concentrations in the exhaust gas stream using an optical spectrometer, it was considered appropriate to take point measurements of carbon dioxide, carbon monoxide, excess air, and oxygen concentrations at various times during the combustion process. This was done in the knowledge that the oxygen and carbon dioxide concentrations are often used to indicate periods during which poor combustion conditions exist.

A traditional sampling gas analyser was therefore used to obtain measurements of the carbon dioxide, carbon monoxide, excess air, and oxygen concentrations.

The sampling probe was inserted into the exhaust gas stream approximately 100 mm downstream of the optical sampling point to ensure that its probe did not disturb the gas flow before the optical measurements were made.

Prior to carrying out the combustion experiment, the size of both the dRDf pellets and the coal pieces were reduced in an attempt to standardise the experimental conditions. Section 7.2 describes how this was achieved.

Chapter 7 Experimental procedure

7.1 Measurement of the $N0_2$ concentration levels in flue gas stream

Although the application of optical techniques in combustion processes has provided new ways for accurate measurements of species concentration, it seems that these techniques have not usually been used in a hostile environment. For example, several authors, including McKinnon et al (1991), employed optical techniques to detect hydrocarbon species in a laminar air/methane diffusion flame and a premixed air/methane flame. It was obvious that the exhaust gases produced from such a laminar air/methane diffusion flame or a premixed air/methane flame would carry relatively fewer dust particles than the exhaust gases produced during the combustion of solid fuel. Consequently, the need to examine the application of optical techniques in a hostile environment must be of considerable practical interest.

Most optical techniques are known to suffer from attenuation of the incident light due to the presence of dust particles in the exhaust gases. However, one optical method which does not suffer from this attenuation of the incident light due to dust particles is the infrared attenuation method as stated by McKinnon et al (1992). The authors found that the attenuation of light energy due to the presence of dust particles (light scattering intensity) is proportional to the product of λ^{-4} so that attenuation reduces as the wavelength increases.

In the present investigation, an optical transmission technique with a UV light source has been employed to measure the $N0_2$ concentration levels in the exhaust gas stream for various mixtures of coal and dRDF.

In choosing to operate in the UV range, however, it was noted that the use of wavelengths shorter than approximately 330 nm would result in interference from the $S0_2$ produced during the combustion of the coal. The data in figure 4.9 also show that in a situation where the UV-visible wavelengths are used to monitor $N0_2$, the presence of $S0_2$ may lead to some interference below approximately 330 nm. In the present investigation, therefore, interference from $S0_2$ was avoided by measuring the absorption due to $N0_2$ in the visible region. Several authors including Svanberg (2001), Weibring et al (2002) have shown that $S0_2$ absorbs light energy within the UV region. On the basis of the above observations, it was concluded that difficulties associated with the presence of $S0_2$ could best be minimised by measuring the absorption characteristics of $N0_2$ in the visible region.

The decision to focus on the measurement of $N0_2$ concentration levels in the exhaust during the co-combustion of dRDF/coal was motivated by various factors including the new EU Directive which requires the reduction of nitrogen dioxide from all waste reactors. Awareness of the growing commercial interest of power generation using fuel made from municipal waste, and especially when in the form of dRDF pellets, has also stimulated the present investigation.

Although there is a growing commercial interest in the use of waste for power generation, most solid fuel users prefer to use fuel with the heating capacity of at least 30 MJ/kg (Gera and Gautam (1993)). Since the heating capacity of dRDF is only two-thirds of this minimum value, it was assumed that adding a certain percentage of coal to the dRDF could be used to boost the heating capacity of the mixture to an acceptable level.

This investigation would then enable the optimum mixture to be determined, based upon the levels of gaseous emissions during the combustion process. A laboratory scale combustion test rig with access for optical and temperature-probing system was constructed. This is described in the next section.

7.2 Preparation of the fuel

As a basis for subsequent discussion, dRDF pellets are manufactured from combustible municipal solid waste. Before the municipal solid waste is converted into dRDF pellets, all non-combustible materials such as glass, aluminium, and ferrous metals are removed. The remaining organic materials are then chopped or crushed to produce a relatively homogeneous waste fuel. This is then mixed with a limestone binder, and is extruded into pellets of approximately 25 mm diameter and varying length.

In an attempt to standardise the conditions for this experimental programme, the length of the dRDF pellets was reduced (by hand) to approximately 10 mm and the coal to a size between 5 to 10 mm. A nominal coal size between 5 and 10 mm was achieved by crushing the coal into smaller sizes. Two standard sieves were then employed to produce the required range of sizes.

Typical dRDF pellets, as received, are shown in figure 7.1 while the standardised pellets are shown in figure 7.2. It was assumed that reducing the size of the dRDF pellets and the coal pieces would improve the combustion characteristics of the fuel mixture and would ensure that some uniformity was achieved.

Then, with the preparation of the fuels completed, both the proximate, and the ultimate analysis for coal and dRDF were obtained prior to the programme of combustion experiments. This analysis were carried out to determine the level of nitrogen in both the dRDF and the coal together with other elements such as the level of volatile matter which might influence the formation of nitrogen dioxide.

Figure 7. 1 typical sample of dRDF fuel as received

Source: **Manufactured by Reprotech (Pebsham) Ltd**

Figure 7. 2 A typical sample of the dRDF after preparation (approximately 10 mm lengths)

7.3 Fuel analysis

The proximate, and the ultimate analysis of coal and dRDF used in the present investigation are presented in table 7.1.

Table 7. 1 Chemical analysis of dRDF and coal

Proximate Analysis % wt as received	Fuel Type	
	dRDF	Coal
Volatile matter	68.1 ± 5%	36%
Moisture	10.2 ± 5%	0.49%
Ash	9.7 ± 3%	21.8%
Fixed carbon	12 ± 2%	52%
Ultimate Analysis % wt as received		
Carbon	38 - 43.3%	71.6%
Hydrogen	5.4 - 6.3%	2.6%
Oxygen	26.2 - 32.5%	9.6%
Nitrogen	0.4 - 0.6%	0.8%
Sulphur	0.12 - 0.2	0.3%
Calorific value MJ/kg	19.9 ± 1.3	29.6

7.4 Method of operation

Prior to each test run, the combustion chamber was thoroughly cleaned and a vacuum cleaner was used to remove any small pieces of ash and clinker. Each thermocouple was then tested and was set to the required depth of insertion. The weight of the fuel was recorded and the bed was charged. To avoid long test runs which could have damaged the grate, the maximum charge for each test run was fixed at 2 kg.

After the charging process, the furnace was moved onto position and connected to the flue gas receiving section (fixed section) as shown in figure 6.17. The data acquisition system was then prepared so that all the relevant data could be recorded.

To perform the data recording process, the optical spectrometer system was first tuned to the scope mode as shown in figure 6.5. Then, with the light source switched on, the data acquisition parameters were adjusted to give an indicated intensity of approximately 3500 counts/second for the transmitted light. The optical path between the two (transmission and receiving) lenses was then blocked so that the dark spectrum could be stored. Subsequently, the optical path was unblocked and the reference spectrum was stored. This allowed the data processing system to determine the absorbance of the gas medium in the optical path at any given wavelength using equation 6.1. Next, the system was switched to the transmission mode as shown in figure 6.6. This was done to test the stability of the radiation arriving at the detector for 100% transmission at a wavelength of 439.34 nm. Finally, the data processing system was switched to the absorbance mode as shown in figure 6.7.

A small (standardised 0.2 kg) mass of crushed charcoal soaked in methylated spirit was spread over the top surface of the fuel charge using a sight window. The charge was then ignited manually by introducing a burning match.

After allowing 2 to 3 minutes for the burning on the top of the bed to establish, the primary airflow rate was slowly increased to the required level. When the temperatures recorded by a thermocouple located at 750 mm above the grate had increased to the chosen threshold temperature of approximately 200°C, measurement of the gas concentration levels and the fuel bed temperatures was initiated.

As explained, in addition to the $N0_2$ concentrations, point measurements of the percentage of oxygen, excess air, and carbon dioxide, together with the concentration of carbon monoxide were made in the exhaust duct using a sample gas analyser[3].

The following equations are used for calculating the percentage of excess air, carbon dioxide and concentration of carbon dioxide.

$$Excess\ air = \left(\frac{0_{2\,set}}{0_{2\,set} - 0_2} - 1 \right) * 100 \qquad 7.1$$

where $0_{2\,set}$ = set oxygen value = 21%

0_2 = measured oxygen content

$$C0_2 = C0_{2\,max} * \frac{0_{2set} - 0_2}{0_{2set}} \qquad 7.2$$

where $C0_{2max}$ = fuel specific

$$C0 = \left(\frac{0_{2set} - 0_{2bz}}{0_{2\,set} - 0_2} \right) * C0\,(ppm) * 1.25 \qquad 7.3$$

where 0_{2bz} = 0_2 reference value

Data for the nitrogen dioxide emission levels and the fuel bed temperatures were recorded every 10 seconds for 35 minutes into the combustion process.At the end of this period, the airflow rate was reduced and held at a low level for 10 to 15 minutes so as to assist to allow the furnace to cool.

[3] Testo 342 – $S0_2$ flue gas analyser. Developed for heavy industrial applications. It enables the simple and precise measurement and control of flue gas temperature, oxygen content, $C0_2$ and C0 content, excess air, efficiency Gross/Net and $S0_2$ content. Test quality certified IS0 9001.

When the furnace had cooled to around room temperature, the ash was removed and weighted. The presence of any clinker was noted and the furnace and the grate were cleaned for the next test.

Since the fan and air control system was located approximately 5 m from the furnace, a CCD digital colour camera TC-5173T was used to transmit an image of the flame image onto a television monitor. This monitor was located next to the air control valve to make it easer for the operator to control the primary airflow rate by observing the reaction of the combustion process as illustrated in figure 7.3. The television monitor also displayed a freeboard temperature which was used to indicate if the ignition process was being delayed due to an excessive rate of airflow. Based on the observed images of the flame and the indicative temperature which was at approximately 750 mm above the grate, it was possible after some practice to supply an appropriate amount of airflow to sustain the ignition process.

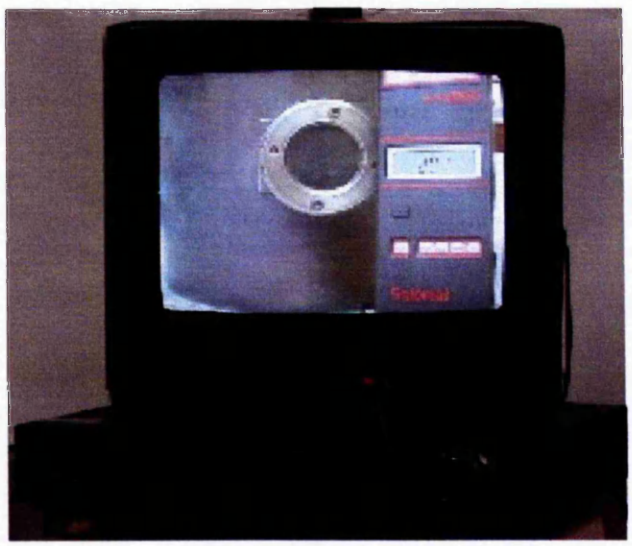

Figure 7. 3 A television monitor showing camera's view of the slight window and a thermocouple digitalmeter

Chapter 8 Results and discussion

8.1 Initial statement

The author performed combustion experiments using different mixtures of fuel. For simplicity, only a sample of the results obtained from these experiments have been presented and discussed in this chapter. This enables the main findings of the research to be identified and explained. The results from the remainder of the combustion experiments are presented in Appendix A with a brief commentary to explain the significance of the data obtained in each case.

8.1.1 Presentation of results

The results obtained during the combustion of different mixtures of coal and dRDF are presented and discussed in this chapter. As already stated in chapter 1, the objectives of the investigation were to determine the thermal characteristics and the emission levels for different mixtures of coal and dRDF. The emission levels covered were those of nitrogen dioxide, carbon dioxide, and oxygen, noting that, in practice, the levels of oxygen and carbon dioxide can be used as indicators to the performance of a full-scale plant. Fuel mixtures consisting of 100% coal, 100% dRDF, 50/50% coal/dRDF, 60/40% coal/dRDF, 70/30% coal/dRDF were tested. These results are presented and discussed in section 8.2 to 8.6 respectively.

The combustion process for each fuel was examined under stoichiometric combustion conditions. Here, the term stoichiometric means that sufficient oxygen was present to sustain the oxidation reactions, enabling the carbon and hydrogen in the fuel to be converted into the by-products of combustion. The corresponding airflow rates for each fuel mixture have been calculated and are presented in Appendix B.

The bulk mean temperatures were measured using the thermocouples, continuous measurements of the nitrogen dioxide levels were obtained using the optical spectrometer, and spot measurements of the oxygen, carbon dioxide, and excess air concentrations were made with an intrusive flue gas analyser as described earlier in section 7.4.

In addition, photographic images of the flames for the different mixtures were recorded at various combustion conditions. The time at which each image, determined by the time needed for the gas analyser to reach a stable reading, was recorded: the corresponding oxygen and carbon dioxide concentration levels are also shown below each flame image. Note, that the temperature reading which is indicated on the left hand side of each flame image was recorded at 750 mm above the grate. Why it was felt appropriate to display the flue gas temperature while monitoring the emission levels generated during the combustion process was discussed earlier in section 7.4.

8.1.2 Identifying the stages in the combustion process

The combustion process for a solid fuel, unlike that for liquid and gaseous fuels, usually takes place in two stages as shown in figure 8.1. These are known as the ignition, and the burnout stages (Spliethoff et al (1999)), Rampling et al (1993), and Gera et al (1993)). The ignition stage is assumed to start when the top of the fuel bed reaches its ignition temperature, while the burnout stage starts when the fuel at the base of the combustion chamber ignites. The burnout phase is assumed to finish when the fuel temperature begins to fall rapidly.

Since the use of dRDF as an alternative energy source for power generation is increasing, it is of practical interest to determine how these two stages of combustion

influence the emission levels generated during the co-combustion of coal and dRDF. the reader should observe that these two stages will not receive so much emphasis subsequently but will often be referred to during the discussion of the experimental results.

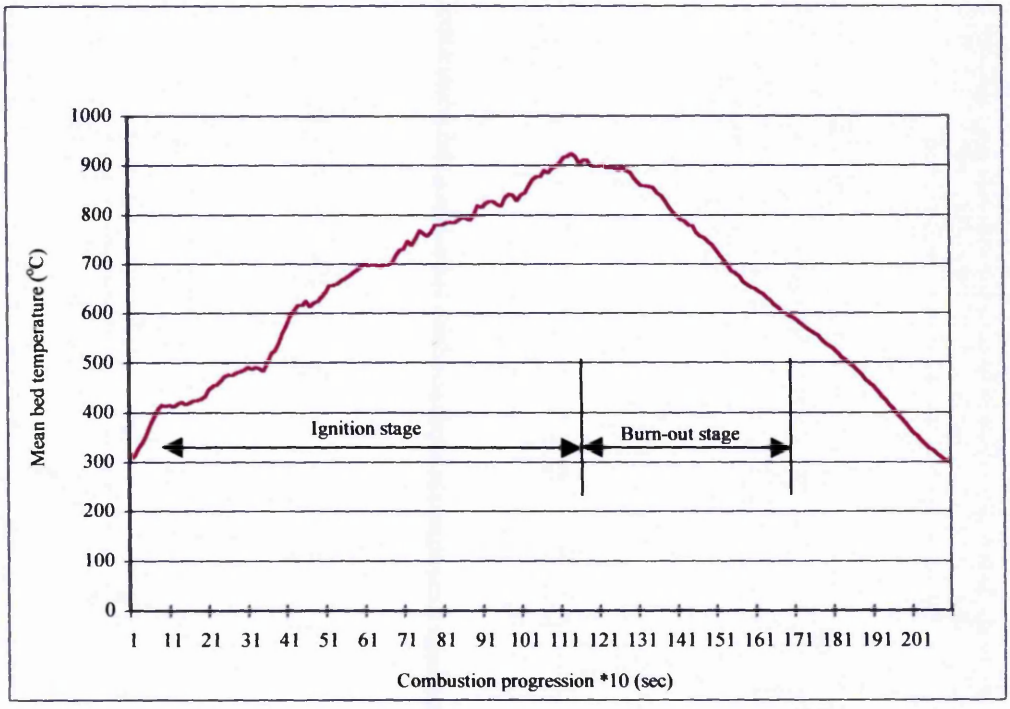

Figure 8. 1 Two stages of combustion for solid fuel

8.1.3 Order of presentation

The results are presented as follows. Figures 8.2 to 8.10 show the emission levels and photographic images of the flames for each of the five different fuels. The rest of the results, including the temperature profiles (bulk temperature versus time) for different fuel mixtures recorded at different positions as described earlier in section 6.8 are presented in Appendix A.

8.2 Combustion performance for 100% coal

Typical temperature profile and emission levels which were observed during the combustion process for 100% coal are shown in figures 8.2 and 8.3. These results indicate that coal char was very reactive. The reactivity of the coal char occurred towards the beginning of the burnout stage as evident in the results of figures 8.2(a) and 8.3 by a relatively low oxygen concentration of 1.4%. Note, that the low oxygen concentration of 1.4% in both figures means that, between the start of the combustion process and the time when this value was recorded, oxygen concentration levels in the flue duct reduced from 21% to 1.4%. In fact, this value of 1.4% was recorded at approximately 1074 seconds (17.9 minutes) in figure 8.2(a) and at 1268 seconds (21 minutes) in figure 8.3 into the start of the combustion process.

These measurements indicate that the combustion of 100% coal produced relatively high carbon dioxide levels towards the burnout stage based on the actually spot measured values of carbon dioxide. The appearance of these relatively high carbon dioxide levels observed towards the burnout stage was taken to confirm the reactivity of the coal char. In fact, the same high level of 17.9% a carbon dioxide was recorded in both figures 8.2(a) and 8.3 (although at slightly different times approaching the burnout stage) as mentioned in the previous paragraph. In both cases, the concentration level of excess air was 7.1%, indicating a negligible energy loss in the form of sensible heat in the excess air. Note that values of excess air are not indicated in the experimental results because of the reasons discussed in section 7.4.

With regard to the emission levels of nitrogen dioxide, the results in figure 8.2(a) for relatively high ignition rates reveal that the $N0_2$ emission levels reached a maximum close to the peak mean temperatures, suggesting that the thermal N0x dominated the

production of NO_2. Overall, the results for the combustion of coal alone show that the NO_2 concentration levels ranged from 8ppm to 41ppm with the maximum being recorded at the peak mean temperature. As discussed in section 4.2, thermal N0x dominates at temperatures above 1200°C. Considering figure 8.2(d) which shows a temperature reading of 851.4°C (recorded at 750 mm above the grate at 1157 seconds (19.6 minutes) into the start of the combustion process), it is appropriate to conclude that the flame temperatures a few millimetres above the fuel would have been higher than the mean temperature indicated in figure 8.2(a). This assumption was based on the fact that at 1157 seconds (19.6 minutes) into the start of the combustion process, the flue gas temperature at 750 mm above the grate was 851.4°C as shown in figure 8.2(d). Based on this observation, it is assumed that of high temperatures could have existed in the combustion chamber which could have influenced the formation of thermal N0x in figure 8.2(a).

Note that the observed variation in the thermal processes and the NO_2 emission levels, as revealed in figures 8.2(a) and 8.3, is believed to have arisen because of variations in the size distribution of the coal particles. Although an attempt was made to control the size of the dRDF fuel particles, no steps except crude size control using coarse filters were taken to control the size distribution of coal particles. It is therefore concluded that the 100% coal sample which was used in the experiments covered by the results in figure 8.2 was dominated by fuel particles near to the lower limit (of 5mm) which resulted in a relatively short ignition delay.

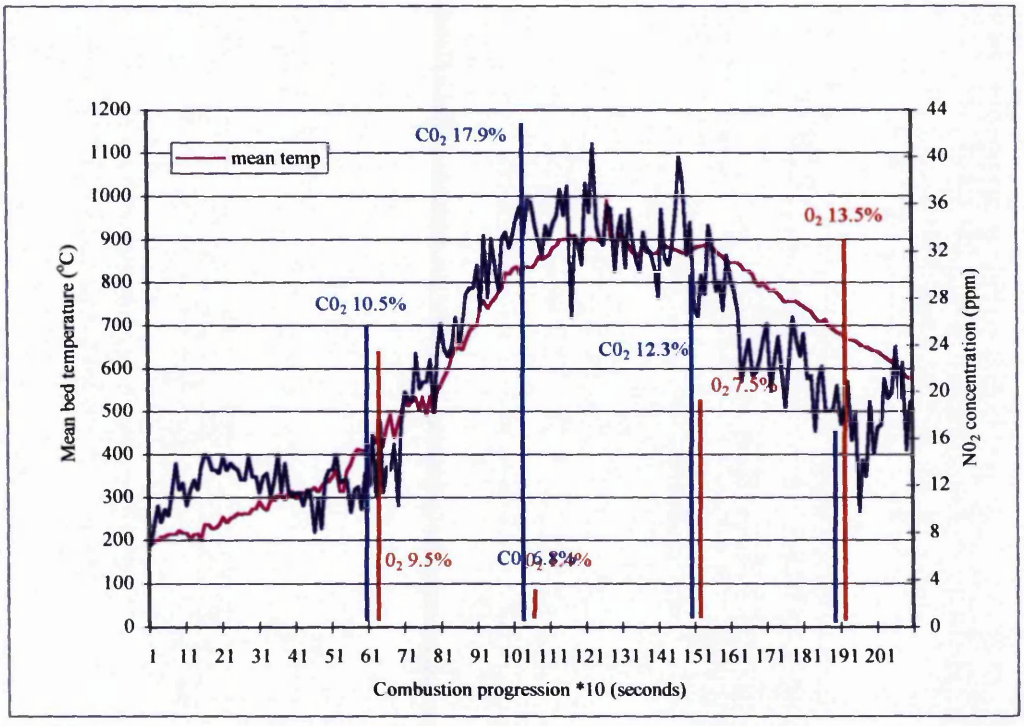

(a)

Flame 1(b)

Recorded at 622 seconds. Oxygen = 9.5%. carbon dioxide = 10.5%.

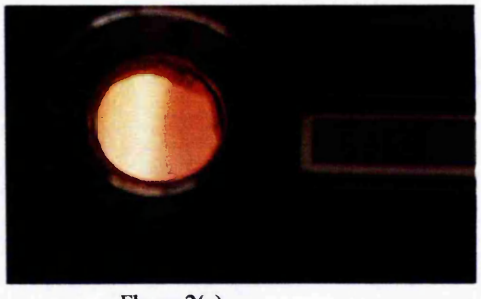

Flame 2(c)

Recorded at 702 seconds. Oxygen = 8% , carbon dioxide = 12%.

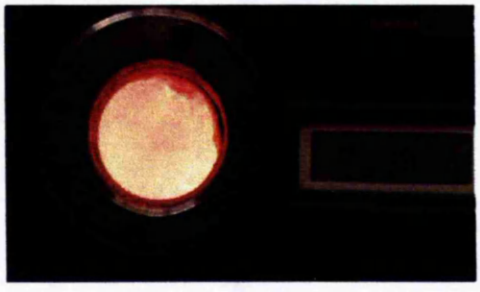

Flame 3(d)

Recorded at 1175 seconds.

Figure 8. 2 Emission levels and flame images for 100% fuel

N.B. images taken during the ignition stage

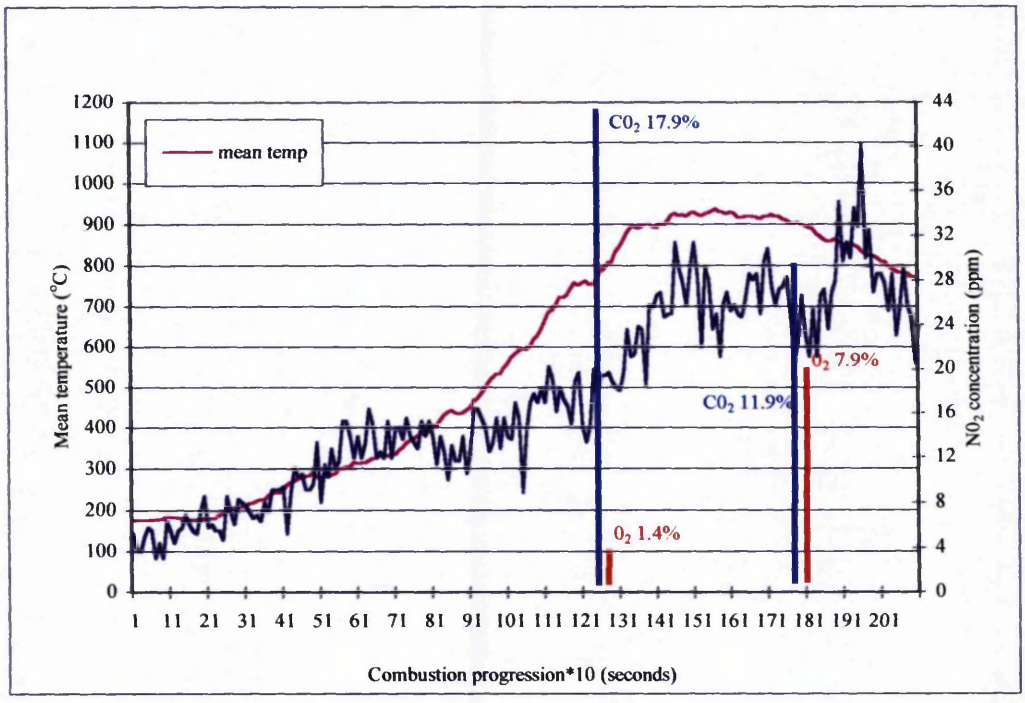

Figure 8. 3 Emission levels for 100% coal

8.3 Combustion performance for 100% dRDF.

Typical temperature and emission levels which were observed during the combustion process of 100% dRDF are shown in figure 8.4(a). These data should be viewed in parallel with Figure 8.4(b) which shows the flame image recorded at approximately 300 seconds (5 minutes) into the combustion process.

Here, it needs to be explained that the emission levels of nitrogen dioxide could not be recorded during the combustion of 100% dRDF. In this situation, relatively high levels of soot were produced which led to the saturation of the optical monitoring system as discussed earlier in section 5.2. For this reason, no $N0_2$ data can be included in figure 8.4(a).

These relatively high emission levels of soot in the combustion chamber were also observable in the flame image shown in figure 8.4(b). It can be seen that figure 8.4(b) recorded during the ignition stage displays a smoky flame despite the relatively high oxygen concentration levels which were above the minimum limit of 6% specified in the new EU Directive 2000/76/EU as described in section 2.8. This smoky flame in the presence of relatively high oxygen concentration levels suggests that the rate in which oxygen was absorbed by the reaction was low. In turn, this suggests that relatively high levels of volatile matter of dRDF were present – table 7.1 supports this assumption.

Comparing the emission levels of carbon dioxide, generated during the combustion of 100% dRDF, with those generated during the combustion of 100% coal, the results in figures 8.4(a) for 100% dRDF shows that the combustion of this fuel produced carbon dioxide emission levels which were lower than those for the combustion of 100% coal. Such an observation strengthens the view expressed earlier by the author that the rate in which oxygen was absorbed in the reaction was relatively low for the combustion of 100% dRDF.

This relatively low emission of carbon dioxide in the combustion of dRDF alone (figure 8.4 (a)) is consistent with the observations made by Swithenbank et al (1999). Additionally, these authors stated that the carbon dioxide produced by the combustion of waste does not actually add carbon dioxide to the carbon cycle of the biosphere because this same waste already forms part of a bio-cycle. Based on this thinking, and particularly on the results in figure 8.4(a) for 100% dRDF fuel, it is clear that the waste-to-energy conversion method should help to reduce the build-up of carbon

dioxide in the atmosphere by reducing our dependence on fossil fuels. Carbon dioxide gas is the major greenhouse gas as discussed in chapter 1.

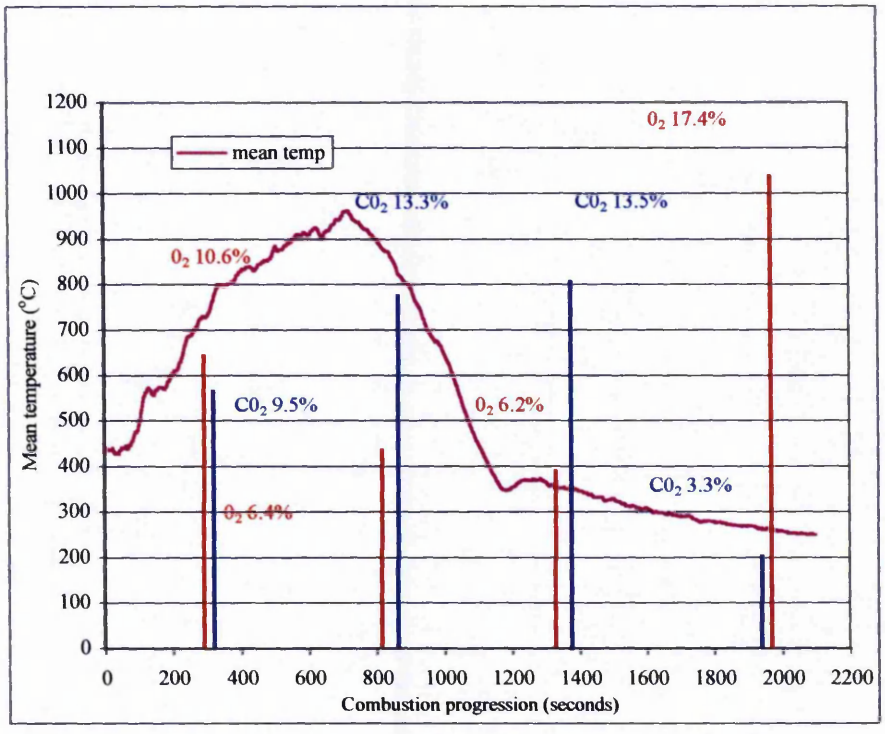

(a)

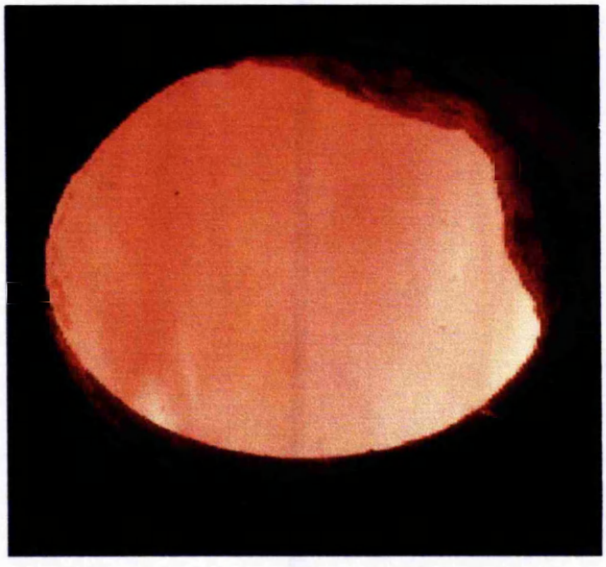

Flame 1(b)

Figure 8. 4 Emission levels and flame image for 100% dRDF
N.B image taken during the ignition stage

8.4 Combustion performance for 50/50% coal/dRDF fuel mixture

Typical temperature profiles and emission levels which were observed during the combustion process for a 50/50% mixture are shown in figures 8.5(a) and 8.6(a). The first observation which can be made, based upon these results is that this mixture burns easily and quickly. The rapid rates of reaction are confirmed by the high rate of depletion of the oxygen which leads to relatively low concentrations of this gas in the exhaust, especially during the ignition stage. For example, figure 8.5(a) shows that the oxygen concentration fell to 3.1% and that this value was reached during the ignition stage at approximately 744 seconds (12.4 minutes) from the start of the combustion process. Clearly, this level of oxygen is significantly below the minimum limit of 6% specified in the new European Directive 2000/76/EC. The low concentration of oxygen which was below the minimum limit of 6% can also be seen in figure 8.6(a) for the 50/50% fuel mixture.

Comparing the peak $N0_2$ emission levels recorded in figures 8.5(a) and 8.6(a) (normally for the same 50/50% fuel mixture and the same combustion conditions), it is clear that there was some variation between the $N0_2$ emission levels for these two experiments (87ppm vs 50 ppm). These changes represent a 43% variation in the $N0_2$ levels.

The variation of $N0_2$ emission levels as shown in figures 8.5(a) and 8.6(a) (for 50/50% fuel mixture) was influenced by the rate of ignition. Thus when the ignition rate was relatively low (based on the bulk mean temperature), the peak $N0_2$ emission level was also seen to be relatively low as shown in figure 8.6(a). Comparing the bulk mean temperature in figure 8.5(a) with those shown in figure 8.6(a) it can be seen that there was delayed ignition evident in the results of figure 8.6(a) by nearly constant

bulk mean temperature between the start of the ignition process and at approximately 310 seconds (5.2 minutes) into the combustion process. It is also believed that the observed variation in ignition rate (based on the bulk mean temperature) was because of the size distribution of fuel mixture and the hydroscopic characteristics of dRDF. Note, that there was no attempt made to control the moisture content of the fuel.

Although there was variation of NO_2 emission levels as shown in figures 8.5(a) and 8.6(a), the results (for the 50/50% fuel show that the peak NO_2 emission levels occurred at the maximum ignition rates and corresponded to the highest recorded (actual) carbon dioxide emission levels during the ignition stage.

In fact, in figure 8.5(a) the flue gas concentrations of carbon dioxide and oxygen of 16.3% and 3.1% were recorded respectively at approximately 744 seconds (12.4 minutes) from the start of the combustion process. These were recorded at the peak range of NO_2 emission levels. Figure 8.6(a) also show a similar profile where the peak range of NO_2 emission levels occurred at the maximum ignition rate and corresponded to the flue gas concentrations of carbon dioxide and oxygen of 14.8% and 4.7% respectively, recorded at approximately 1045 seconds (17.4 minutes) from the start of the combustion process. Note, that the variation in the time at peak NO_2 emission levels as shown in figures 8.5(a) and 8.6(a) was because of the reasons discussed earlier in the present section and in sections 8.2 and 8.3.

The rapid nature of the combustion for the 50/50% coal/dRDF fuel mixture, producing low levels of oxygen in the exhaust duct during the ignition stage, was also observable in the flame images shown in figure 8.5(b), (c) and (d): these were recorded during the ignition stage. It can be seen that these flame images display smoky regions with relatively low intensity when compared with the flame image in

figure 8.4(b) for 100% dRDF. It can also be seen that the corresponding level of oxygen in the exhaust for the three images (referred to as flames (1, 2 and 3) were well above the specified limit of 6% indicating that there was sufficient oxygen but the rate at which it was absorbed in the reaction was relatively low. Based on this observation, these smoky regions are taken to confirm similar view as described in section 8.3.

The flame images in figure 8.5(b), (c) and (d), taken during the ignition stage, can be compared with the image in figure 8.6(b), obtained for the same 50/50% coal/dRDF fuel mixture but at a later time corresponding to the end of the ignition stage. This shows a relatively high flame intensity and an absence of smoky regions. In fact, an oxygen concentration of 9.2% was achieved at approximately 792 seconds (13.2 minutes) into the combustion process as shown in figure 8.6, suggesting that the ignition rate at this stage was relatively low so that the rate at which oxygen was absorbed in the reaction was correspondingly high. The 9.2% oxygen concentration at 792 seconds (13.2 minutes) compares with an oxygen concentration of 8.8% for the flame image shown in figure 8.5(d) taken at 457 seconds (7.6 minutes) into the combustion process. This comparison strengthens the conclusion that the oxygen was consumed very rapidly during the ignition stage for the 50/50% fuel mixture in figure 8.5(a).

Despite the rapid depletion of the oxygen levels during the ignition stage for the combustion of 50/50% coal/dRDF fuel mixture, the data presented in figure 8.5(a) show that the oxygen values began to rise towards the end of the ignition stage. This rise in the oxygen level was associated with a fall in the $N0_2$ concentration. For example, between 744 seconds (12.4 minutes) and 1392 seconds (23.2 minutes) from

the start of the combustion process, the oxygen concentration showed an increase from 3.1% to 10.4%, corresponding to an increase of excess air from 17.4% to 98.1%. Note, that the values for the excess air concentrations are not shown in any of the figures, although values were recorded at various combustion conditions as mentioned earlier in section 8.1.2.

For this increase in both the oxygen and excess air levels between 12.4 and 23.2 minutes, the $N0_2$ concentration fell from 60.8ppm to 12.2ppm. This reduction in the $N0_2$ concentration, while the oxygen and excess air concentrations both increased, confirms that the combustion process for the dRDF (assumed to be the major source for the formation of prompt N0x,) was nearly completed.

In figures 8.5(a) and 8.6(a), for the 50/50% fuel mixture, the results reveal that the mean temperatures at which the peak $N0_2$ appeared were well below the lower limit of 850°C specified in the European Directive. In fact, the mean temperature observed in figure 8.5(a) at approximately 744 seconds (12.4 minutes) into the combustion process was 800°C while in figure 8.6(a) the same mean temperature was reached at approximately 1045 seconds (17.4 minutes) into the combustion process.

The results in figure 8.5(a) (for the 50/50% fuel mixture) show that the peak $N0_2$ emission levels occurred at approximately 744 seconds (12.4 minutes) from the start of the combustion process. It is worth noting that these peak $N0_2$ emission levels occurred at the maximum ignition rates and corresponded to the highest carbon dioxide emission levels during the ignition stage. On the basis of this, and other evidence such as the smoky flame images in figure 8.5(b), (c) and (d), it is concluded that "prompt N0x" dominated the formation of nitrogen dioxide in the ignition stage.

As discussed in section 4.2, prompt N0x is formed by a relatively fast reaction between combustion air and the hydrocarbon radicals released during the combustion process, and is generally most important at lower temperatures (Baukal and Romano (1992)).

In fact, Baukal and Romano (1992) noted that thermal N0x, which is formed by the high temperature reaction of atmospheric nitrogen with oxygen, only becomes a dominating mechanism at temperatures above 1200°C. A similar observation has been highlighted in the UK Guidance Note (S2 1.05). This states that $N0_2$ formation by thermal processes requires relatively high temperatures and that the thermal formation of N0x is relatively low below 1200°C. Such observations strengthen the view that "prompt N0x" dominated the formation of $N0_2$ in the ignition stage for this 50/50% fuel mixture.

Overall, the results for the 50/50% fuel mixture shown in figures 8.5(a) and 8.6(a) reveal that the $N0_2$ concentration levels ranged from 5ppm to 87ppm with the maximum being recorded at approximately 894 seconds (14.9 minutes) into the combustion process as shown in figure 8.5(a). However, it is clear that the $N0_2$ concentration levels recorded during the combustion of this 50/50 coal/dRDF fuel mixture remained well below the specified limit of 200ppm given in the new European Directive 2000/76/EC.

Considering the link between the levels of carbon dioxide and carbon monoxide in the exhaust, the results in figure 8.5(a) show that the carbon dioxide emission levels fall rapidly toward the end of the burnout stage for the 50/50% fuel mixture. In this same period, the carbon monoxide concentration levels rise. For example, in figure 8.5(a) when the carbon dioxide fell from 14.3% to 9.6%, the corresponding carbon

monoxide emission levels were 26ppm and 60ppm respectively. These results are consistent with the observations made by Swithenbank et al (1999) that such changes indicate that the charred fuel continues to burn by converting carbon dioxide to carbon monoxide.

In a practical full-size situation, where the moving grate will be designed to mix the bed in the vertical direction whilst transporting the waste towards the ash pit, all of the complex combustion processes described in chapter 8 will co-exist.

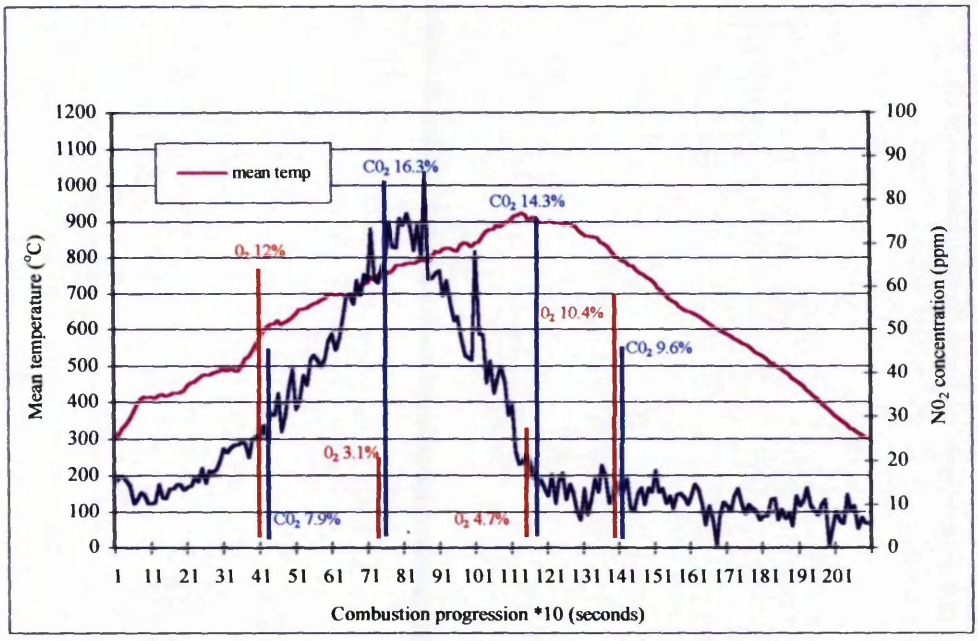

(a)

Flame 1(b)

Recorded at 350 seconds. Oxygen = 12.1%, carbon dioxide = 7.9%.

Flame 2(c)

Recorded at 400 seconds. Oxygen =11.1%, carbon dioxide = 8.9%.

Flame 3(d)

Recorded at 457 seconds. Oxygen = 8.8%, carbon dioxide = 11.2%

Figure 8. 5 Emission levels and flame images for 50/50% coal/dRDF

N.B. images taken during the ignition stage

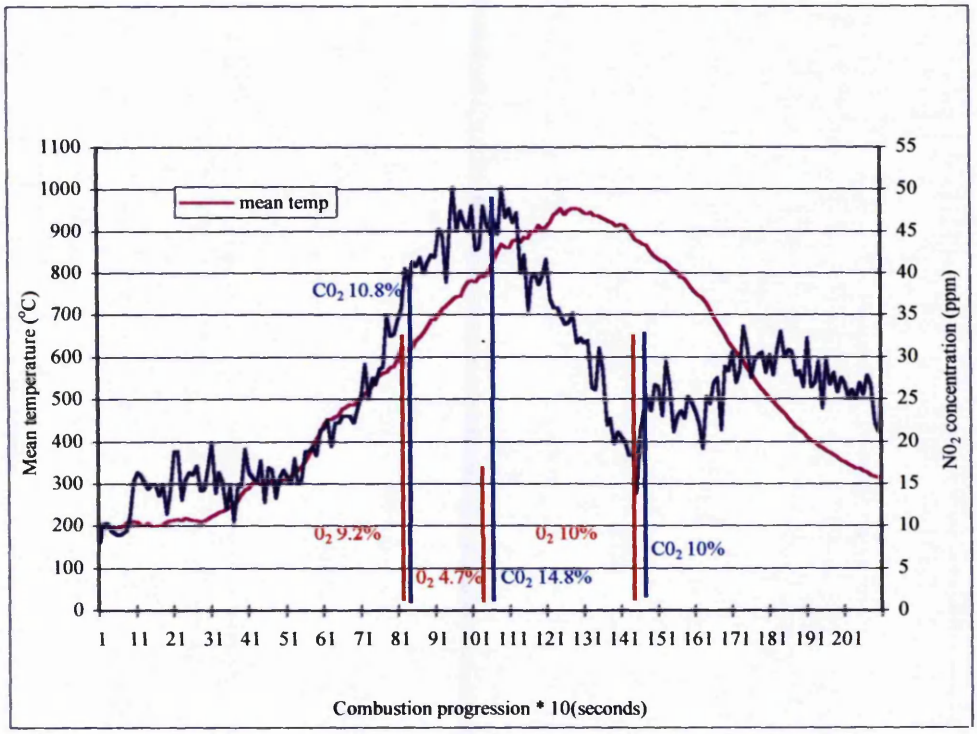

(a)

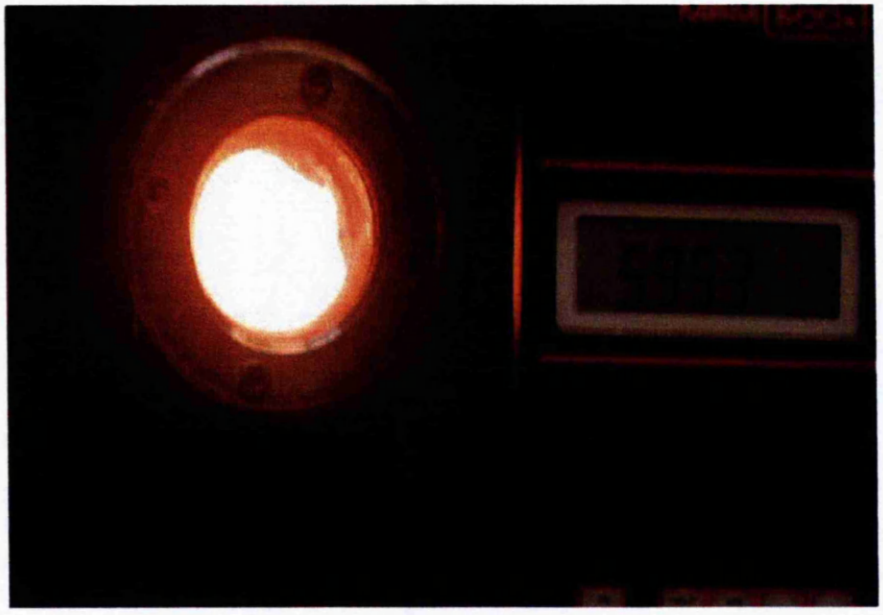

Flame 1(b)

Recorded at 794 seconds. Oxygen = 9.2%, carbon dioxide = 10.8%

Figure 8. 6 Emission levels and flame image for 50/50% coal/dRDF

N.B. images taken during the ignition stage

8.5 Combustion performance for 60/40% coal/dRDF

Typical temperature and emission levels observed during the combustion process for the 60/40% coal/dRDF fuel mixture are shown in figures 8.7 and 8.8. The results in both figures show that the oxygen concentration in both the ignition and burnout stages were relatively high. Interestingly, the $N0_2$ emission levels recorded in figures 8.7(a) and 8.8(a) ranged from 11ppm to 37ppm. These relatively low $N0_2$ levels and the relatively high oxygen concentrations, suggest that the fuel sample actually used was dominated by coal particles close to the upper size (of 10 mm).

Considering the results in figure 8.7(a) and 8.8(a), it can be seen that the temperature and emission profiles are nearly similar, confirming that repeatable combustion results can only be expected if the sample size distribution remains the same. Note, that achieving the same combustion conditions requires that the same oxygen levels are maintained and the distribution of fuel particles must remain unchanged for every test of the same fuel mixture.

Although the $N0_2$ emission levels recorded in figures 8.7(a) and 8.8(a) ranged from 11ppm to 37ppm, it is believed that if the oxygen levels in both figures had reduced to a value below 6% (as it was the case in figure 8.10 (a) for the 70/30% fuel mixture), then the $N0_2$ emission levels could have increased above 37ppm. This assumption is based on the finding that the $N0_2$ emission levels produced during the co-combustion of coal and dRDF increase with the increase in the rate of combustion.

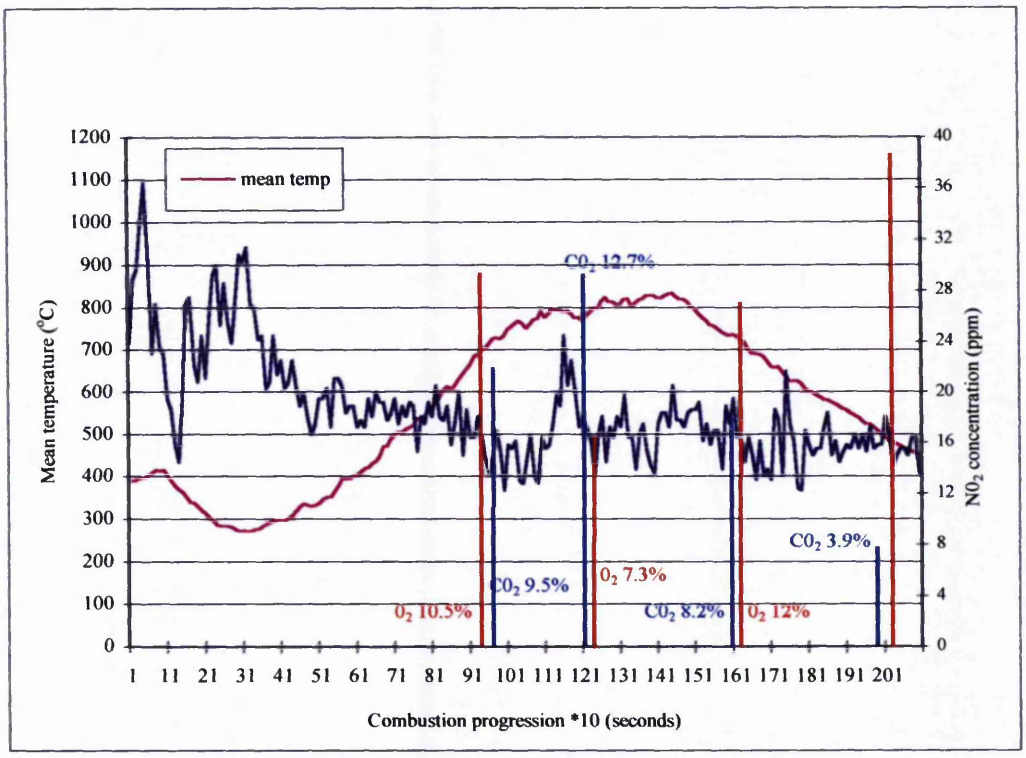

(a)

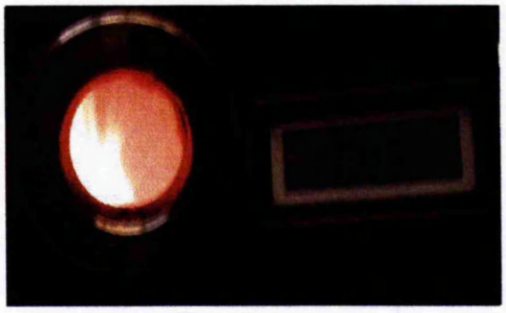

Flame 1(b)

Recorded at 920 seconds. Oxygen = 10.5%, carbon dioxide = 9.5%.

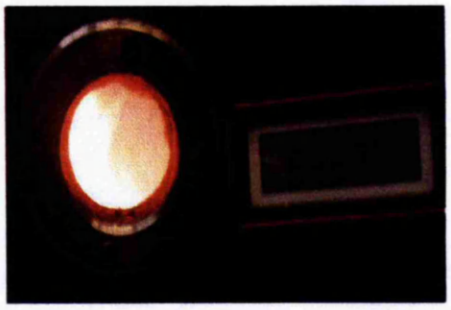

Flame 2(c)

Recorded at 980 seconds. Oxygen = 9.8%, carbon dioxide = 10.2%.

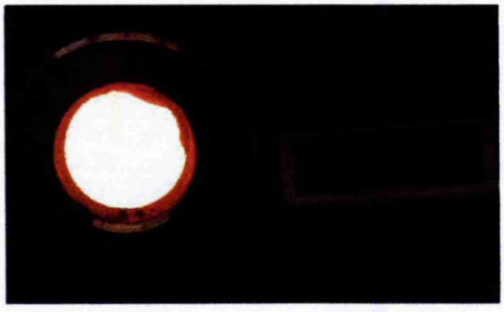

Flame 3(d)

Recorded at 1178 seconds. Oxygen = 7.1%, carbon dioxide = 12.9%

Figure 8. 7 Emission levels and flame images for 60/40% coal/dRDF

N.B. images taken during the ignition stage

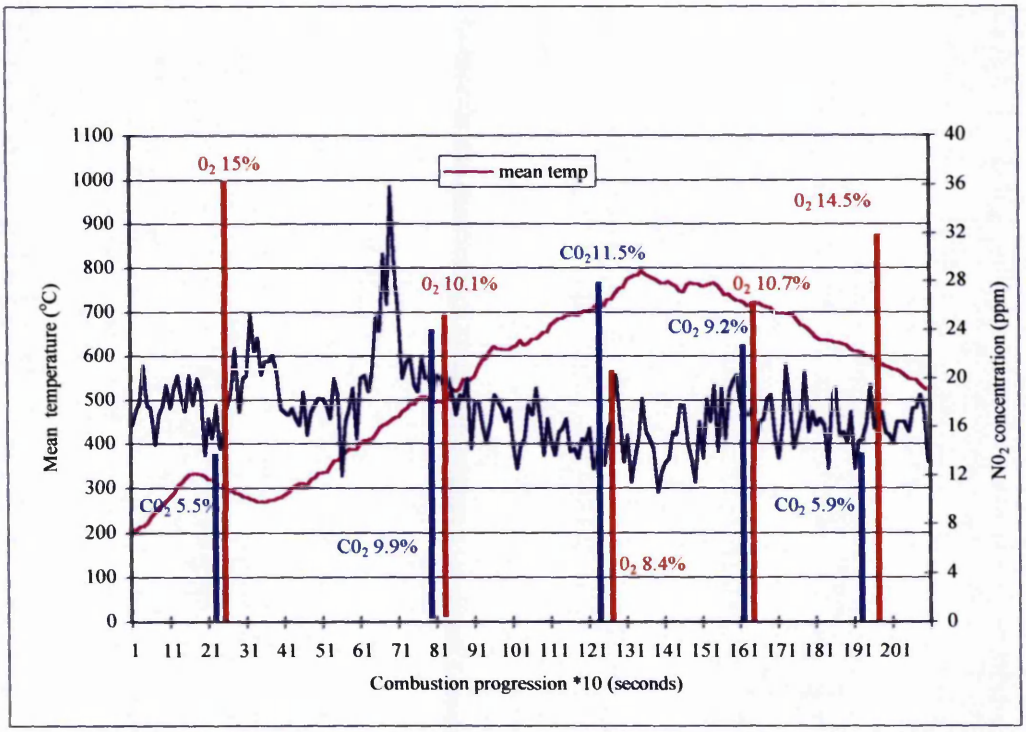

(a)

Flame 1(b)

Recorded at 154 seconds. Oxygen = 14.5%, carbon dioxide = 5.5%

Flame 2 (c)

Recorded at 588 seconds. Oxygen = 12.5%, carbon dioxide = 7.5%

Flame 3(d)

Recorded at 800 seconds. Oxygen = 10%, carbon dioxide = 10%

Figure 8. 8 Emission levels and flame images for 60/40% coal/dRDF

N.B. images taken during the ignition stage

8.6 Combustion performance for 70/30% coal/dRDF

Results for the 70/30% coal/dRDF fuel are presented in figures 8.9 and 8.10. Figure 8.9 shows that the oxygen concentration levels in both the ignition and the burnout stages were relatively high. Presumably, this could have been due to the relatively poor ignition characteristics of the fuel sample. In many cases, this caused the fuel bed to burn from one side during the early stages of ignition as clearly shown in the flame image (referred to as 1(b), (c) and (d) in figure 8.10.

Comparing the results in figures 8.9(a) and 8.10(a) for the 70/30% coal/dRDF fuel mixture, a long ignition delay is indicated by a fall in the mean temperature during the first few minutes from the start of the combustion process – figure 8.9(a). This was believed to be the cause of relatively high oxygen concentration levels in both the ignition and burnout stages, leading to relatively a low mean temperature and NO_2 emission levels in figure 8.9(a).

In practice, the effect of the high levels of excess oxygen, and hence the excess air, is to increase the sensible heat energy carried away in the flue gases.

Such combustion behaviour will result in a delayed ignition process as mentioned earlier and is consistent with the observations made by Swithenbank et al (1999). These authors noted that oxygen concentrations between 8% and 10% in the flue gas represent a great waste of energy which will reduce the thermal efficiency.

In the present investigation, it was noted that the oxygen concentration level of 6% given in European Directive 2000/76/EU yielded an excess air level of 40%. This can be compared with an excess air level of 76.5% corresponded to the oxygen concentration of 9.1% recorded in figure 8.9(a) at approximately 1264 seconds (21

minutes into the start of the combustion process. In terms of the thermal efficiency of the combustion process, any excess air can be equated with the loss of sensible heat and reduced conversion efficiency.

Although the was ignition was delayed for the experiment covered by figure 8.10(a), these results show that at approximately 410 seconds (6.8 minutes) the ignition rate improved, leading to relatively low concentration of oxygen especially during the ignition stage. Note, that the $N0_2$ emission levels towards the end of the burnout stage were relatively high in figure 8.10(a). It is believed that this was due to the difficulty in achieving a uniform spread of flame on top of the flue bed, suggesting that the combustion of dRDF (assumed to be the major source for the formation of the prompt N0x) was prolonged leading to relatively high levels of $N0_2$ towards the end of the burnout stage in figure 8.10(a).

These differences in the rates of combustion for normally identical tests using the same fuel mixture made it extremely difficult to produce repeated results for various fuel mixtures. Despite the difficulties in achieving a uniform spread of flame on top of the fuel bed as shown in figures 8.10(b), (c) and (d), these particular flame images do not show any significant smoky regions. These images can be compared with the flame images in figure 8.5(a), (b) and (c) for the 50/50% fuel mixture where smoky regions are evident.

Overall, the results for the 70/30% fuel mixture shown in figures 8.9(a) and 8.10(a) show that the $N0_2$ concentration levels ranged from 9ppm to 33ppm.

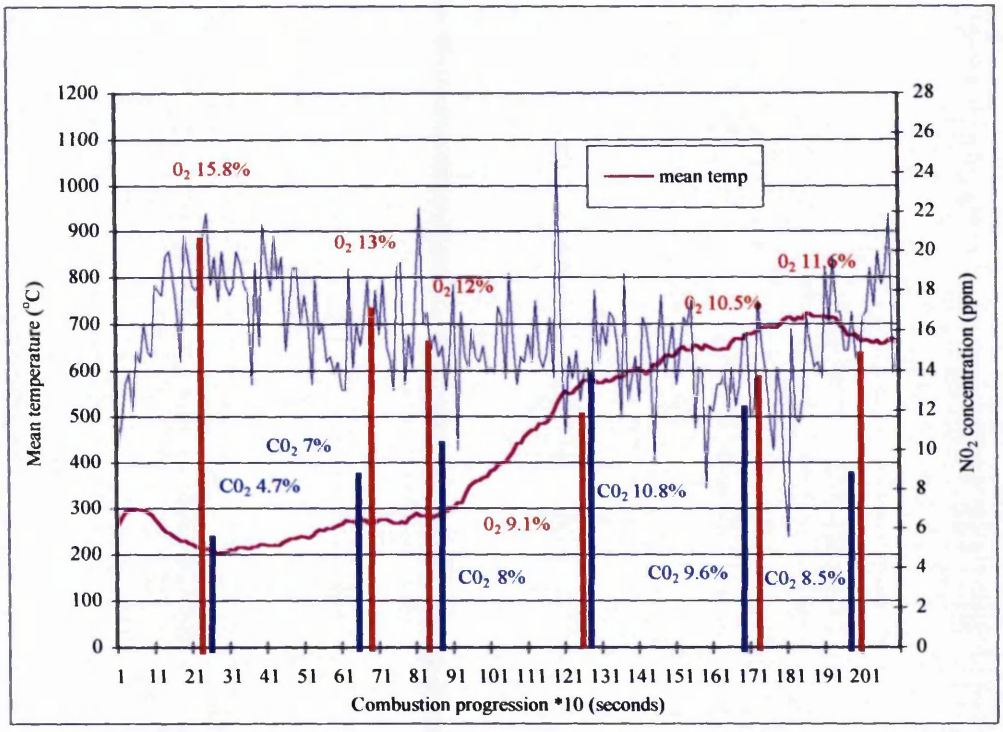

(a)

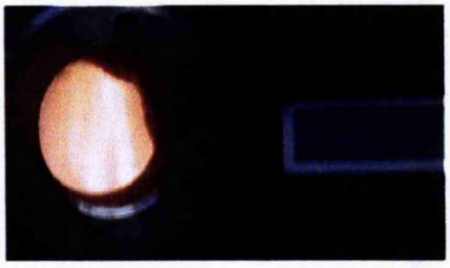

Flame 1(b)

Recorded at 676 seconds. Oxygen = 13%, carbon dioxide = 7%.

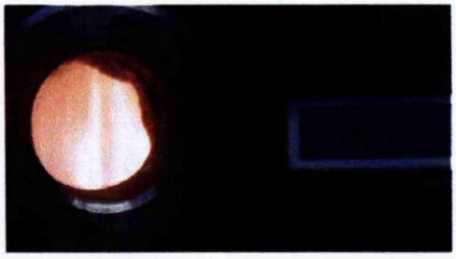

Flame 2(c)

Recorded at 830 seconds. Oxygen = 12%, carbon dioxide = 8%.

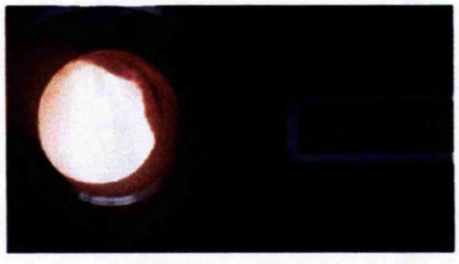

Flame 3(d)

Recorded at 1030 seconds. Oxygen = 10.5%, carbon dioxide = 9.5%.

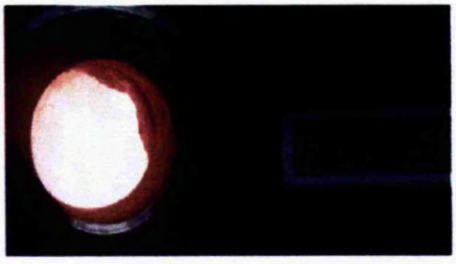

Flame 4(d)

Recorded at 1200 seconds. Oxygen = 9.4%, carbon dioxide = 10.6%.

Figure 8. 9 Emission levels and flame images for 70/30% coal/dRDF

N.B. images taken during the ignition stage

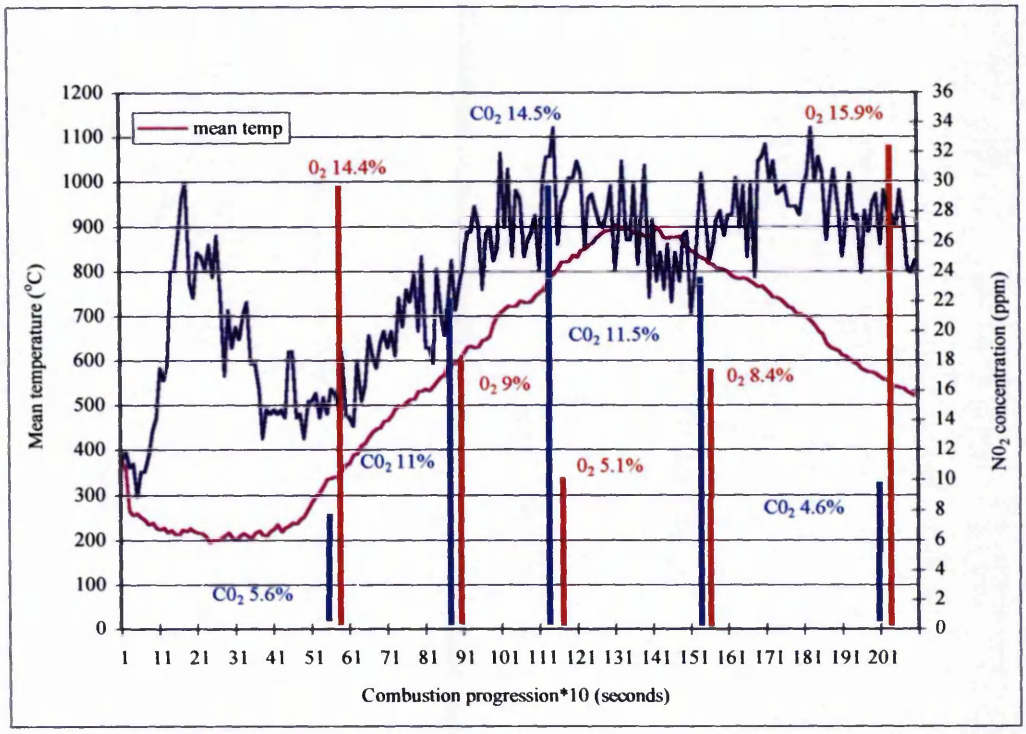

(a)

Flame 1(b)

Recorded at 597 seconds. Oxygen = 14.4%, carbon dioxide = 5.6%

Flame 2(c)

Recorded at 898 seconds. Oxygen = 9%, carbon dioxide = 11%

Flame 3(d)

Recorded at 787seconds. Oxygen = 11.2%, carbon dioxide = 8.8%

Flame 4(e)

Recorded at 1017 seconds. Oxygen = 6.7%, carbon dioxide = 13.3%

Flame 5(f)

Recorded at 1099 seconds. Oxygen = 6% , carbon dioxide = 14%

Figure 8. 10 Emission levels and flame images for 70/30% coal/dRDF

N.B. images taken during the ignition stage

8.7 Final comment on the results

The high temperature achieved in the combustion of dRDF is assumed to stem from the high levels of plastic materials in the fuel as revealed in figure 2.6. On the basis of the high flue gas temperatures achieved by the combustion of the dRDF, it is safe to conclude that the combustion of this fuel in a power generating plant would not require any supplementary fuel. However, the results of the present study have indicated that mixing the dRDF with coal leads to a reduction in the levels of the gaseous pollutants. For example, at 201 seconds (3.4 minutes) into the combustion process for the 50/50% fuel mixture in figure 8.6 the recorded carbon monoxide concentration level was 1247ppm. This value can be compared with the concentration of 4092 ppm recorded at 300 seconds (5 minutes) into the combustion process for the combustion of 100% dRDF in figure 8.4. This is one clear advantage of the mixed fuel approach.

8.8 Repeatability of testing

The experiments were repeated for various fuel mixtures and the results show that there are clear discrepancies between the different sets of results obtained for nominally the same fuel/fuel mixture. This lack of repeatability demonstrates one of the principal difficulties encountered by the author and other worker (Gera and Gautam (1993)) in making this type of experiment.

Discrepancies arise between the data for the same fuel/fuel mixture because of the following uncontrolled features of the experiments performed by the author.

i. It was impossible to control the ignition and combustion rates to the required levels.

ii. Variation in the size distribution of the coal and dRDF fuel particles proved to be more important than anticipated.

iii. There were almost certainly variations in the physical and thermal characteristics of the coal and dRDF used in the series of experiments. These could only have been accounted for if a detailed analysis has been performed for every fuel sample at the time of testing. With the facilities available to the to the author, this was never a possibility.

Chapter 9 Conclusion

Measurements of the gaseous emission levels and temperature variations have been made for various combinations of coal and pelletised waste derived fuel (dRDF).

- Observations of the thermal output of the dRDF based on the maximum mean temperature as shown in figure 8.4(a) confirm that the use of this fuel for power generation would not require it to be mixed with a supplementary fuel.

- Mixing dRDF with coal reduces the levels of soot and carbon monoxide produced during the combustion of dRDF alone as shown by the discussion in section 8.3.

- The combustion of dRDF alone produces relatively low carbon dioxide emission levels as shown by the data in figure 8.4(a).

- When the combustion rates are relatively high, a 70/30% coal/dRDF fuel mixture appears to represent the optimum. The results reveal a mean temperature around 900°C and relatively low levels of gaseous emissions which are comparable to those generated during the combustion of the coal alone. These findings are confirmed by the results presented in figures 8.2(a) and 8.10(a).

9.1 Suggestions for further work

- Mount the combustor chamber on a sensitive weighing balance. This would enable the ignition and combustion rates to be calculated.

- Improve the ignition process by incorporating gas burners a few millimetres above the fuel bed. These burners could then be switched off when the ignition is fully established.

- Improve the repeatability of the combustion process by controlling the size distribution of the dRDF and coal particles.

- Measure the moisture content of the dRDF and determine the chemical composition of each batch of fuel, with the intention of improving the repeatability of the combustion experiments.

- Replace the present particle separator with a cyclone and incorporate finer flue gas filters to eliminate any possibility of false optical signals.

- Improve the air delivery system into the combustion chamber to ensure a more even distribution of the flow across the fuel charge on the grate.

Chapter 10 References

1. **Acharya, P, DeCicco, S, G, and Navak, R, G.** Factors that can influence and control the emission of dioxides and furans from hazardous waste incinerators. Journal of the Air and Waste Management Association, volume 41, Part 1, 1991, pp 1605 - 1615.

2. **Alter, H. and Dunn, J. JJr.** Solid waste conversion to energy. Current European and US Practice. Ed. R. A. Young, P. N. Cheremisinoff. New York. Marcel Dekker, 1980, pp. 69-85.

3. **Andrews D. L.** Lasers in Chemistry. London, 1990, pp. 88 - 87.

4. **Anson, D.** Waste incineration as core of combined heat and power system. Energy Digest, volume 15, number 5, 1986, pp. 45-50.

5. **Barton, J.** Recycling and resources recovery. Harwell Waste Management Symposium. Waste management in the UK, 1988, pp, 54 - 62.

6. **Baukal, C. E, Romano, F. J.** Reducing N0x and particulate. Journal of Pollution Engineering, September 1, 1992, pp, 76 - 79.

7. **Beine, J. H, Dahlback, A, and Orback, J. B.** Measurements of $N0_2$ at Ny – alesund svalbard. Journal of Geophysical Research, volume 104, number D13, 1999, pp. 16009 - 16019.

8. **Brereton, C.** Municipal solid waste - incineration, air pollution control and ash management. Pollution control and management and environmental toxicology. Conservation and Recycling, volume 16, number 1-4, 1996, pp. 227-264.

9. **British Oxygen Company**. Gas data and safety sheet, special gases, nitrogen dioxide.

10. **Brown, T. M, Pitz, R. W, Hess, C. F, and Wood, C. P.** Smoke and $N0_2$ measurements by pulsed photothermal laser deflection. Applied Physics volume 59, 1991, pp. 351 - 356.

11. **Bulley, M. M.** Medical wastes management in Australasia. Medical waste incineration and pollution prevention. Ed. A. E. S. Green. Norstrand Reinhold. New York, 1992, pp. 65-70.

12. **Bury, K.** The Waste Industries in the UK. Journal of Waste Age, April, 1994, pp. 247-252.

13. **Chagger, H. K, Kendall, A, McDonald, A, Pourkashanian, M and Williams, A.** Formation of dioxides and other semi-volatile organic compounds in biomass combustion. Journal of Applied Energy, volume 60, 1998, pp. 101 - 114.

14. **Chagger, H. K., Jone, J. M, Pourkashanian, M. Williams, A.** The formation of VOC, PAH and Dioxins during incineration. Second International Symposium on Incineration and Flue Gas Treatment Technologies, 4 - 6 July, 1999, Sheffield University, UK, pp 3 - 12.

15. **Chamberlain, C. T.** Waste heat recovery from combustible wastes. Management and conservation of resources. IChemE. Pergamon Press, 1982.

16. **Commission of the European Communities.** Energy from municipal waste. Summary Report. Luxembourg, 1980/81.

17. **Commission of the European Communities.** Energy from waste. An evaluation of conversion technology. Eds. Parker, C. and Roberts, T. Elevier London Applied Science, 1985.

18. **Curlee, T. R., Susan, S. M., David, V. P., Amy Wolfe, K., Michael, K. P., and David, F. L.** Waste-to-energy in the United States. A Social and Economic Assessment. USA, Greenwood, 1994, pp 10 – 20.

19. **Darley, P. C.** Steam generation in industrial waste incineration plants. Power Generation by Combustion of Waste. IMechE, 1993, pp. 19-27.

20. **Davidson, J. A, Cantrell, C. A, McDaneil, A. H, Shetter, R. E, Madronich, S, and Calvert.** Visible – ultraviolet absorption cross-section for $N0_2$ as a function temperature. Journal of Geophysical Research, volume 104, 1988, pp. 7105 - 7111.

21. **Department of Health.** Report (COC/2000/S1) on cancer incidence near municipal solid waste incinerators in Great Britain by the Committee on Carcinogenicity, 2000.

22. **Department of the Environment and Welsh Office.** Making waste work. A Strategy for Sustainable Waste Management in England and Wales. HMSO, London, 1995.

23. **Department of the Environment, Transport and the Regions and National Assembly for Wale.** Waste Strategy for England and Wales, Part 1, CM 4693 – 1, London, 2000.

24. **Department of the Environment, Transport and the Regions.** A better quality of life. A Strategy for Sustainable Development for the UK, HMSO, London, 1999.

25. **Department of the environment.** A review of options, Waste Management Paper No 1. HMSO, London, 1992.

26. **Department of the environment.** Recycling, Waste Management Paper No 28. HMSO, London, 1992.

27. Digest of Environmental Statistics No. 20 1998, pp 171.

28. Directive of the prevention of air pollution from exciting municipal waste incineration **(89/429/EEC)**. Official Journal of the European Communities, December 1989.

29. Directive of the prevention of air pollution from new municipal waste incineration **(2000/76/EU).** Official Journal of the European Communities, December 2000.

30. Directive of the prevention of air pollution from new municipal waste incineration **(89/369/EEC).** Official Journal of the European Communities, December 1989.

31. **EC Coll EC 348 / S.** An energy policy for the European Union. White Paper of the European Commission, January 1996.

32. **Eduljee, G. H.** Organic micro-pollutant emissions from waste incineration. Waste incineration and the environment. Issue in environmental science and technology. Eds. R. E. Hester and R. M. Harrison. Royal Society of Chemistry. Great Britain, 1994, pp, 47 – 60.

33. **Elliot, S. J.** A comparative analysis of public concern over solid waste incinerators. Journal of Waste Management and Research, volume 16, number 4, 1998, pp. 351 - 364.

34. **Elliott. P, Shaddick, I. Kleinchmidt. I, Jolley. D, Walls. P, and Grundy, C.** Cancer incidence near municipal solid waste incinerators in Great Britain. British Journal of Cancer, volume 73, 1996, pp. 702 - 710.

35. **ENDS.** Report 245. Environmental Data Service Ltd. Bowling Green Lane, London, June 1995.

36. **ENDS.** Report 246. Environmental Data Service Ltd. Bowling Green Lane, London, July 1995.

37. **ENDS.** Report 265. Environmental Data Service Ltd. Bowling Green Lane, London, February 1997.

38. **ENDS.** Report 285 Environmental Data Service Ltd. Bowling Green Lane, London, 1998.

39. **Environment Agency.** Combustion of fuel manufactured from or comprised of solid waste in appliances 3 MW (th) and over S2 1.05, London, HMSO, 1996.

40. **Environment Agency.** Making solid fuel from waste. IPC guidance note. Waste Disposal and Recycling Sector S2 5. 02. London MHSO, 1996.

41. **Environment Agency.** Processes subject to integrated pollution control, waste incineration. Guidance Note S2 5.01, October 1996.

42. **Environment Agency.** Processes subject to integrated pollution control, combustion of fuel manufactured or comprised of solid waste. Guidance Note S2 1.05, September 1995.

43. **Environment Agency.** Processes subject to integrated pollution control, making solid fuel from waste. Guidance Note S2 5.02, July 1996.

44. **Environmental Protection Act 1990.** Process Guidance Note IPR 5/3. Municipal waste incineration, HMSO, London.

45. **Environmental Protection Act.** Waste management. The duty of care. A code of practice 1996. London, HMSO, 1990.

46. **Floyd, H.** Relationship between input and output. Medical waste incineration and pollution prevention. Ed. A. E. S. Green. Norstrand Reinhold. New York, 1992, pp. 109-110.

47. **Gera, D. and Gautam, M.** Emissions from RDF/coal blended fuel combustion. Chemosphere, volume 27, number 12, 1993, pp. 2353-2363.

48. **Gerstrom, P., Meredith, J. and Bailly, N.** DeN0x systems. The SELCHP experience. SELCHP Ltd, UK. Second International Symposium on Incineration and Flue Gas Treatment Technologies. Sheffield, UK, July 1999, pp 15 – 23.

49. **Goodger, E. M.** Alternative fuels. Chemical Energy Resources. London 1980, pp, 75 – 102.

50. **Green, D.** Combined heat and power, Levy exempt energy. Journal of Water, Energy and Environment, issue No 6, February 2000, pp 12 – 14.

51. **Grubb. M, Vrolijk C, and Brack D.** The Kyoto Protocol. Energy and Environmental Programme. The Royal Institute of International Affairs, 1999, pp, 1 - 45.

52. **Hall, G. S. and Knowles, M. J. D.** Heat recovery boiler for gas turbines. Incinerators and gas furnaces. Energy and the process industrial. IMechE, London, 1985.

53. **Harwood, L. M. and Claridge, T. D.W.** Introduction to organic spectroscopy. Oxford University Press, 1997, pp. 2 - 20.

54. **Integrated Waste Services Association Report**, waste-to-energy directory of United States Facilities, 1997/98.

55. International Standard Organisation EN ISO 5167-1 issue 2, February 1999.

56. **Jahnke, B.** Waste Incineration. An important element of the integrated waste management system in Germany. Waste Management and Research, volume 10, number 4, 1992, pp. 303 - 315.

57. **James, H., Bechtel, C. J. Dasch, and Rechard, E. T.** Combustion research with laser, in laser applications. Eds. John, F. R. and Robert, K. Academic Press Inc. London, 1984, pp. 130 - 191.

58. **Janhke, J. A.** Continuous emission monitoring. John Wiley and Sons, Inc, New York, 2000, pp 10 – 125.

59. **Knowles, M. J. D.** Energy and heat recovery in the chemical, steel making, and refuse disposal industries. Energy Recovery in Process Plants IMechE, London, 1974.

60. **Landy, M.** Energy from waste option. Harwell Waste Management Symposium. Waste Management in the UK, 1988, pp 35 – 42.

61. **Laufer, G.** Introduction to optics and lasers in engineering. Cambridge University Press, 1996, pp. 305 - 320.

62. **Liem, A. J, and Wilson, M. A.** A quantitative method for evaluating incinerators test burns results. Journal of the Air and Waste Management Association, volume 41, Part 1, 1991, pp. 47 - 55.

63. **Lindan, L.** N0x effects on flue gas opacity. Journal of the Air and Waste Management Association, volume 41, 1991, pp. 1098.

64. **Mark, H. and Workman, J**. Statistics in spectroscopy. Academic Press Inc, London, 1991, pp 271 – 276.

65. **McKinnon, J. T, Abraham, E, Miller, J. H.** An infrared laser fault detection method for hazardous waste incineration. Journal of Combustion, Science and Technology, volume 85, 1992, pp. 391 - 403.

66. **Metcalfe, E. D, Prichard, F. E, (Eds).** Atomic absorption and emission spectroscopy. John Wiley and Sons, London, 1994, pp. 51 - 57.

67. **Miyawaki, J., Yamanouchi, K. and Tsuchiya, S.** State-specific unimolecular reaction of $N0_2$ just above the dissociation threshold. Journal of Chemical Physics, volume 99, 1995, pp. 254 - 264.

68. **Mott, D.** Measurement of Nitrogen Dioxide by Laser Techniques. Postgraduate Dissertation, University of Manchester, 1989.

69. **Nasserzadeh, V, Swithenbank, J, Lawrence, D, Garrod, N and Jones, B.** Measuring gas-residence times in large municipal incinerators, by means of a pseudo-random binary signal tracer technique. Journal of the Institute of Energy, September, volume 68, 1995, pp. 106 - 120.

70. **Niessen, W. R.** Combustion and incineration process. Applications in environmental engineering. Eds. R. A. Young and P. N. Chermisinoff. Barrington, New York 1978, pp 65 – 76.

71. **Ocean Optics Europe**. Spectrometer PC 2000 manufactures manual.

72. **Oppelt, E. T.** Incineration of hazardous waste, a critical review. Journal of Air Pollution Control Association, volume 37, 1989, pp. 558 - 586.

73. **Parr, E. A.** Industrial Control and Handbook. Butterworth Heinemann, London, 1995, pp. 233 - 236.

74. **Paul and Ellen Connect.** Municipal waste incineration, wrong question and wrong answer: The Ecologist, volume 24, 1994, pp. 14 - 20.

75. **Pavia, D. L, Lampman, G. M, Kriz, G. S.** Introduction to spectroscopy. Harcourt brace College Publishers, London, 1996, pp. 14 - 16.

76. **Peng, W. X, Ledingham, K. W. D, Marshall, A, and Singhal R. P.** Urban air pollution monitoring. Laser-based procedure for the detection of N0x gases. Analyst, volume 120, 1995, pp. 2537 - 2542.

77. **Penner, S. S., Chang, D. P. Y. Gouland, R. and Lester, T.** Waste incineration and energy recovery. Energy, volume 13, number 12, 1988, pp. 845 - 851.

78. **Porteous, A.** Energy from waste incineration – a state of the art emission review with an emphasis on public acceptability. Journal of Applied Energy, volume 70, 2001, pp. 157 - 167.

79. **Porteous, A.** Energy from waste, a wholly acceptable waste – management solution. Journal of Applied Energy, volume 58, 1998, pp. 177 - 208.

80. **Rampling, T. W, and Gill, P. J.** Fundamental research on the thermal treatment of waste and biomass. ETSU B/T1/00208/ REP/2. Warren Spring Laboratory, 1993.

81. **Rappe, C, Per-Anders, B. and Stellan, M.** Analysis of polychlorinated dibenzofurans and dioxins in ecological samples. Department of Organic Chemistry. University of Umea, Sweden, 1985.

82. **Rashid, R. A. and Frantz, G. C.** Municipal solid waste incinerator. Ash as aggregate in concrete and masonry. Journal of Materials in Civil Engineering, volume 4, 1992, pp. 353 - 368.

83. **Rhyner, C. R, Schwartz, L. J, Wenger, R. B. and Kohrell, M. G.** Waste Management and Resources Recovery. Lewis Publishers, London, 1995, pp. 241-270.

84. **Rogoff, M. J.** How to implement waste-to-energy projects. New Jersey, Noyes, 1987.

85. **Royal Commission on Environmental Pollution 17th Report.** Institute of Waste Management. London, HMSO, 1993.

86. **SELCHP.** Technical literature. South East London Combined Heat and Power, London, 1997.

87. Sheffield University Waste Incineration Centre (SUWIC). Second International Symposium on Incineration and Flue Gas Treatment Technologies - Sheffield UK, July 1999, pp, 15 - 23.

88. **Smith, D. J.** Industrial power plants reduce operating costs with waste fuels. Journal of Power Engineering, March 1992, pp 18 – 19.

89. **Stessel, R. I.** Recycling and resources recovery engineering. Principles of waste processing. Eds. U. Forstnee., J. Murphy, and W.H. Rulkens. New York, Heidelberg, 1996, pp 45 – 60.

90. **Stessel, R. I.** Recycling and resources recovery engineering. Springer, London, 1996, pp 205 – 221.

91. **Stohr. M, Schutz, M, Kruger, H.** Status of and experience with N0x reduction in coal-fired turbine plant. Journal of Power and Energy. I Mech.E volume 21, 1997, pp. 27 - 41.

92. **Sustainable development.** The UK Strategy. HMSO, London, 1994.

93. **Svanberg, S.** Geophysical gas monitoring using optical techniques - volcanoes, geothermal fields and mines. Applied Optics, volume 3, July 2001, pp. 245 - 266.

94. **Swithenbank J, Nasserzadeh V, Wasantakoran A, Lee P.H, and Swithenbank C.** Future integrated waste, energy and pollution management (WEP) system exploit pyrotechnology. Second International Symposium on Incineration and Flue Gas Treatment Technologies, Sheffield University, UK, 4 - 6 July 1999.

95. **Swithenbank, J, Nasserzadeh, V, Ewan, B. C. R, and Delay, I.** Research investigation at the municipal (2*35 MW) and clinical (2*5 MW) waste incineration centre. Sheffield University waste incineration centre. International FBC Conference. Savannah, Georgia, USA, May 1999, pp, 47 - 54.

96. **Swithenbank, J, Nasserzadeh, V, Goh, R, and Siddall, R, G.** Fundamental principles of incinerator design. Sheffield University Waste Incineration Centre. International FBC Conference. Savannah, Georgia, USA, May 1999, pp, 75 - 82.

97. **Swithenbank, J, Taib, R. Basire, S. Wony, W. Y. Oung, Y lu.K. and Nasserzadek, V.** Sludge incineration in a spinning fluidised bed incinerator. Waste Incineration Centre University of Sheffield. UK. 15th International FBC Conference. Savannah, Georgia, USA, May 1999, pp, 102 - 112.

98. **Takacs, L, and Moilanen, G, L.** Simultaneous control of PCDD/FCDF, HCI, and N0x emissions from municipal solid waste incinerators with ammonia injection. Journal of the Air and Waste Management Association, volume 41, Part 1, 1991, pp 716 - 722.

99. **The Composting Association.** Report SCA03, composting standards for composts, January 2002.

100. **The Kyoto Protocol and Beyond**. Action against climate change, OECD Coll, 1999, pp, 7 – 83.

101. **Tillman, D. A.** The combustion of solid fuels and wastes. Academic Press Inc. London, 1991, pp. 223 – 244.

102. **Warmer Bulletin 44.** Information sheet. Journal of the World Resources Foundation. Tonbridge, 1995, pp, 12 - 17.

103. **Weibring, P, Swartling, J, Edner, H, Svanberg, S, Caltabiano, T, Condarelli, D, Cecchi, G, and Pantani, L.** Optical monitoring of volcanic sulphur dioxide emissions – comparison between four different remote – sensing spectroscope techniques. Applied Optics, volume 37, 2002, pp. 267 - 284.

104. **Whiting, K. J.** The future of solid waste processing. Combustion, gasification or pyrolysis? Independent consultant. Second International Symposium on Incineration and Flue Gas Treatment Technology. Combustion, July 1999, pp. 4 - 6.

105. **William, M. S.** Laser industrial applications springer – verlag. London, 1991, pp. 23 - 31.

106. **Williams, D. H, and Fleming, I.** Spectroscopic methods in organic chemistry. McGraw – Hill, London, 1993, pp. 1 - 8.

107. **Williams, P. T.** The sampling and analysis of dioxines and furans from combustion sources. Journal of the Institute of Energy, volume 65, March 1992, pp. 46 - 54.

108. **Williams, P. T.** Waste treatment and disposal. Department of Fuel and Energy, University of Leeds, UK. John Wiley, Chichester, England, 1998, pp. 283 - 330.

109. **Wolpert, V. M.** Incineration of municipal solid waste combined with energy production. Latest development. Climate change. Energy and the Environment. Part 2. Renewable Energy, volume 5, number 5 - 8, 1994, pp. 782 - 785.

110. **Wurster, W., Kamada, S. and Laser, M.** Latest development of waste incineration in the Julich incineration process. Low and intermediate level radiative waste management. ASME, New York, 1989, pp, 69 - 74.

111. **Zacharias, H,. Geilhaupt, M. Meier, K and Welge, K. H.** Statte – specific unimolecular reaction of $N0_2$ just above the dissociation threshold. Journal of Chemical Physical, volume 101, No6, 1994, pp, 4505.

Appendices

Appendix A The results from the remainder of the combustion experiments.

The results from the remainder of the combustion experiments are presented in this Appendix. Figure A.1 to A.5 shown the emission levels and photographic images of the flames for each of the five fuels. Figure A.6 to A.7 show the temperature profiles (bulk temperature versus time) for different fuels. Figure A.1 and A.2 show the linear relationship between the absorbance and the nitrogen dioxide concentration for selected test run.

Overall, the measurements in figures A.1 to 11 confirm the findings discussed in section 8.2 to 8.6 that the $N0_2$ emission levels produced during the co-combustion of coal and dRDF increase with the increases in the rage of combustion. The measurements in figure A.12 to A.28 helps to explain the variations in the temperature profiles observed in the combustion chamber for the repeated tests of the same fuel and the same combustion conditions.

The results in figure A.29 and 30 helps to explain that the absorbance levels observed during the combustion experiments were below useful practical limit of 1 as described in section 5.2.

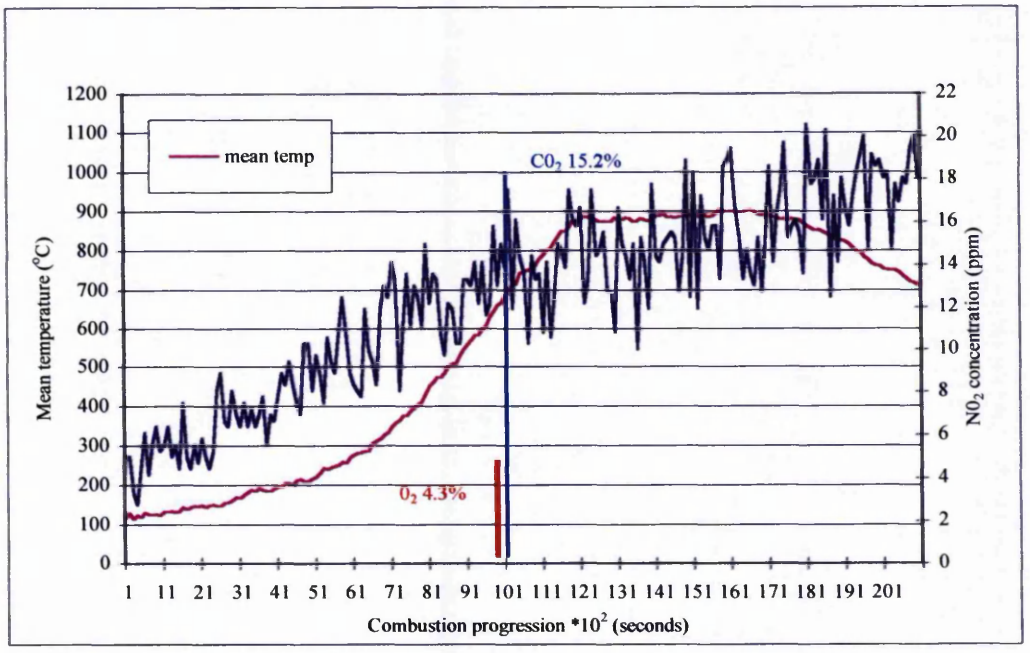

Figure A. 1 Emission levels for 100% coal

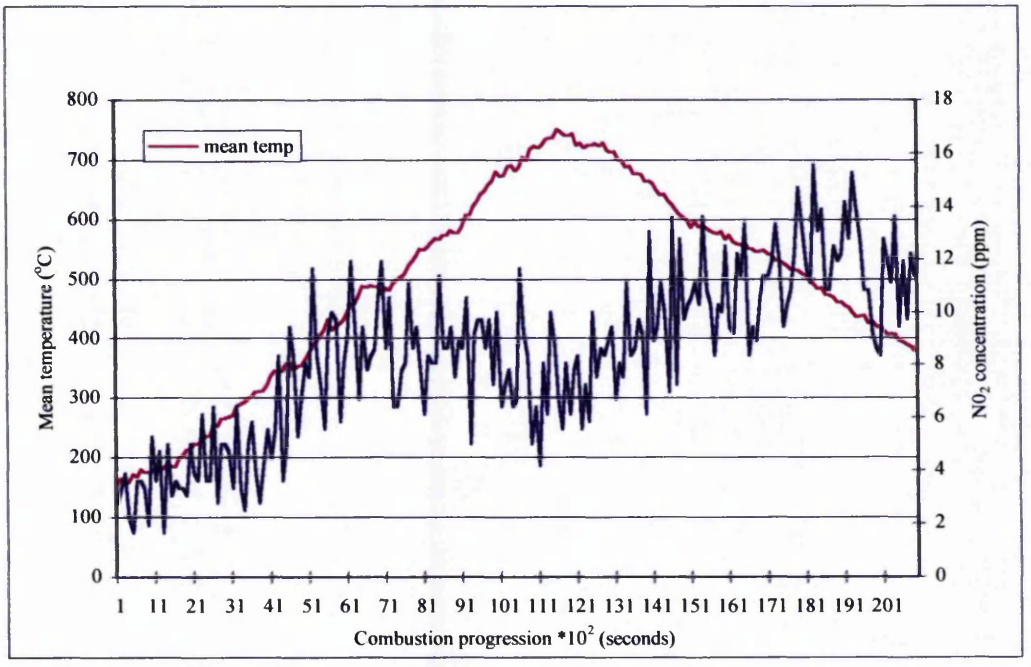

Figure A. 2 Emission levels for 100% coal

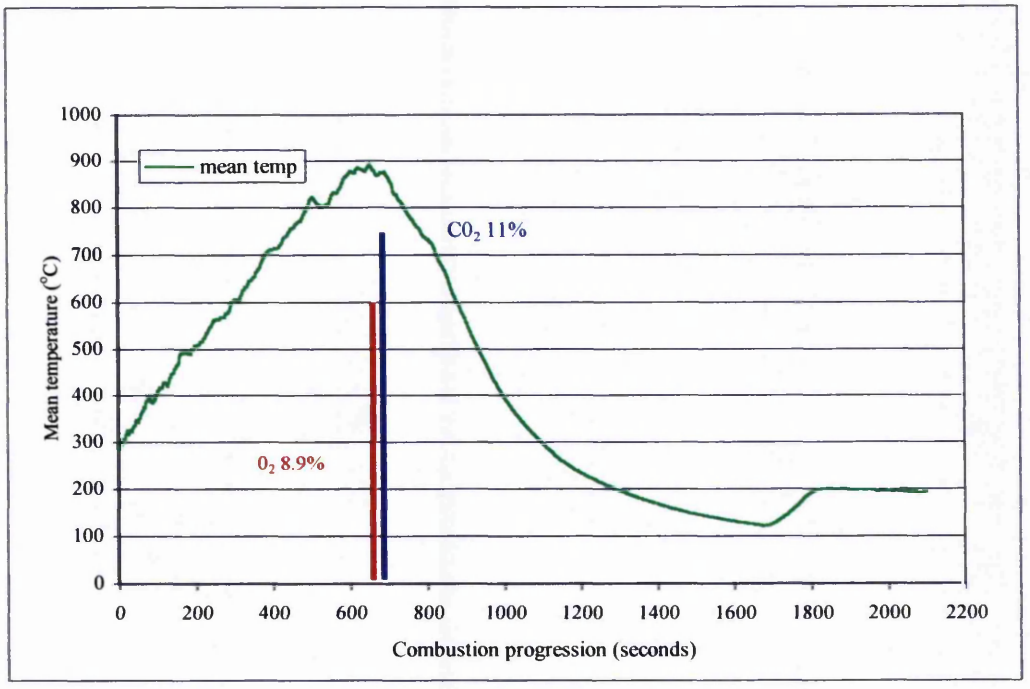

Figure A. 3 Emission levels for 100% dRDF

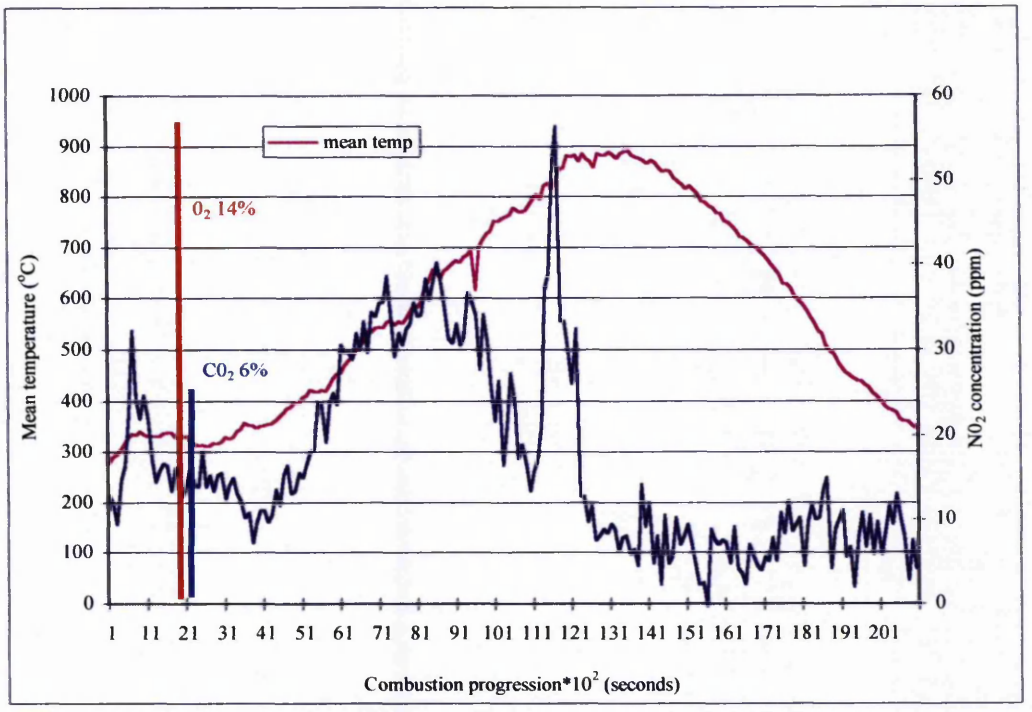

(a)

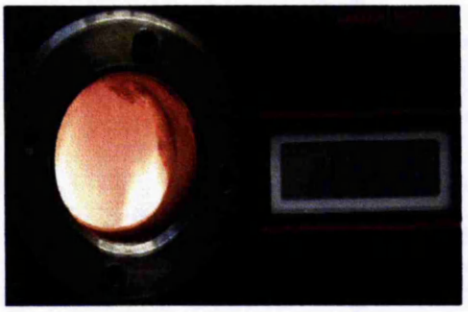

Flame 1 (b)

Recorded at 64 seconds.

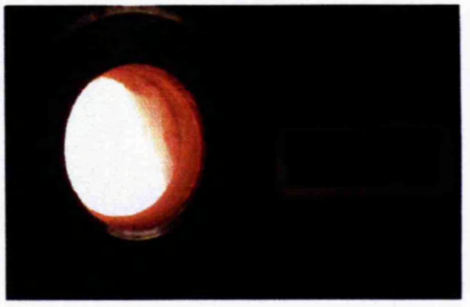

Flame 2 (c)

Recorded at 157 seconds. Oxygen = 14%, carbon dioxide = 6%

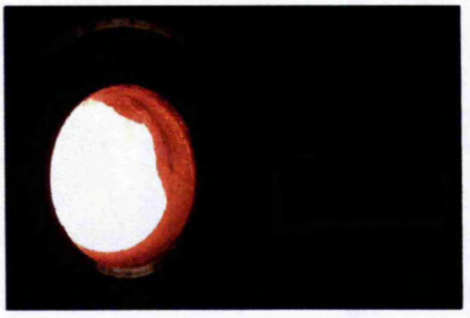

Flame 3 (d)

Recorded at 346 seconds

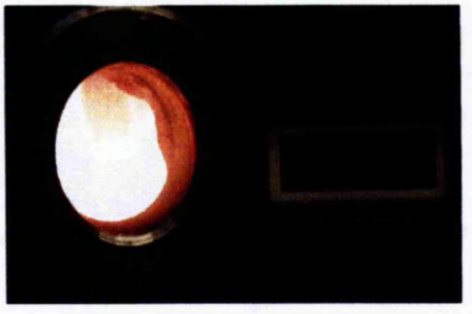

Flame 4(e)

Recorded at 617 seconds

Figure A. 4 Emission levels and flame images for 50/50% coal/dRDF

N.B. images taken during the ignition stage

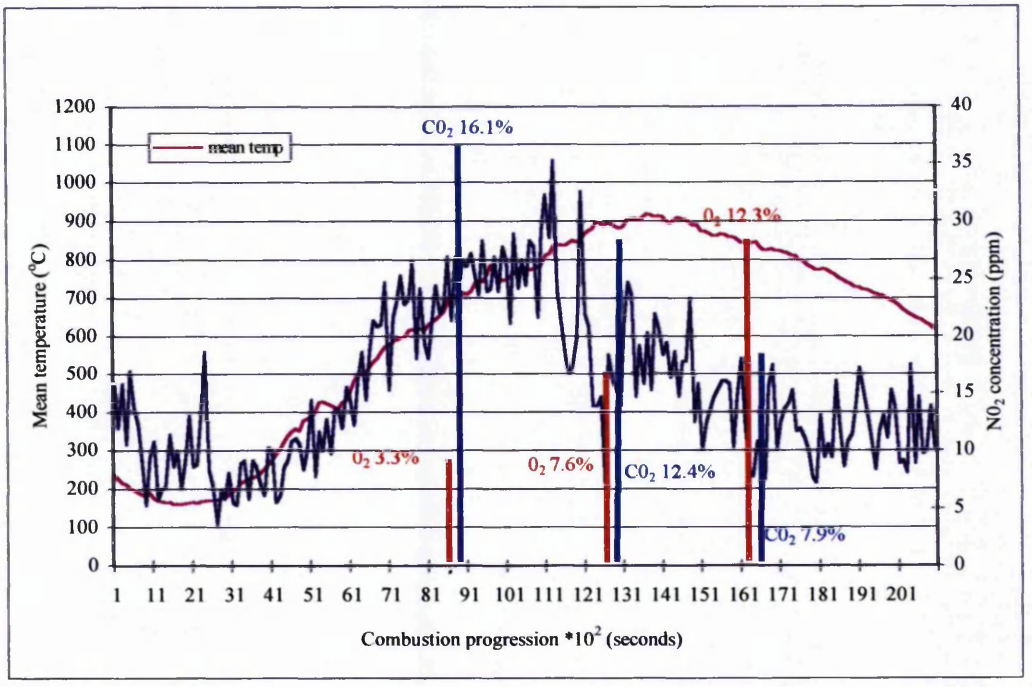

Figure A. 5 Emission levels for 50/50% coal/dRDF

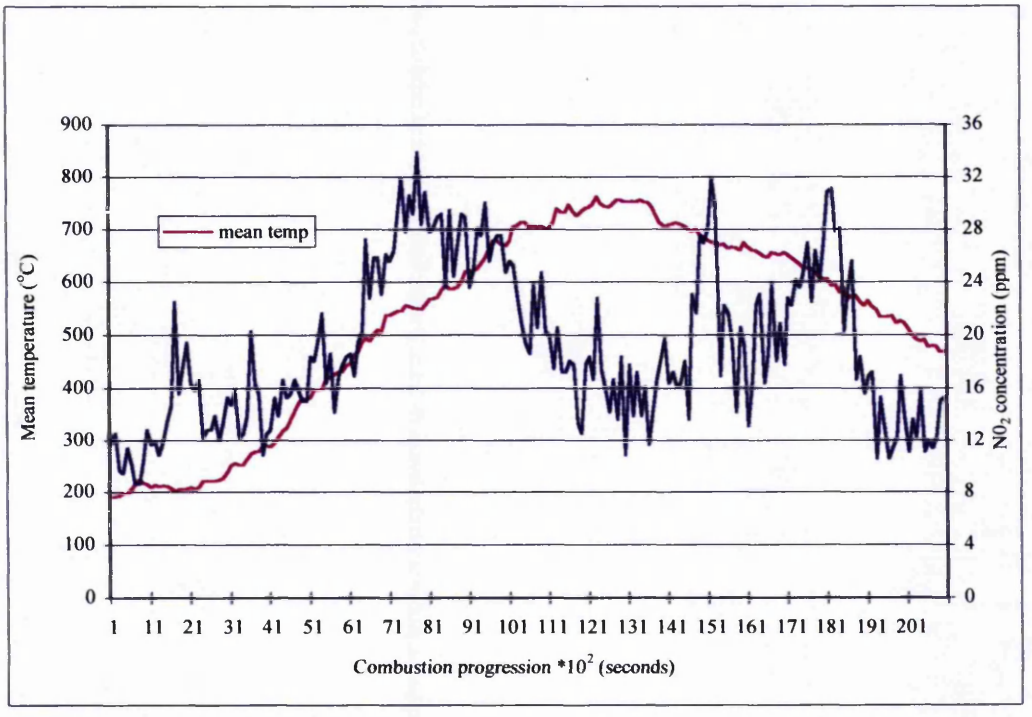

Figure A. 6 Emission levels for 50/50% coal/dRDF

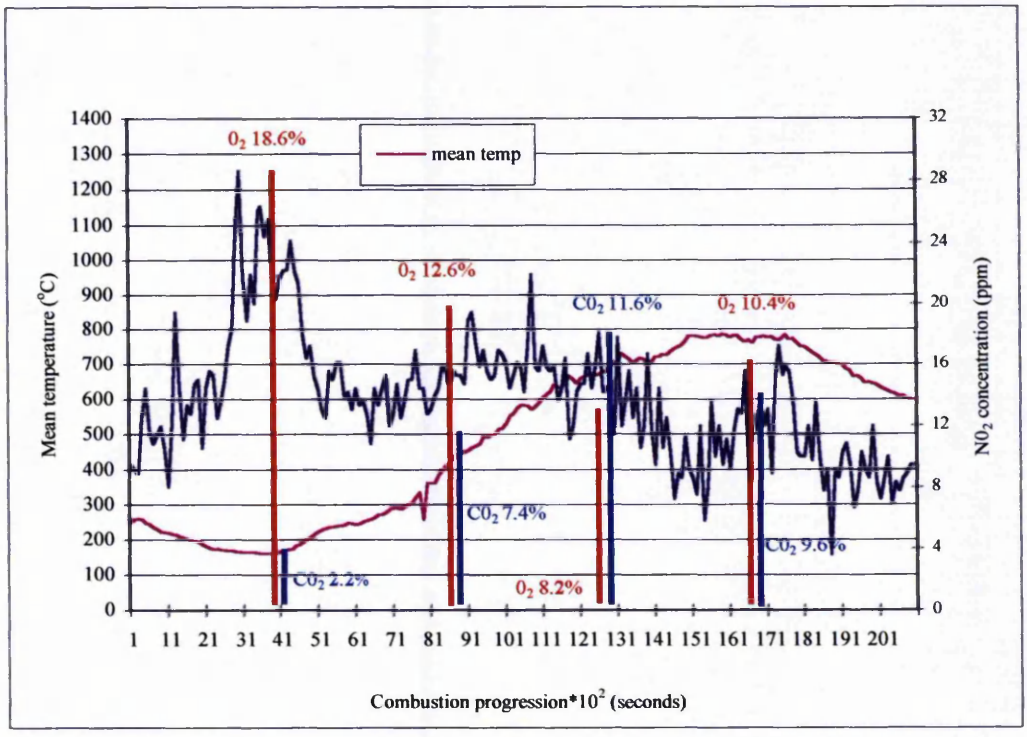

(a)

Flame 1(b)

Recorded at 900 seconds. Oxygen = 12%, carbon dioxide = 7.4%

Flame 2(c)

Recorded at 1021 seconds. Oxygen = 10.4%, carbon dioxide = 9.6%

Flame 3(d)

Recorded at 1100 seconds. Oxygen = 9.2% , carbon dioxide = 10.8%.

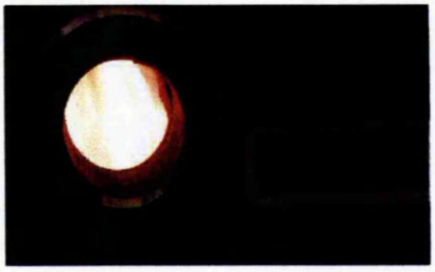

Flame 4(e)

Recorded at 1197 seconds. Oxygen = 8.4%, carbon dioxide = 11.6%.

Figure A. 7 Emission levels and flame images for 60/40% coal/dRDF

N.B. images taken during the ignition stage

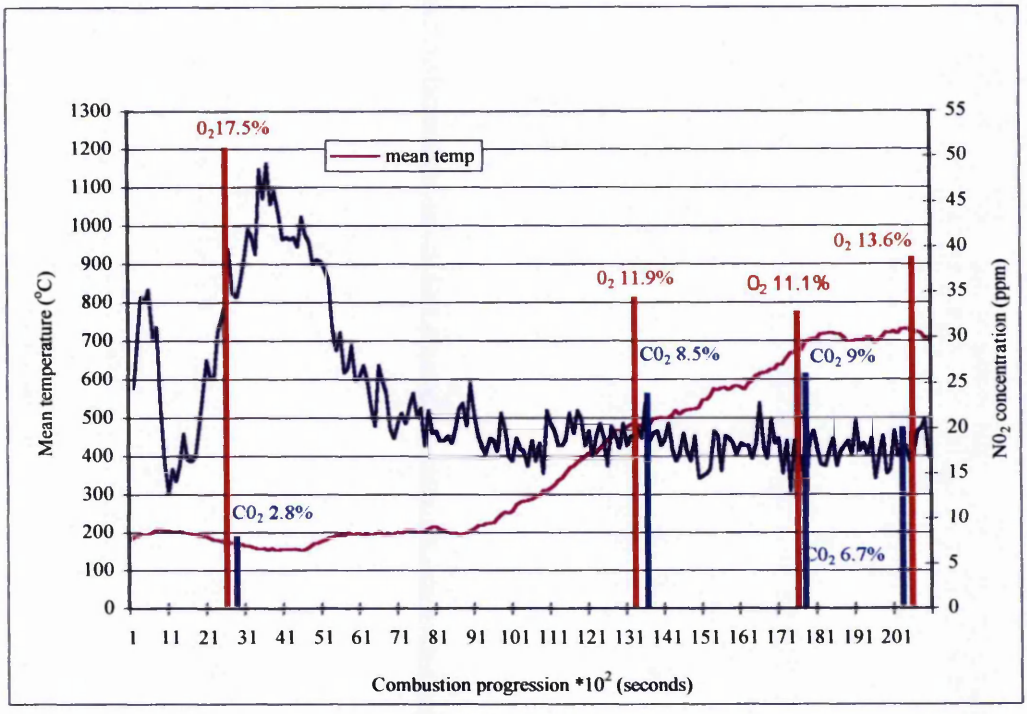

(a)

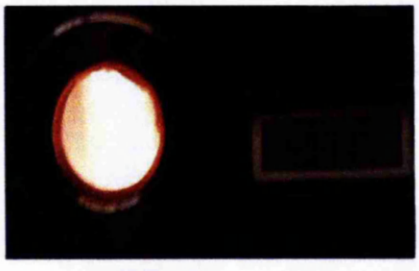

Flame 1(b)

Recorded at 1149 seconds. Oxygen = 12.9% , carbon dioxide = 7.1%.

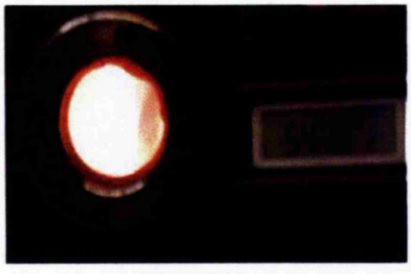

Flame 2(c)

Recorded at 1650 seconds. Oxygen = 11.5% , carbon dioxide = 8.5%.

Figure A. 8 Emission levels and flame images for 60/40% coal/dRDF

N.B. images taken during the ignition stage

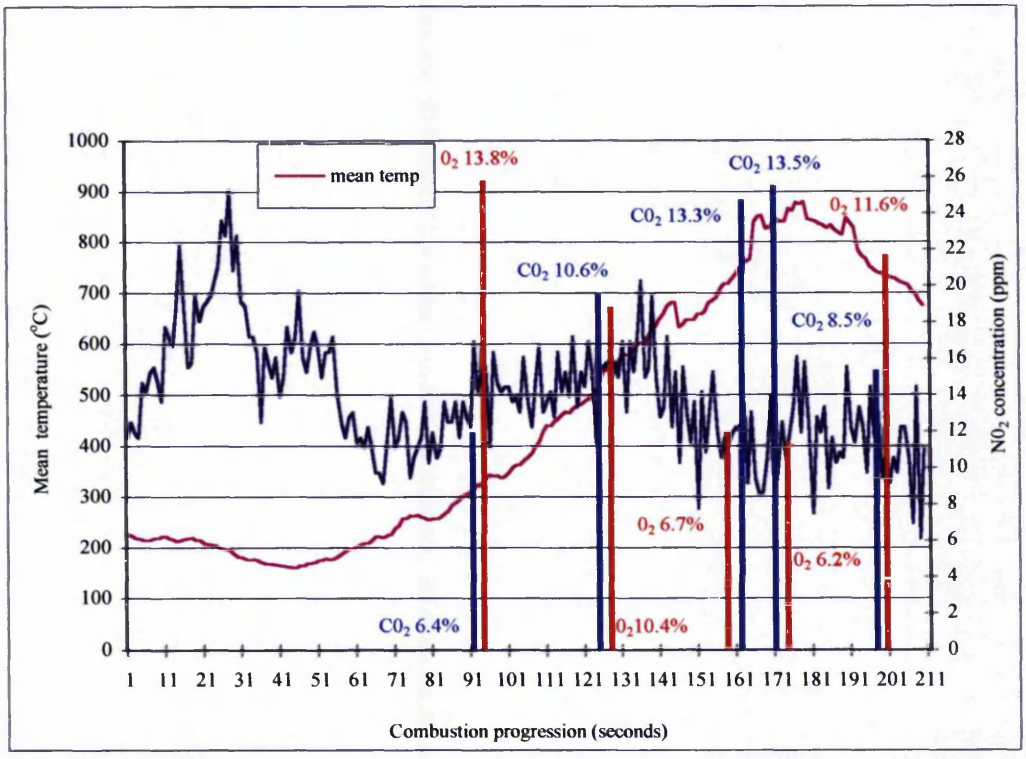

(a)

Flame 1(b)

Recorded at 684 seconds

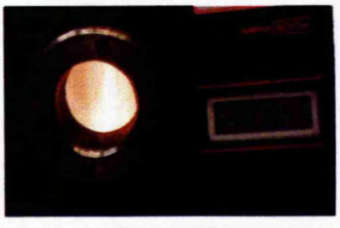

Flame 2(c)

Recorded at 930 seconds. Oxygen = 13.8%, carbon dioxide = 6.4%

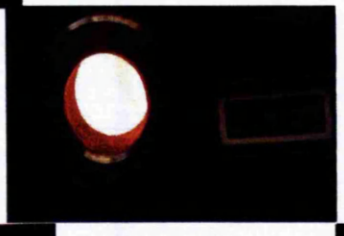

Recorded at 1280 seconds. Oxygen = 10.4% carbon dioxide = 10.6%

Flame 3(d)

Flame 4(e)

Recorded at 1468 seconds. Oxygen = 7.5% , carbon dioxide = 12.5%

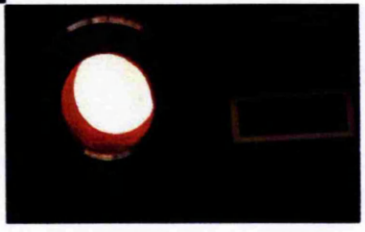

Flame 5(f)

Recorded at 1630 seconds. Oxygen = 6.7%, carbon dioxide = 13.3%

Figure A. 9 Emission levels and flame images for 70/30% coal/dRDF

N.B. images taken during the ignition stage

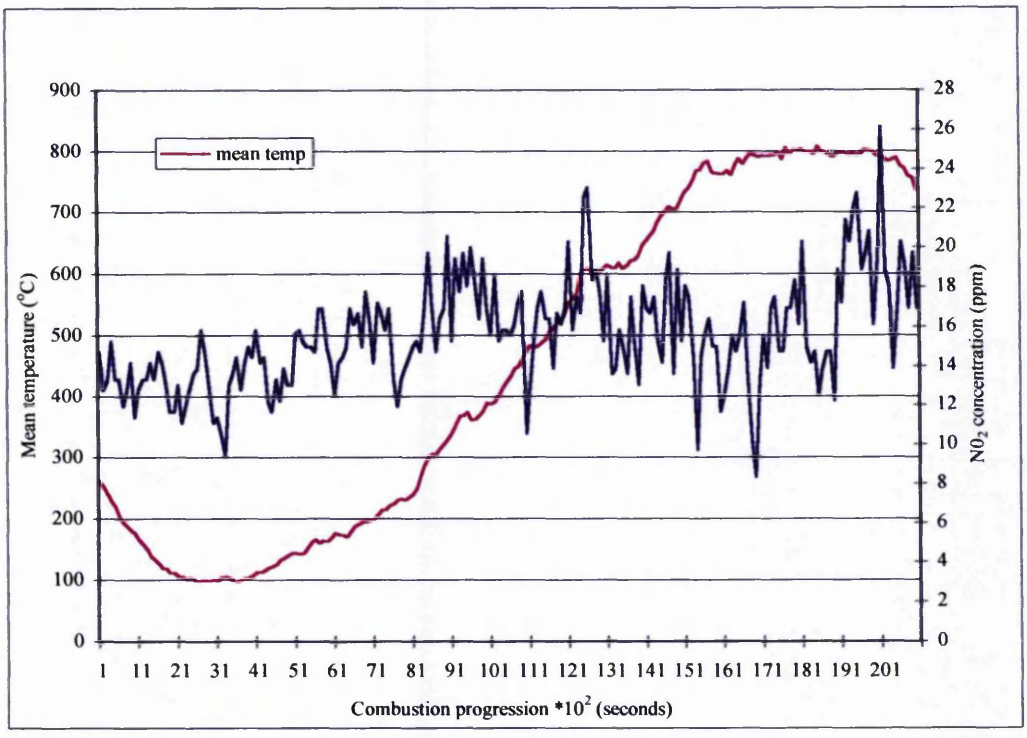

Figure A. 10 NO_2 emission levels for 70/30% coal/dRDF

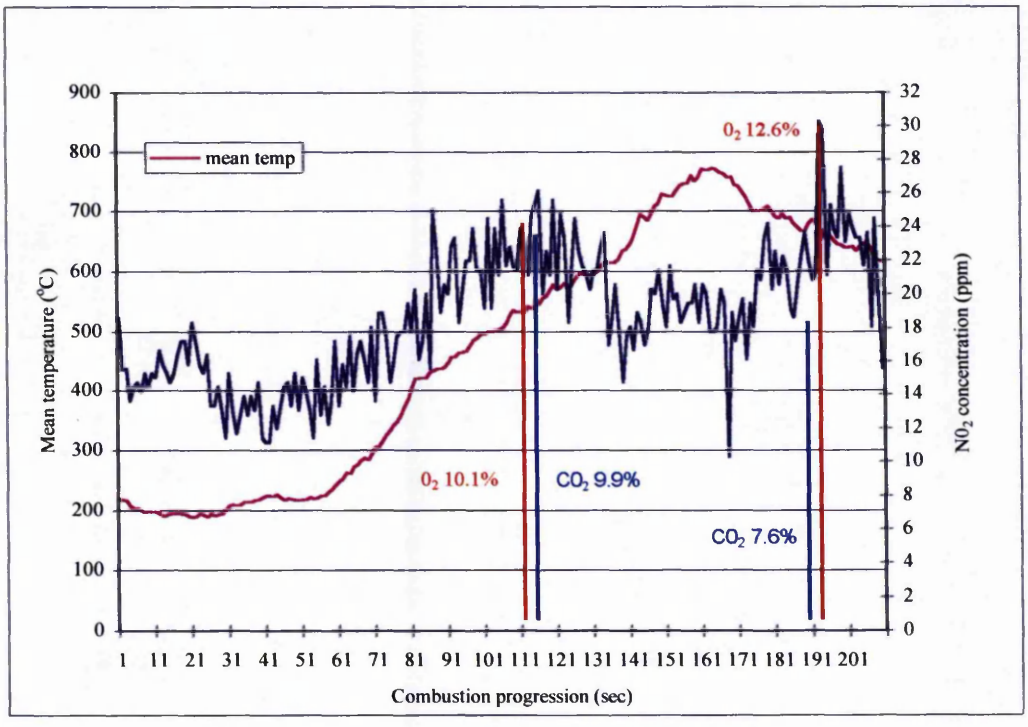

Figure A. 11 NO_2 emission levels for 70/30% coal/dRDF

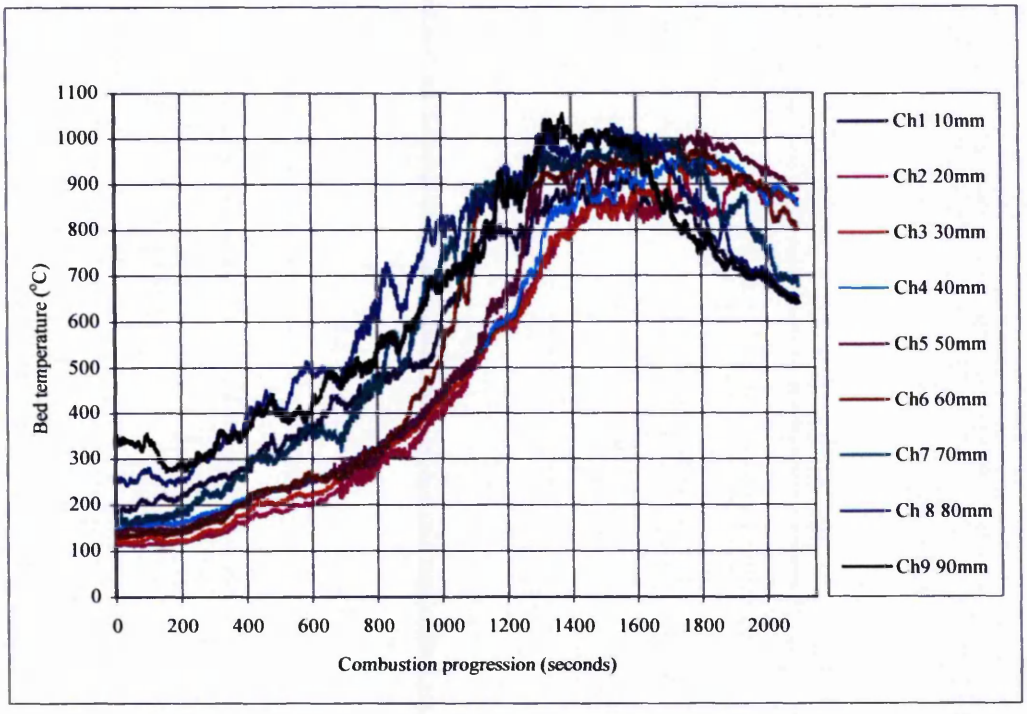

Figure A. 12 Temperature profiles for 100% coal

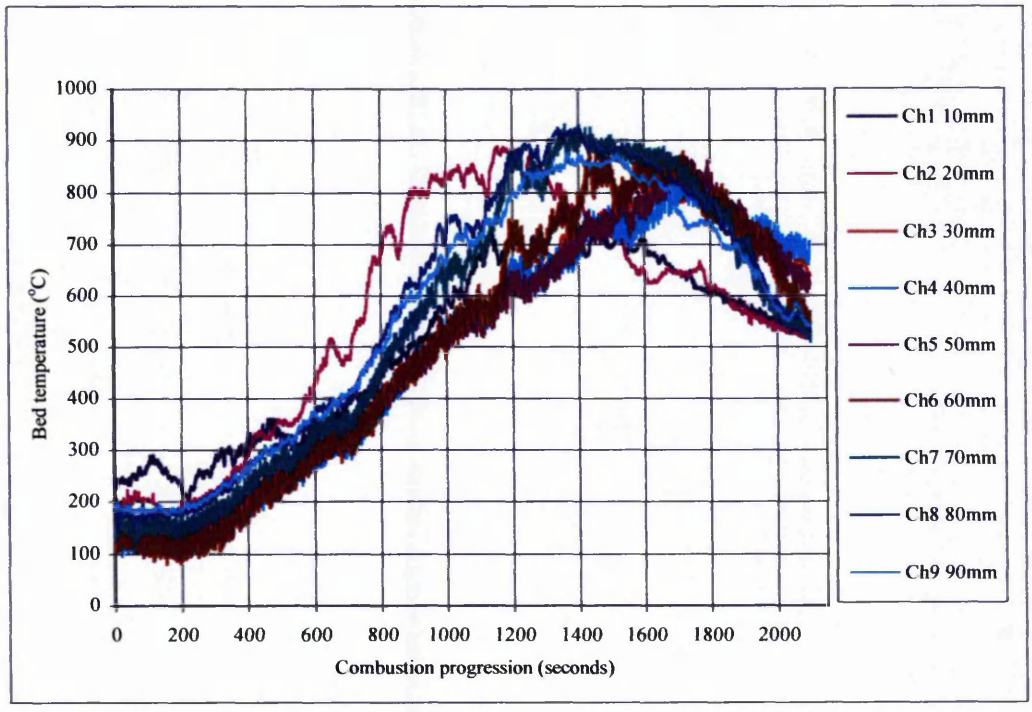

Figure A. 13 Temperature profiles for 100% coal

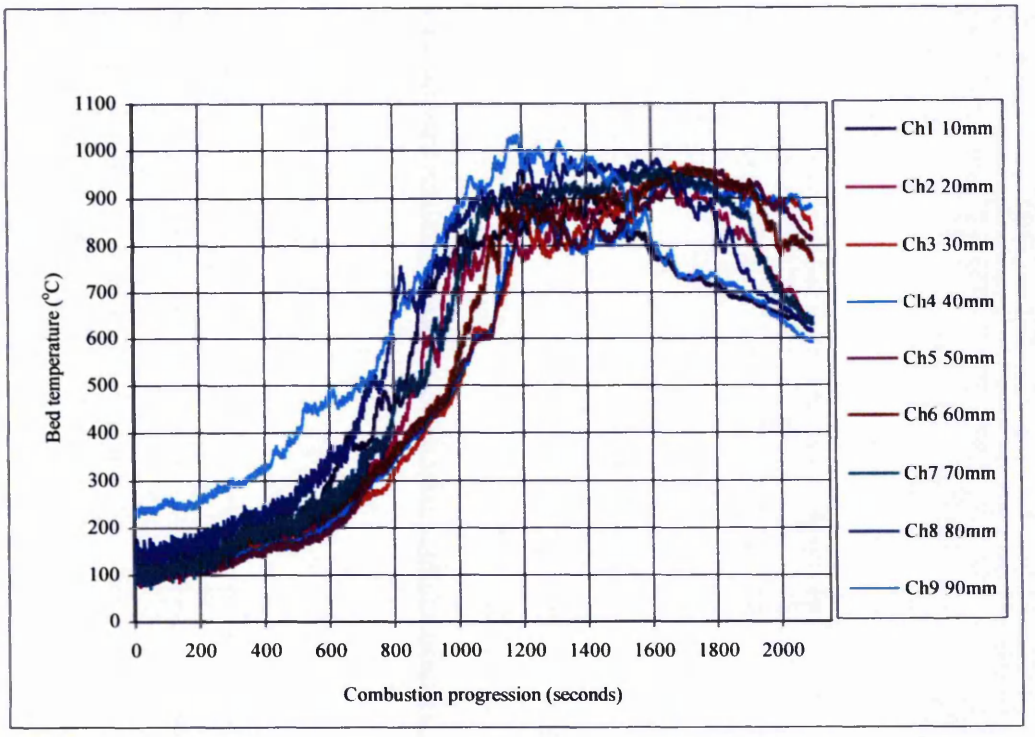

Figure A. 14 Temperature profiles for 100% coal

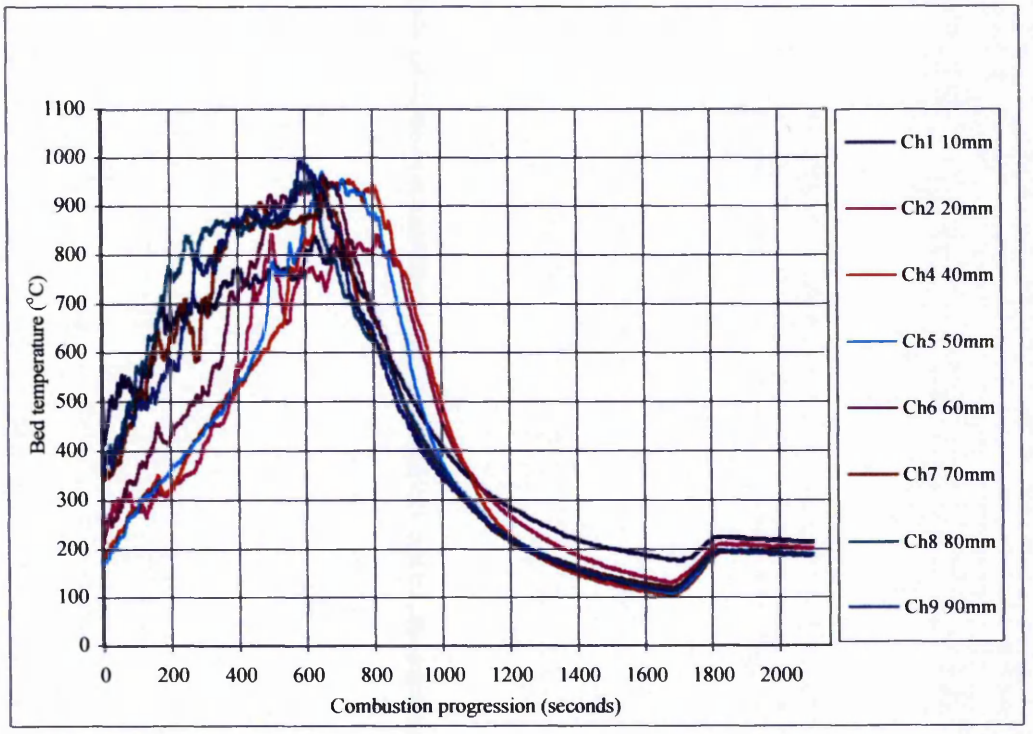

Figure A. 15 Temperature profile for 100% dRDF

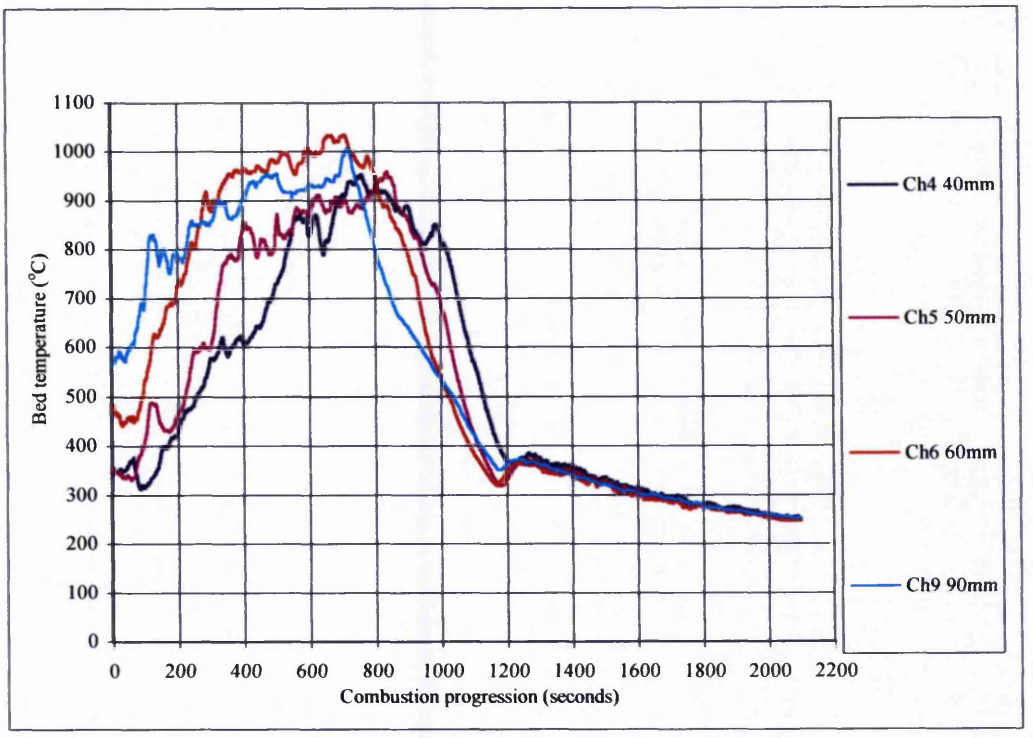

Figure A. 16 Temperature profiles for 100% dRDF

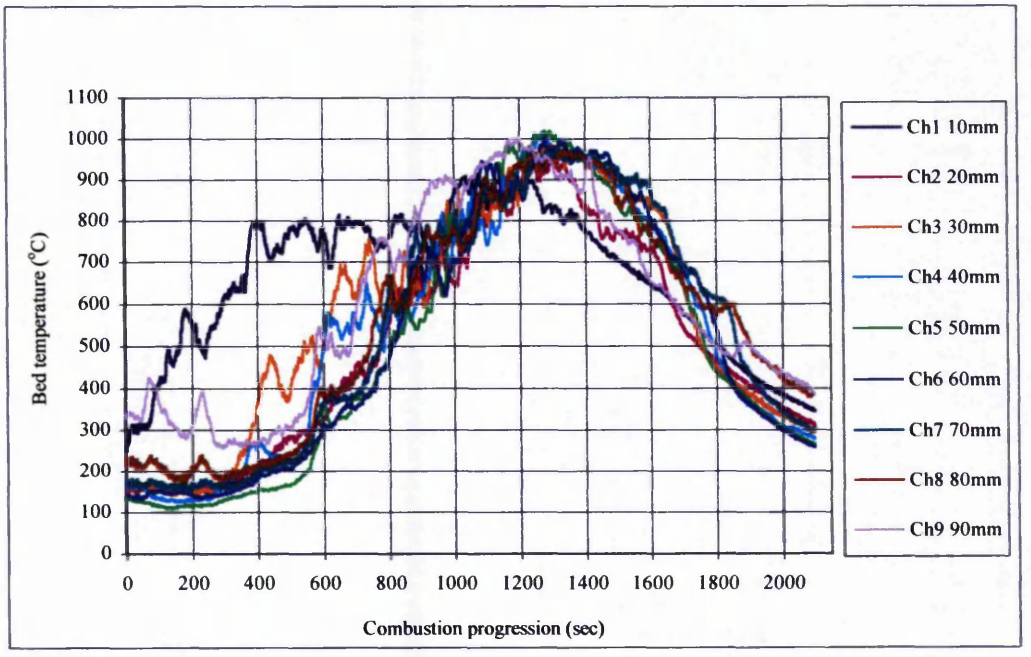

Figure A. 17 Temperature profile for 50/50% fuel mixture

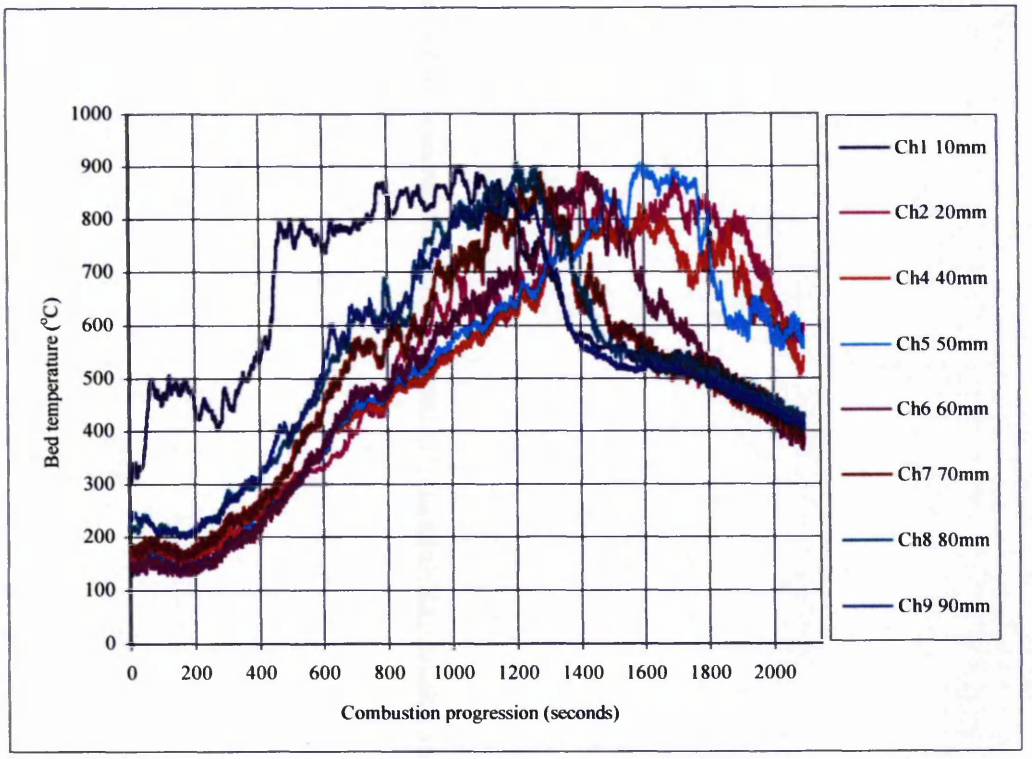

Figure A. 18 Temperature profiles for 50/50% fuel mixture

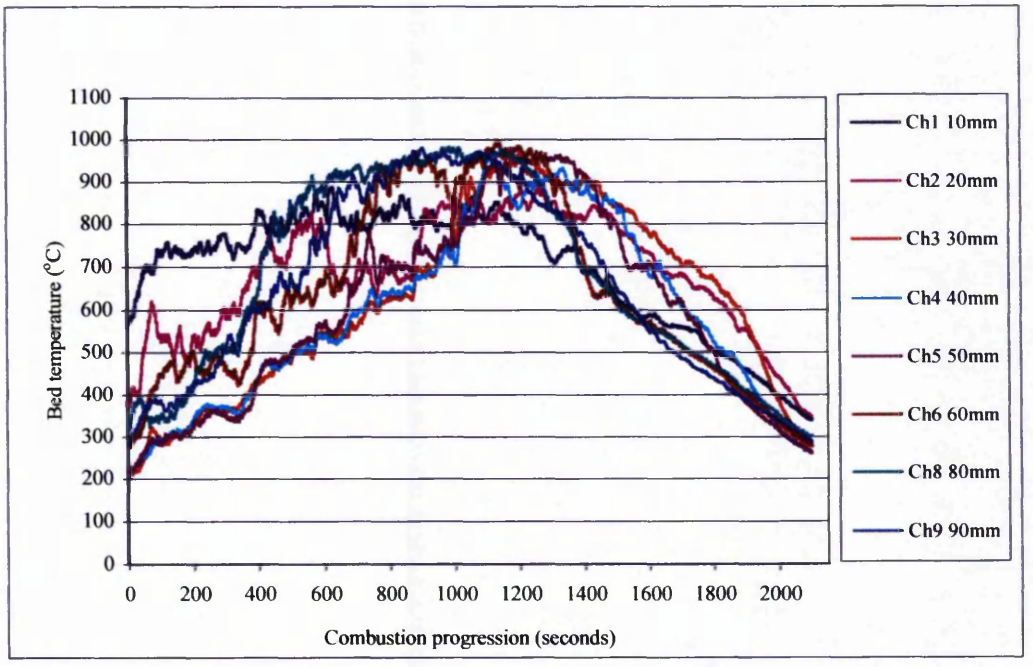

Figure A. 19 Temperature profile for 50/50% coal/dRDF

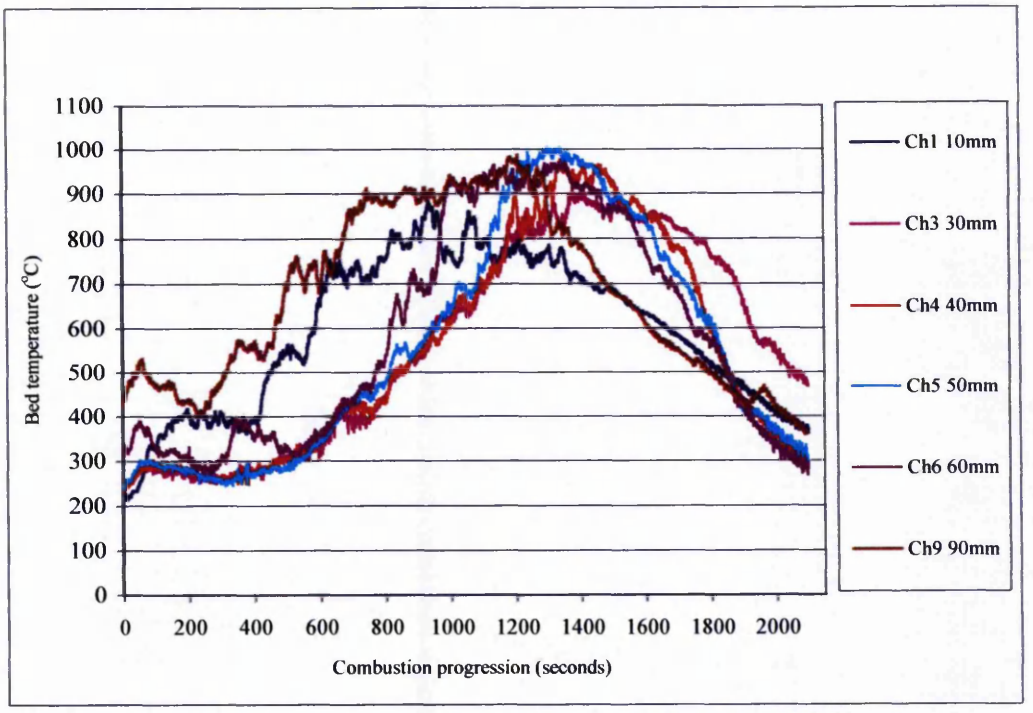

Figure A. 20 Temperature profiles for 50/50% coal/dRDF

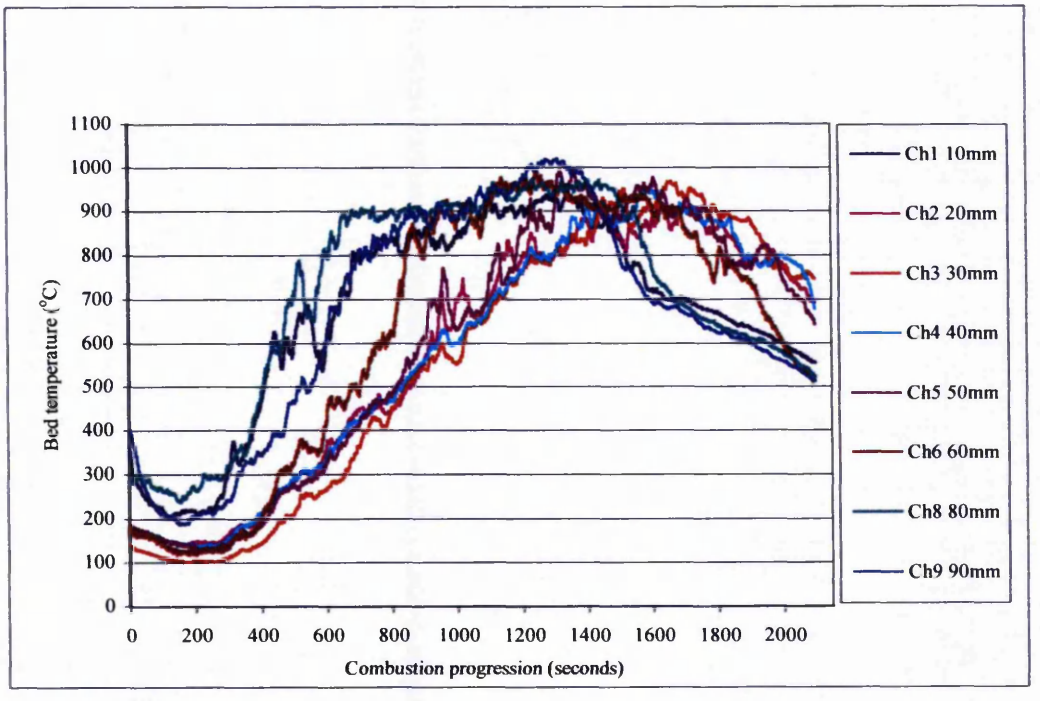

Figure A. 21 Temperature profiles for 50/50% coal/dRDF

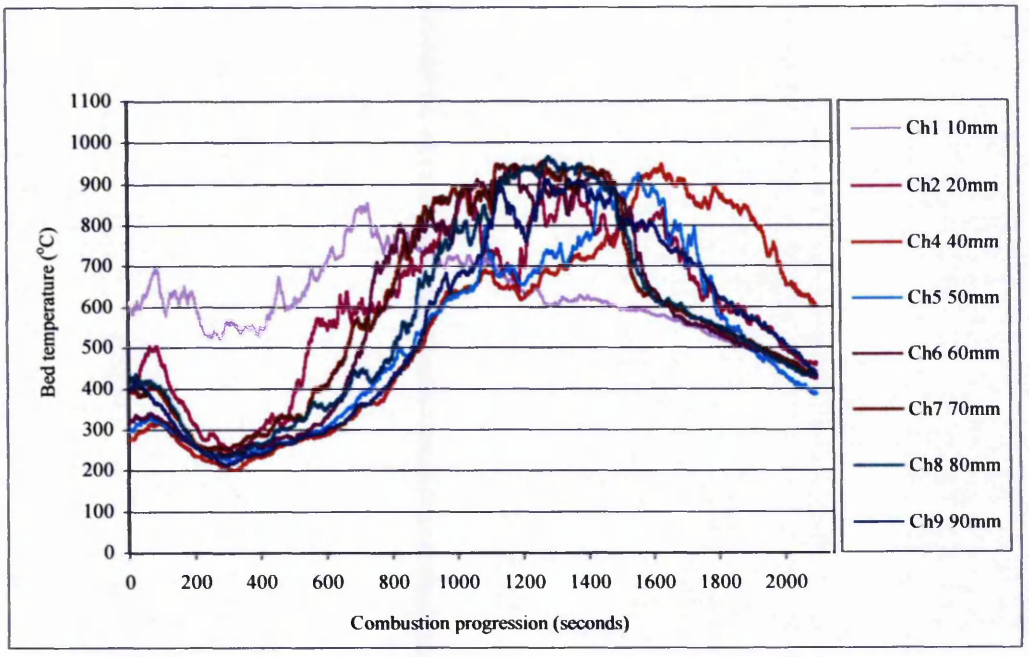

Figure A. 22 Temperature profiles for 60/40% coal/dRDF

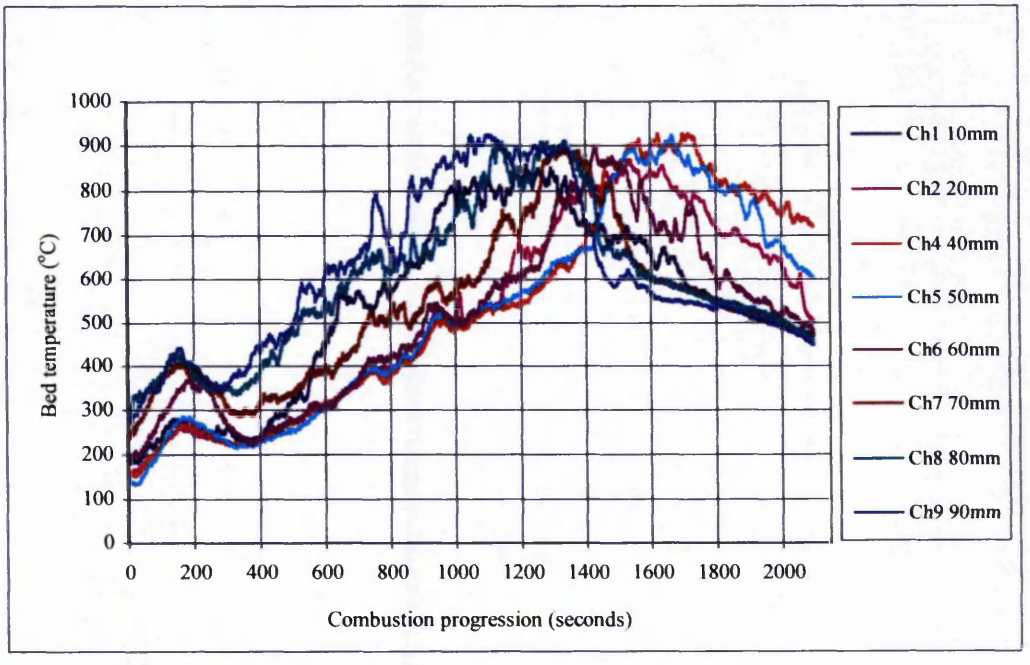

Figure A. 23 Temperature profiles for 60/40% coal/dRDF

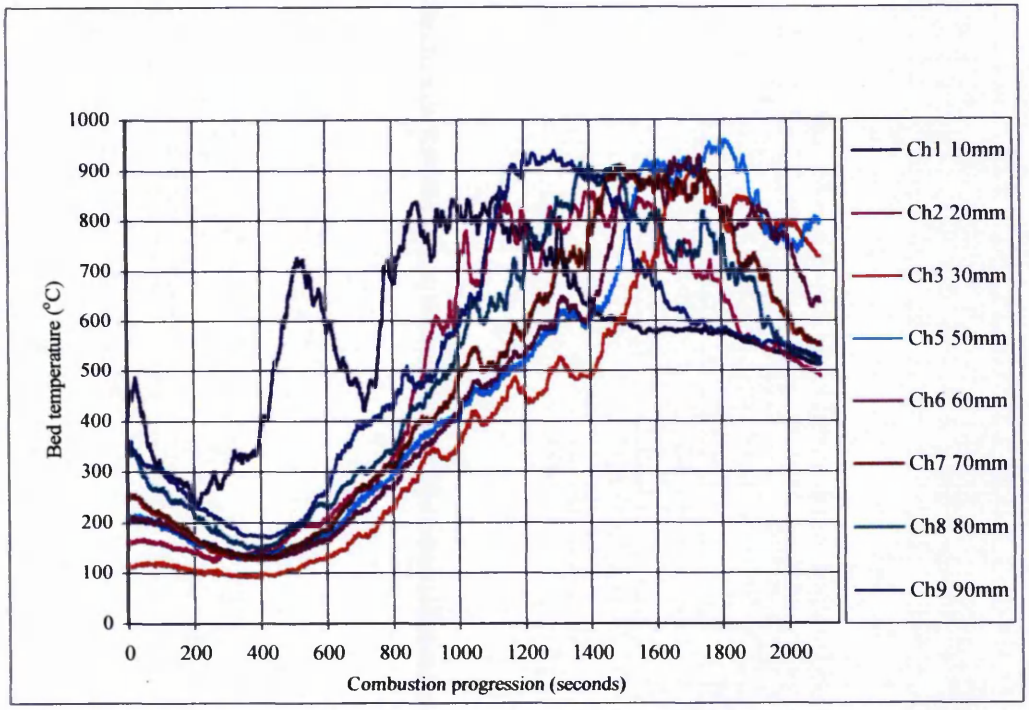

Figure A. 24 Temperature profiles for 60/40% coal/dRDF

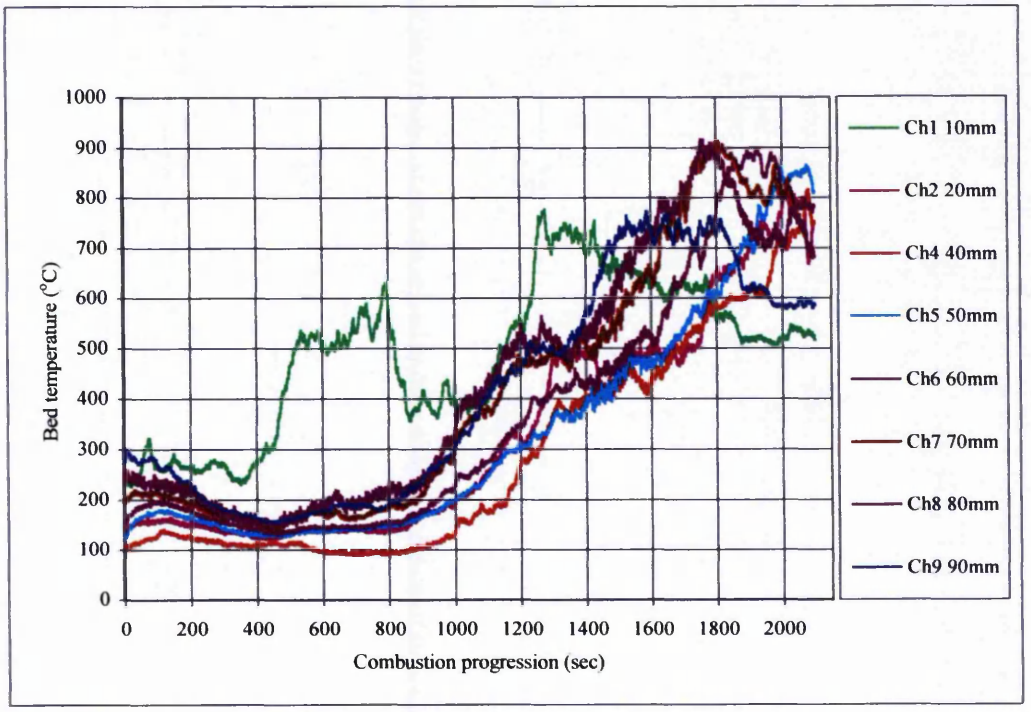

Figure A. 25 Temperature profile for 60/40% coal/dRDF

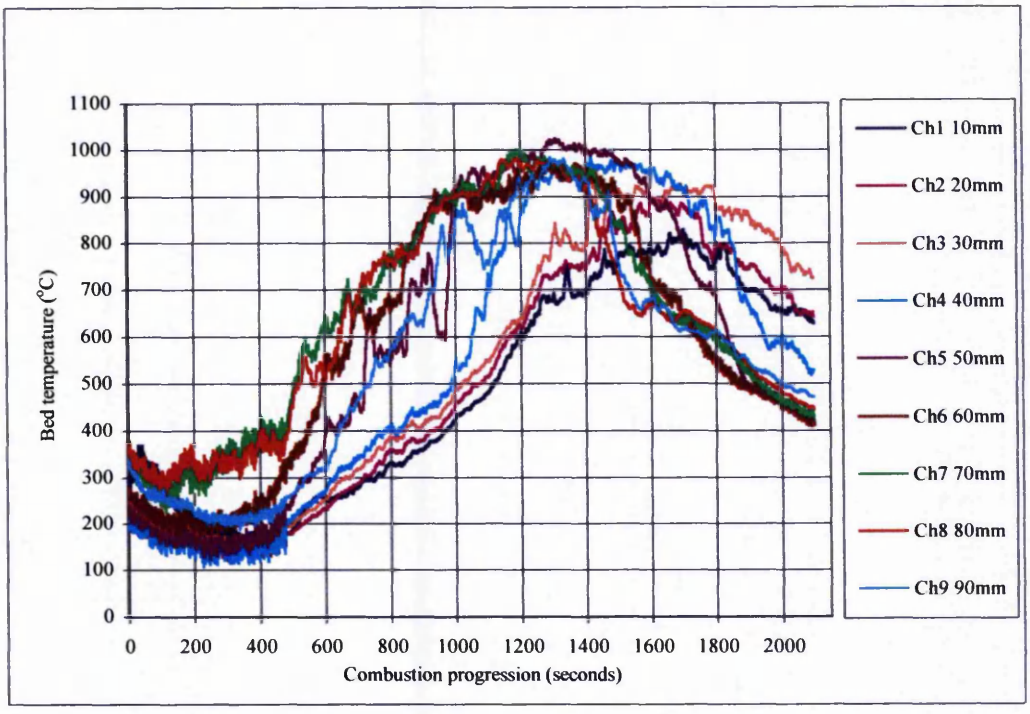

Figure A. 26 Temperature profile for 70/30% coal/dRDF

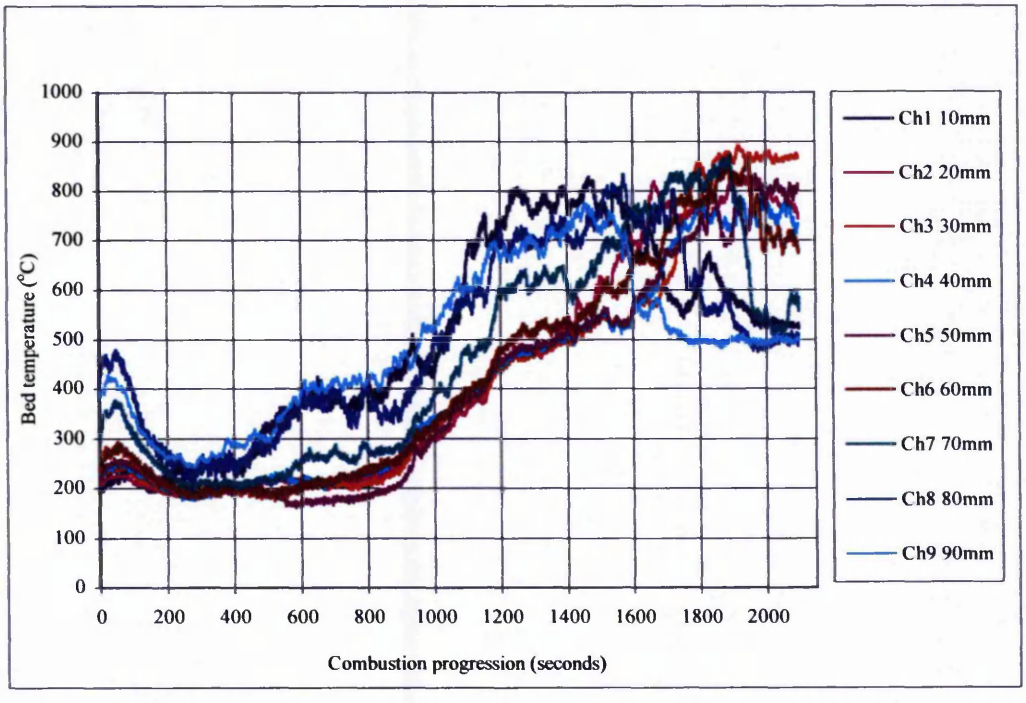

Figure A. 27 Temperature profiles for 70/30% coal/dRDF

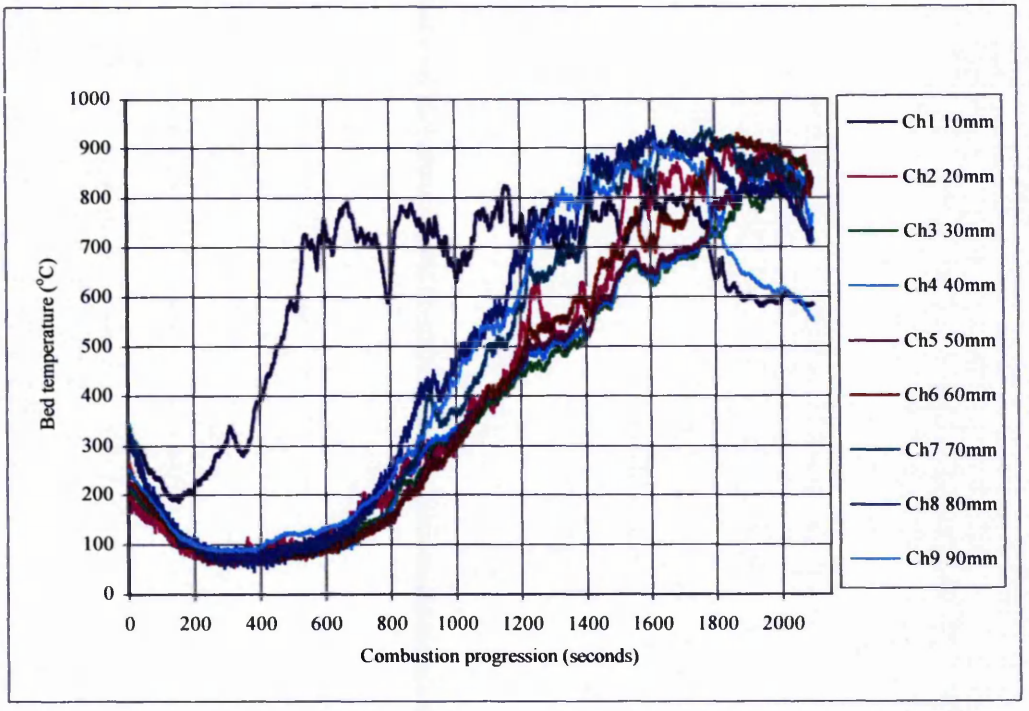

Figure A. 28 Temperature profiles for 70/30% coal/dRDf

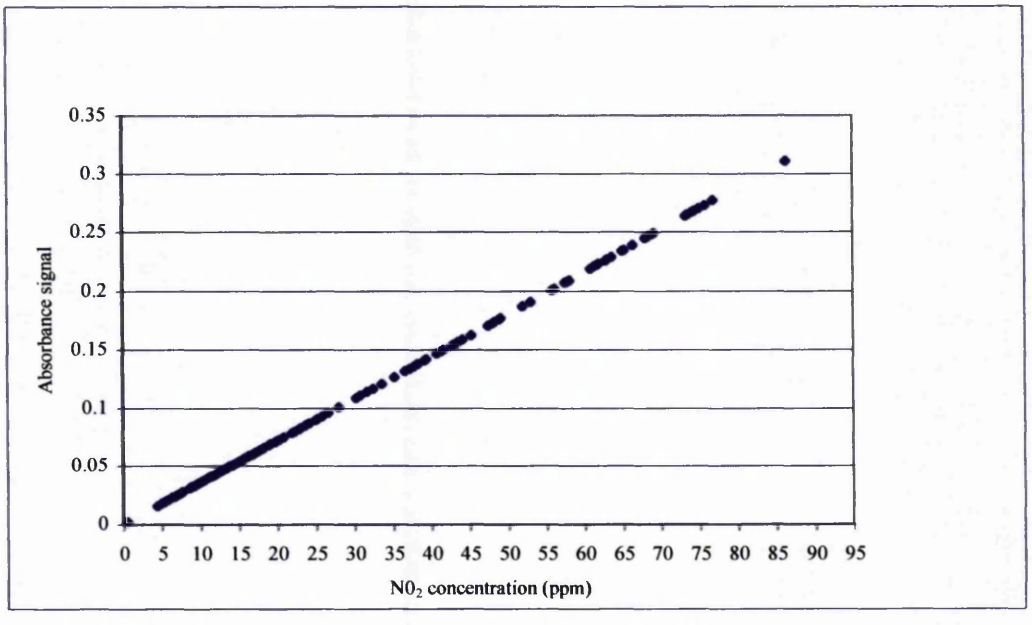

Figure A. 29 Absorbance vs $N0_2$ concentration for the 50/50% fuel mixture

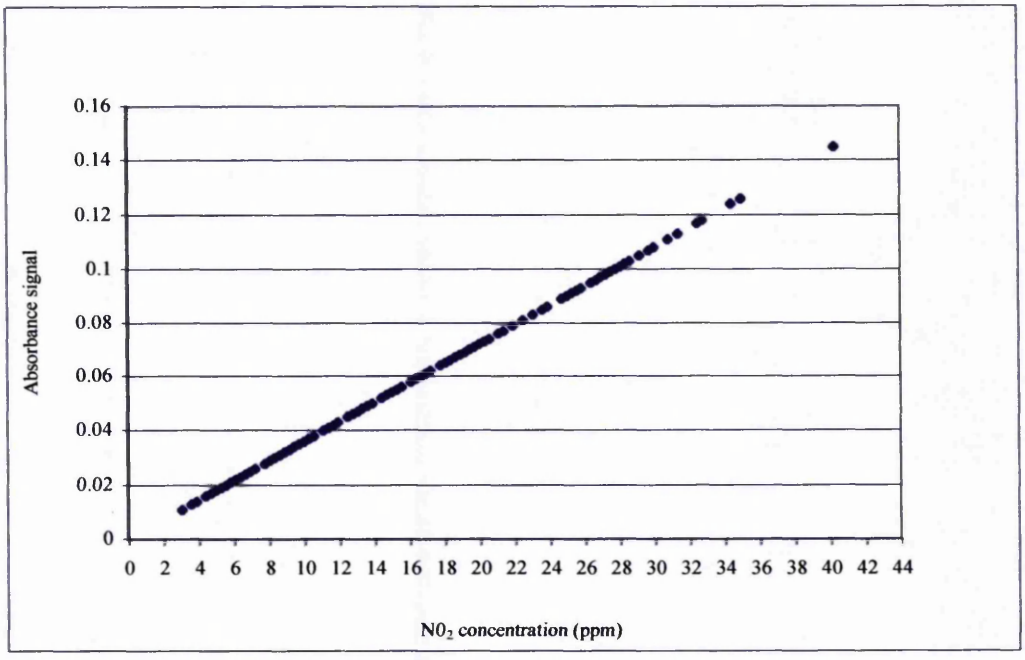

Figure A. 30 Absorbance vs $N0_2$ concentration for the 100% fuel

Appendix B Air mass flow rates

The data on the air mass flow rate across the fuel bed calculated according to the International Standard Organisation (EN ISO 5167 - 1 (1999)) are given in this Appendix.

TEST N0	Composition ratio % by wt		Bed weight (kg)	Primary air (kg/h/m^2)
	Coal	dRDF		
58	50% + 50%		2	3.76
61	50% + 50%		2	3.76
62	50% + 50%		2	3.76
66	50% + 50%		2	3.76
67	50% + 50%		2	3.76
68	50% + 50%		2	3.76
49	60% + 40%		2	3.57
50	60% + 40%		2	3.57
51	60% + 40%		2	3.57
52	60% + 40%		2	3.57
53	60% + 40%		2	3.77
48	70% + 30%		2	3.15
54	70% + 30%		2	3.15
55	70% + 30%		2	3.15
69	70% + 30%		2	3.15
70	70% + 30%		2	3.15
	Coal			
56	100%		2	4.16
57	100%		2	4.16
63	100%		1.3	4.16
64	100%		1.4	4.16
65	100%		2	4.16
	Densified refuse derived fuel			
32	100%		2	3.62
60	100%		2	3.62

JOHN RYLANDS
UNIVERSITY
LIBRARY OF
MAN